

https://dspace.org/

Reconstruction of the Early-Middle Miocene Palaeoenvironment in Gorongosa National Park, Mozambique

Maphutha, Mmatolo Julliet

2025-06

University of the Witwatersrand, Johannesburg

https://hdl.handle.net/10539/47690

Maphutha, Mmatolo Julliet. (2025). Reconstruction of the Early-Middle Miocene Palaeoenvironment in Gorongosa National Park, Mozambique. [Master's dissertation, University of the Witwatersrand, Johannesburg]. WIReDSpace. https://hdl.handle.net/10539/47690

Downloaded from a DSpace repository. https://dspace.org/

UNIVERSITY OF THE WITWATERSRAND JOHANNESBURG



FACULTY OF SCIENCE

Reconstruction of the Early-Middle Miocene Palaeoenvironment in Gorongosa National Park, Mozambique

by Mmatolo Julliet Maphutha

(1085894) (0000-0003-1609-8009)

A Masters Research Project Dissertation (DRAFT) in PALAEONTOLOGY

at the Evolutionary Studies Institute, Faculty of Science, University of the Witwatersrand, Johannesburg, South Africa

Supervisor: Prof Marion Bamford

DECLARATION

I declare that this dissertation is my own, unaided work. It is being submitted for the Master of Science at the University of the Witwatersrand, Johannesburg. It has not been submitted before for any degree or examination at any other University.



_____

(Signature of candidate)

_June_____day of _02_____2025_____at_Limpopo, Apel_____

.

Abstract

The origin of our flora and fauna is of general interest, and the Miocene (between 23.0 - 5.3 million years ago) was a crucial period for the development of our modern flora. Generally, there is a poor Miocene record in Africa but new Miocene sites have been discovered in Gorongosa National Park, central Mozambique; a park with an incredible diversity of fauna and flora. With newly discovered fossil shark teeth, molluscs, marine vertebrates and invertebrates, this is the first study to use palynological analysis to reconstruct the environment surrounding the Miocene fossils. The study aimed to use pollen, phytoliths, microcharcoal and other microremains to 1)reconstruct the palaeoenvironment and palaeoclimate from Early-Middle Miocene sediment deposits at the Gorongosa Palaeontological Locality number 12 (GPL-12); and 2)test the fidelity of the microremains recorded in the modern soils of the known vegetation types in the park. The pollen and phytolith samples for both fossil sediments and modern soils were processed using the standard method, which involves acid treatment and analysed in the lab. Overall, fungal material dominated most of the slides, and fossil non-pollen palynomorphs (NPPs) aided the most in palaeoenvironment reconstruction compared to fossil pollen and phytoliths. Fourteen phytolith morphotypes were found across the modern soil samples of which nine distinctively belonged to C4 grasses, the others were non-specific, and the rest were from woody dicotyledons. Overall, the results support other publications done in the area that the sea was more inland during the Miocene and GPL-12 was more wet and of an estuarine environment.

To the family that carried me in prayers and were a shoulder to cry on when it got tough, I dedicate this to you. Thank you for caring me in the Lord.

Acknowledgements

I am grateful to my supervisor Prof Marion Bamford firstly, for entrusting me with this project, and secondly for guiding me throughout. To say that the journey was bumpy would be an understatement- it was mountainous. I am grateful to have received support and guidance from my supervisor and for going the extra mile to assist me.

I am thankful to PAST for funding my degree so that we were able to do fieldwork, paying the institution and granting me peace of mind. I would not have done it without them.

Thanks to Dr Abraham Dabengwa for working with me through the codes and phytolith identifications, and being a big brother in the journey.

Thanks to Wade Harris for also assisting with an R-lesson that was very impactful to my codes.

Big thank you to our lab technician MS Prosper Bande for always being available to process samples, and also training and teaching me how to process pollen and phytoliths. Her kindness and patience made lab work easier.

Lastly, I am thankful to the University for granting me an opportunity to pursue my studies here. In addition to the Evolutionary Studies Institute (ESI) for providing an environment to carry out my experiments and laboratory work, I am thankful for all the resources they provided.

1. CHAPTER ONE- INTRODUCTION 9
1.1. General Introduction 9
1.1.1. Evolution of grasses and grasslands 9
1.1.2. Introduction to Gorongosa 13
1.1.3. The Civil War 18
1.2. Literature Review 19
1.2.1. Palaeoecology 19
1.2.2. Phytolith records 21
1.3. Aims and Objectives 26
Objectives. 27
2. CHAPTER TWO- MATERIALS AND METHODS 27
2.1. Introduction 27
2.2. Fossil Sampling 27
2.3. Modern Sampling 29
2.4. Laboratory method 32
2.4.1. Pollen Processing 32
2.4.2. Phytolith Processing 33
2.5. Data analysis 34
3. CHAPTER THREE- Fossil Pollen Results 35
3.1. Introduction 35
3.2. Results 35
3.2.1. Fossil Pollen 35
3.2.2. Fossil Non-Pollen Palynomorphs 37
4. CHAPTER FOUR- Modern Samples Results 46
4.1. Introduction 46
4.1.1. Modern Pollen Results 46
4.2. Non-Pollen Palynomorphs from Modern Soils 60
4.3. Modern Phytolith results 69
5. CHAPTER FIVE- DISCUSSION 83
5.1. Introduction to Discussion 83
5.2. Fossil Palynomorphs Preservation 84
5.3. Modern Climate and Vegetation 86
5.3.1. Pollen Interpretation 86
5.3.2. Non-pollen palynomorphs 87
5.4. Phytolith, Microcharcoal, and Indices 88
5.4.1. Phytolith Assemblages 88
Conclusion 91
Appendix 1 92
REFERENCES 95

Table of figures

Figure 1.1. A topographic map and cross-section extracted from (Habermann et al., 2019), showing the southern extent of the East African Rift System (EARS) and four regions of central Mozambique in which Gorongosa National Park lies.
Figure 1.2. The geological map also extracted from (Habermann et al., 2019) with different geological time scales of Gorongosa and Palaeontological localities from the lower member of the Mazamba formation.
Figure 2.1. Miocene deposit with stratigraphic layers that soil samples were collected from
Figure 2.2. Study site, Gorongosa National Park in central Mozambique.
Figure 2.3. GNP regional ecosystems with sampling sites showing samples MS-003, 005, 011, and 027 at boundaries of vegetation types.
Figure 4.1. Phytolith morphotypes from modern soil samples.
Figure 4.2. The summary of phytolith morphotypes in different biomes at GNP.
Figure 4.3. Phytolith morphotypes distribution and abundance across Gorongosa National Park.
Figure 4.4. Summary of taxa and their proportions in the different vegetation types across Gorongosa National Park.
Figure 4.5. The distribution and correlation of multivariable factors influencing the vegetation of GNP.

List of tables

Table 1.1. Mark Stalmans' Vegetation Samples in Gorongosa National Park, 2008.

Table 3.1 Fossil NPPs and their Affiliated Environments

Table 3.2. Fossil non-pollen palynomorphs groupings and possible affiliated environments following the scoring and grouping of Shumilovskikh and van Geel (2020).

Table 4.1 Pollen family and species as observed.

Table 4.2 A list of modern non-pollen palynomorphs and their affiliated environment and/or predominant behaviour.

Table 4.3 Summary of phytolith morphotypes described by Lloyd Russow.

Table 4.4 Sample data from GNP showing lithology, vegetation types and GPS localities where.

1. CHAPTER ONE- INTRODUCTION

1.1. General Introduction

The origin of our flora and fauna are of general interest as they are highly diverse, and their evolution seems to influence each other one way or the other. Modern flora has diversified and adapted to a variety of habitats, however, the Miocene is foundational for the establishment of the floras (Habermann *et al*., 2019). Generally, there is a poor Miocene record in Africa but new Miocene sites have been discovered in Gorongosa National Park (GNP); the Palaeontological Primate Project group of researchers set up to study the palaeontology of these Miocene settings in Gorongosa. This dissertation is the first to work on the pollen and phytoliths of these deposits.

1.1.1. Evolution of grasses and grasslands

The expansion of grasslands and hominid evolution in the Plio-Pleistocene are strongly correlated (Bobe and Behrensmeyer, 2003; Bobe, 2006; Bonnefille, 2010), along with faunal diversification in response to the increase of open vegetation from closed woody-dominated vegetation (Jacobs, 2004). The diversification of landscapes and ecosystems' structures and functions, house a variety of animal species, and thus add to the species richness and abundance (Carlier *et al*., 2009). The adaptability of grasses to different environments and climates remains high beginning in the Late Cretaceous with warm temperatures (Bremer, 2002; Prasad *et al*., 2005; Strömberg, 2011); and to grass-dominated ecosystems then springing up in the Cenozoic in Africa (Bobe and Behrensmeyer, 2003; Bonnefille, 2010; Strömberg, 2011) with interchanging temperatures of warm to cold and to warm again. However, there is still a gap in the woody vegetation- savannas and grassland expansion

during the Cenozoic. Nonetheless, fossil fauna can also aid and put past environments and climates into context due to the relationship fauna has with the flora. Prasad *et al*., (2005) used Gondwanatherian dinosaur coprolites ascribed to Titanosaur sauropods, as well as phytoliths and pollen from the Late Cretaceous in India; the fossil evidence provided records of C_3 Poaceae subclades already being present, along with dicotyledons, conifers, and palms. The hypsodont teeth of Titanosaurs posed a strong argument that they were grazing animals. This evidence supports the utilisation of faunal and floral relations in understanding vegetation and ecosystem dynamics; mammalian morphology and function (e.g., tooth hypsodonty for diet, size of chewing muscles, body size, and leg length), can be used to decipher grass-dominated environments (Linder, 1987; Gallaher *et al*., 2022; Prasad *et al*., 2005; Strömberg, 2011).

To comprehend how earlier habitats evolved, alternative proxies can be employed. Strömberg (2011) using atmospheric CO_2, fossil phytoliths and pollen records, and fossil macroflora (fossilised plant structures i.e., leaves, stems, reproductive structures) studied the shift from woody vegetation to open habitat grasslands on all seven continents of the Earth. Strömberg's research reveals a significant rift in the evolution of grasslands in Africa between the Late Cretaceous and the Middle Miocene; only in the Middle Miocene (between 17 and 12 Mya) did open grass-dominated habitats and potential faunal grassland taxa with C_4 grasses first appear. However, there is still a lack of fossil evidence to narrate the story of these historical events.

The disadvantage of using fossil macroflora is that grasses are greatly misrepresented as they are hard to distinguish from other monocots (Stockey, 2006). Herbaceous plants are poorly preserved, similar to pollen and phytoliths under arid, sandy soils that have been

oxidized (Berihuete-Azorin *et al*., 2023); the outer walls get warn out and become unidentifiable or it gets to the extremes of destruction of the microfossils (pollen and phytoliths) as Halbritter (1998) mentions.

Molecular evidence from the Late Cretaceous deposits in India suggests that the Poaceae family originated about 83 Mya, followed by the distinction of the subclades (Bambusoideae, Ehrhartoideae, and Pooideae= BEP; Panicoideae, Arundinoideae, Chloridoideae, Micrairoideae, Aristidoideae, and Danthonioideae= PACMAD) around 55 Mya (Prasad *et al*., 2005). The BEP grass subclade is primarily C_3 and adapted to cooler, temperate and tropical environments. At the same time, PACMAD is C_4, common in tropical and subtropical environments, and thrives in low CO_2 levels, high temperatures, and more open sunny habitats (Kellogg, 2001, Bond *et al*., 2003). The Bambusoideae (members of Bambuseae, the most primitive and an ancestor of grasses), are forest dwellers and Ehrartoideae inhabit moist open or closed habitats (Clayton, 1981; Strömberg, 2011). Clayton (1981), Lamb (1912), and Strömberg (2011) strongly suggest that the diversification and expansion of Poaceae occurred when some grasses adapted to new warm, arid habitats compared to their ancestors. Most floras from the Cretaceous-Palaeocene did inhabit wet forests or mangroves (Macphail and Hill, 2002). Sediment deposits rich in tropical forests from pollen records in Cameroon were found to have existed around 39-26 Mya, 28 Mya in northwestern Ethiopia (Bonnefille, 2010; Jacobs, 2004), and 46 Mya in northern Tanzania with some *Acacia* species (Bobe, 2006; Jacobs, 2004). Grass-dominated savanna expanded about 16 Mya in the Middle Miocene with evidence from pollen and carbon isotopes from East and West Africa (Jacobs, 2004). Tropical ecosystems are sensitive to changes in temperature, precipitation, and soil nutrient availability, as noted by Bobe (2006). Extended fluctuations in these variables can influence the structure and

functions of the ecosystem by modifying the composition of the vegetation and subsequently the fauna. As the climate got warmer and arid, tropical forests reclined and grass-dominated savannas expanded. Furthermore, environments can change as keystone species disappear. Dense woods expanded because there were fewer large terrestrial species at the end of the Mesozoic era (Wing and Sues, 1992) to browse or knock over trees similar to the behaviour of modern elephants in the savanna. However, as temperatures and humidity increased in the Palaeocene, grasses found an opportunity to advance as the canopy cover got less dense (Clayton, 1981).

In the Early Cenozoic, C_3 and C_4 photosynthetic pathways were already distinct in grasses. C_3 is the ancestral photosynthetic pathway (Edwards *et al*., 2010) that developed in rich atmospheric CO_2 environments and wet equatorial rainforests (Hopley *et al*., 2007; Polissar *et al*., 2019). On the other hand, the C_4 photosynthetic pathway has more than 30 independent origins (Sage *et al*., 2012). (Gallaher *et al*., 2022; GPWG, 2001; Scott, 2001) agree that the evolutionary process of transitioning to a C_4 photosynthetic pathway was not a one-way stream, but a series of independent convergence both within and among clades.

The shift in the photosynthetic C_3 pathway to the C_4 and CAM photosynthetic pathways is the main example of the adaptive reaction to environmental pressures, particularly to those arising out of high light intensity, temperature, and aridity (Barboni *et al*., 1999; Bremond *et al*., 2005; Cordova, 2023; Novello *et al*., 2012).

1.1.2. Introduction to Gorongosa

Gorongosa is located at the southern end of the East African Rift System (EARS) and is a 10,090 km^2 area (see fig 1.1). The existing National Park (6330 km^2) is located in central Mozambique in the southern extent of the EARS (Bobe *et al*., 2020; Habermann *et al*., 2019;

Stalmans and Beilfuss, 2008), and is separate from Mt Gorongosa. However, there are plans to extend the parks from the mountains in eastern Zimbabwe to the coast.

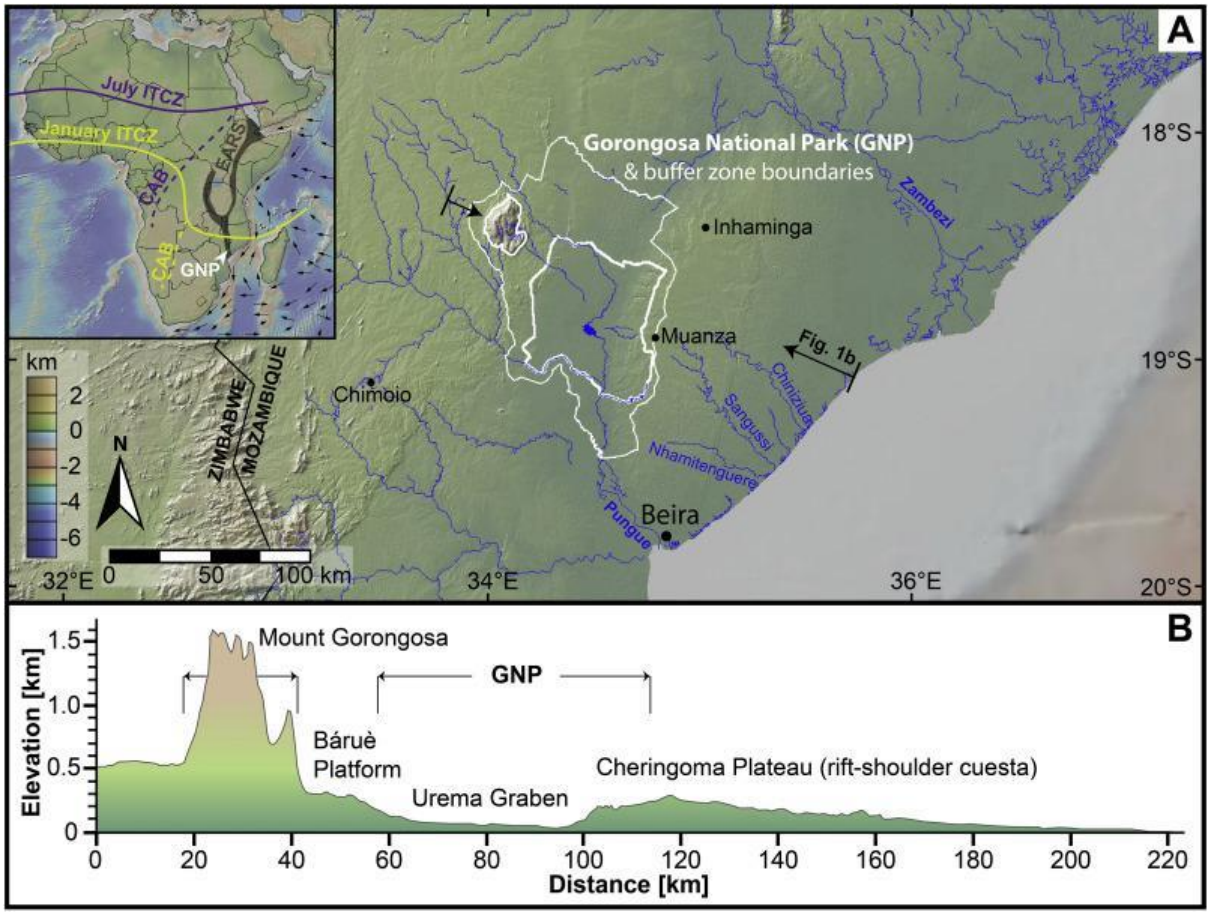


Figure 1.1. A topographic map and cross-section extracted from (Habermann *et al*., 2019), showing the southern extent of the East African Rift System (EARS) and four regions of central Mozambique in which Gorongosa National Park lies.

Muala (2016) on his Master's thesis chronologically explains how colonization and wars impacted Gorongosa landscapes and its people negatively and means put in place to restore former ecosystems of the park. The people of Gorongosa were well adapted to using ecosystem services without exploitation; there was no eminent danger to the landscapes of

Gorongosa (Muala, 2016). Gorongosa's natural landscapes did not only house the people of Mozambique but they also provided a home for the Khoisan and Bantu hunter-gatherers as they settled, and still they were not a threat to the wildlife (French, 2009; Muala, 2016). Exploitation and wars threatened the wildlife of Gorongosa and this is explained in the Civil War section below.

Tinley (1977) studied the ecosystem and diversity of the area after the Civil War, and the famous biologist, Edward O. Wilson, highlighted the incredible diversity of fauna and flora in the park, after his studies on ants, biodiversity, and conservation in the area. This awareness brought the plight of the decimated park after the Civil War to the attention of the philanthropist, Greg Carr. Today, the Gorongosa Restoration Project, funded by Carr and others, has restocked the park with game, rebuilt the infrastructure and developed a thriving research Centre at Chitengo. The park is now known for its insect, bat and primate evolutionary studies (Wilson, 2014) as well as a mosaic of different vegetation (see Tab.1, and Fig.3) types such as *palm-acacia* woodlands, *Combretum* open woodlands, Miombo woodlands, heterogeneous grasslands and many others (Bobe *et al*., 2020; Stalmans and Beilfuss, 2008).

In addition, Gorongosa has several Miocene study sites with silicified wood, marine, estuarine and terrestrial fossils (Bobe *et al*., 2023). These are the first of their kind to be discovered in Southern Africa in the EAST African Rift (Bobe *et al*., 2021; Habermann *et al*., 2019). Gorongosa National Park is also home to geological formations dating from the Cretaceous to the Eocene, and now the Miocene too (Bobe *et al*., 2021). Studies such as Bobe *et al.*, (2020) and Habermann *et al*., (2019) described the current habitat to support a

large number of non-human primates, lions, waterbuck, and wild dogs as well as other African grassland and woodland animals.

The study area, (GPL-12 - Gorongosa Palaeontological Locality number 12), falls within the lower member of the Mazamba Formation (see fig 1.2) in the southernmost extent of the Rift Valley (Steinbruch and Weise, 2014); it is also opposite GPL-1 eastward. The Mazamba Formation unconformably overlies the Eocene marine limestones of the Cheringoma Plateau (Habermann *et al*., 2019). The latter has quartzitic sandstone and greywacke (Böhme, 2005; Habermann *et al*., 2019). Soil types and textures described in detail by Böhme (2005) differ in each region. Gorongosa Mountain has base-leached soil and fine-grained acid granite. The soil in Cheringoma is heterogeneous having leached calcareous material and a sandy sesquioxide-rich quartz, with a cemented clayey subsoil containing lime. The red sandy fersiallitic soils of the Báruè Midlands have a high infiltration rate, while the Rift Valley has both fine clayey soils with high phosphorus content and coarser sandy soils from alluvial fans.

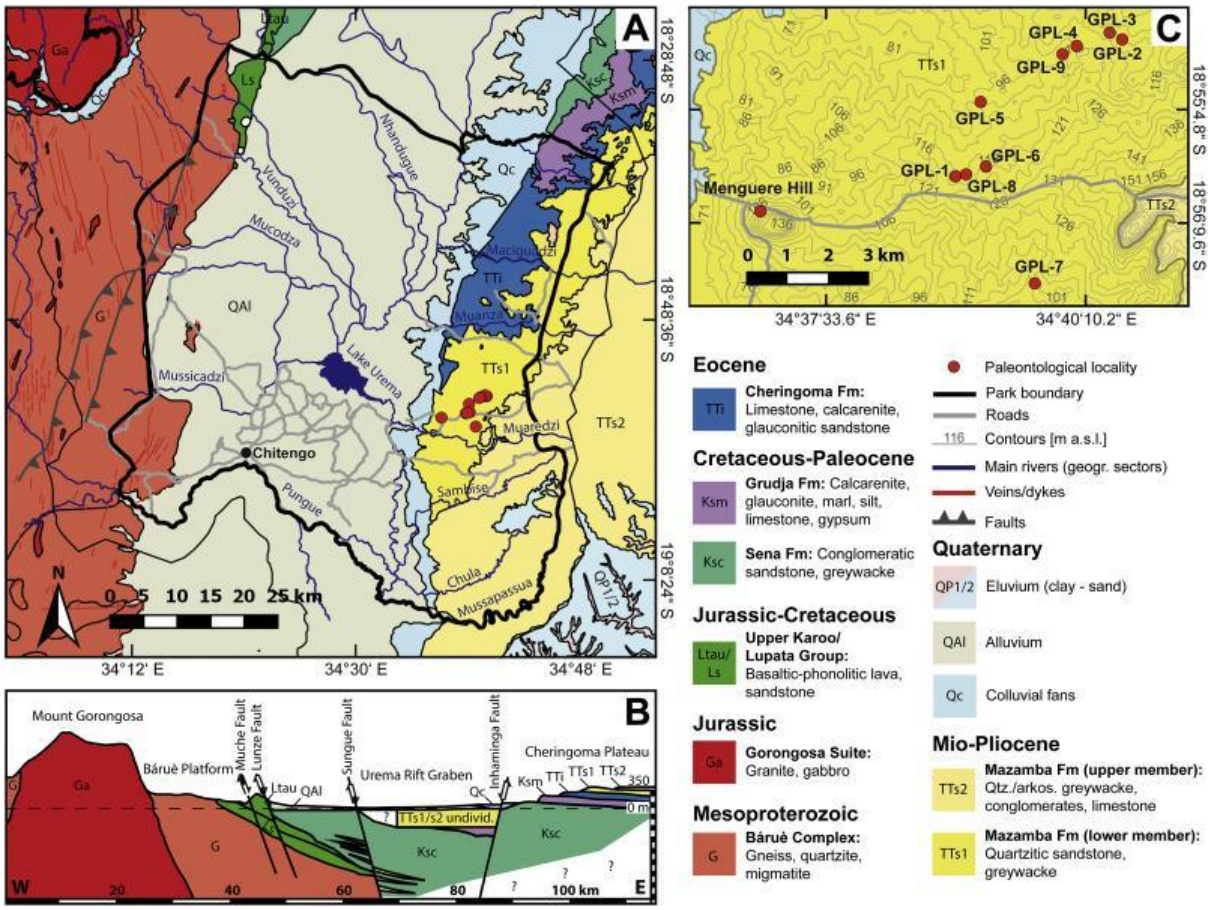


Figure 1.2. The geological map also extracted from (Habermann *et al*., 2019) with different geological time scales of Gorongosa and Palaeontological localities from the lower member of the Mazamba formation.

There is a corresponding high variety of ant communities within each region (Stalmans and Beilfuss, 2008). Stalmans and Beilfuss (2008) described the plant communities in detail. Gorongosa Mountain has lower montane grassland and woodland, montane forest, montane grassland and shrub forest. The midland region has defined moist Miombo with short open to closed pan grassland, a *Combretum* short open woodland, and closed *Acacia* woodland. There is a dry Miombo and mixed woodland with tall Miombo riverine forest, *Combretum* short open woodland. In addition, there are Alluvial and Inselberg settings with different plant communities. The Rift Valley has four different landscapes with the alluvial fan

landscape having almost a dozen plant communities. Lastly, the Cheringoma region has four landscapes with either closed humid Miombo woodland, riverine forests, or Dambo grasslands.

Lake Urema contributes more than 95% to the hydrology of the area (Böhme, 2005), and its main water sources come from the four regions of Gorongosa National Park (i.e. the Gorongosa Mountain, Báruè Platform/ Midlands, Rift valley, and the Cheringoma Plateau (see fig.1.1). Tinley (1977) added that the area of the lake can range from 10 km^2 in drier seasons to a flooding maximum of 200 km^2 as multiple rivers discharge into the lake. The monsoon circulation, having heavy rainfall seasons from December to February (Böhme, 2005), regulates the climate of the study area as well as majorly causing erosion. Gorongosa Mountain has relatively shorter drier periods receiving an average of 2000 mm rainfall per year. Cheringoma receives between 1000 mm to 1400 mm, Báruè Midlands between 800 to 1200 mm, and the Rift Valley about 600 to 800 mm (Owen, 2004).

Stalmans and Bielfuss (2008) described the different vegetation types of Gorongosa shown in Table 1 below. The co-occurence of grasses and trees (which is the definition of a savanna) is unstable and sensitive to disturbances from grazing, fires and climate variability. Moisture availability, fire frequencies, as well as herbivory (Archibald *et al*., 2012; Lehmann *et al*., 2014); mostly drive the structure and function of savannas. GNP has a variety of grasslands. According to Stalmans' records, the grass subfamily Panicoideae appeared to be the most dominant in all the different types of grasslands. Will phytolith records of modern vegetation show us a similar concept or a different one?

1.1.3. The Civil War

Although amid repair, the park underwent severe ecological and biological deterioration in the 1900s because of the wars that followed from 1969 until 1992 (Pringle and Gonçalves, 2022; Tinley, 1977). There was Mozambique's War of Independence from Portuguese colonialism in 1969, with the park serving as a focal point for battle; poachers had also put the park's animals in jeopardy. The Civil War against the newly independent government took place from 1977 to 1992, five years after the struggle for independence (Pringle and Gonçalves, 2022). Tinley (1977) conducted a wildlife survey and found that while some animals, like the black and white rhinos, had vanished entirely from the park, others, like elephants, hippos, and buffalos, were still surviving. However, after the Civil War, the park's wildlife nearly disappeared, with more than 90% of the species that had been present disintegrating (Pringle and Gonçalves, 2022). The conflict not only affected the park's fauna but also its landscape, which was linked to the significant reduction in the number of mammal species there (Pringle and Gonçalves, 2022). Daskin *et al*., (2016) used satellite imagery from 1977 and 2012 at high resolution and found the woody vegetation to have increased widely in the park by 34% and up to 96% in the Rift Valley savannas. Guyton *et al*., (2020) and Herrero *et al*., (2020) have identified the woody plants to be composed of mostly *Mimosa pigra*- a highly invasive woody plant proliferating floodplains and wetlands. Using the Normalised Difference Vegetation Index (NDVI), Herrero *et al*., (2020) recorded *Mimosa pigra* to have spread throughout the tropical forests as well as to have reduced the abundance of riparian forests in the park.

1.2. Literature Review

1.2.1. Palaeontological background

Martin Pickford discovered the Menguere Hill fossil wood site in 2011 and Marion Bamford (Pickford, 2012) identified the wood. In 2016, the newly established research team PPP-G (Palaeo Primate Project – Gorongosa) led by Profs Susana Carvalho and Rene Bobe (Oxford University) and funded by their university and the GRP (Gorongosa Restoration Project), began their first field season to explore the rest of the park for fossil deposits. At the end of the second field season, they found the rich site, called GPL-12, along a stream cutting in the Miombo woodland, 3 km from Menguere Hill. From the third field season excavations focused on this site and a variety of early to middle Miocene fauna has been discovered (Bobe *et al*., 2020) including extinct terrestrial fauna, brackish and marine fauna (bivalves, crustaceans, gastropods, and foraminifera). Habermann *et al*., (2019) postulated that Gorongosa was much closer to the sea in the past and perhaps the site was an estuary. The woods from Menguere Hill show that the woody vegetation was mixed woodland around a pan (Bamford and Pickford, 2021). Bobe *et al*., (2021) found palms that represent the humid and hot lowlands of tropical Africa. Recently, Bobe and team published a study including the first dentognathic specimens of fossil vertebrates belonging to tiger sharks from the Miocene-aged Mazamba formation (Bobe *et al*., 2023). The most abundant plant species implied tropical environments, but there is still a question of what was the environment closely associated with the fossil deposit.

Neumann and Bamford (2015) reviewed the older biomes of southern Africa and showed that the Miocene woodland vegetation of southern Africa was shifting to more open savanna when C_4 grasslands were spreading. Much of this research for environmental reconstruction

is based on pollen and phytolith records, therefore, this is the logical approach to studying the environment of this rare middle Miocene deposit.

Both Roberts *et al*., (2011) and Sciscio *et al*., (2013) studied earlier Miocene palynomorphs in Langebaanweg West Coast in Western Cape, South Africa, and found tropical/subtropical climate represented by high percentages of Podocarpus pollen and palm trees. Working with a 33-metre deposit, at a depth of 33-30 m (Sciscio *et al*., 2013) traced a decline in aquatic plants, algae, Restionaceae and *Tricolporopollenites* indicating a decrease in groundwater level allowing Podocarps to be abundant. Poaceae was recorded to be very well established during this time with C_4 grasslands spreading (Neumann and Bamford, 2015). The overall vegetation ranged from subtropical/tropical forests to a drier climate determined by very low Restionaceae and Ericaceae counts, and finally to an increase in marine environments indicated by a high dinoflagellate count at about 8-6 metres (Sciscio *et al*., 2013). Roberts *et al*., (2013) made another study in Rondeberg Western Cape, South Africa, and found the palynomorphs, also advocated by Podocarpus lignified fossil wood to be in correspondence with those from Langebaanweg. Overall, the vegetation had a diverse range of plant communities as it ranged from forests to shrubs, ferns, and fynbos (Roberts *et al*., 2011; 2013) and sea-level and currents had some influence on the vegetation (Fitchett and Bamford, 2017; Steinbruch and Weise, 2014).

Pollen and spores are resistant microscopic parts of plants that are often preserved in lacustrine environments (Neumann *et al*., 2008). However, when dried or in varying water levels they can be affected by oxidation and this makes them difficult to identify (Neumann and Bamford, 2015), thus lowering the pollen count of important plant species that would be a significant contribution to the reconstruction of palaeoclimates. Nevertheless, since

they are abundant and unique for each plant species, their recovery and identification mean that the plants that produced them can be identified (of those that are not weathered and broken). In addition, the distribution of vegetation is controlled by moisture, temperature and soils (Fitchett and Bamford, 2017; Scott and Neumann, 2018), therefore by identifying the vegetation, we can determine the environment and climate in which the plants grew. In a diverse flora (vegetation), the reconstruction from the pollen can be complex because not all pollens and spores are deposited close by, some are transported by wind and some are not as abundant as others (i.e. wind-pollinated plants produce lots of light and easily dispersed pollen while insect-pollinated plants produce fewer and heavier pollen grains). Bearing these facts in mind, it is important to understand the pollen record that we can expect from certain vegetation types. This will be the fidelity of the pollen record.

1.2.2. Phytolith records

Most early studies in South Africa paired fossil phytolith data with carbon isotopes from the fossil tooth enamel to compare diet and grassland expansion during the Miocene, intending to reconstruct the palaeoenvironment. Phytolith records from the southern west coast of South Africa's fossil soil deposits alluded to C_3 grasses still prevailing in the Miocene (Rossouw *et al*., 2009). The study recorded an expansion of C_4 grassland and a decline of woody dicots in C_3 grass dominated ecosystems. In other parts of East Africa, the carbon 13 isotope showed that the C_3 diet ceased to be dominant in the Late Miocene in most faunas (i.e., Elephantidae, Suidae, Sivatherium, Equidae, and Hippopotamidae), with the C_4 diet being most dominant (Ségalen *et al*., 2007). Few records in Southern Africa show a C_3 diet in the Early Miocene, a mixed diet of C_4 grasses in the Pliocene, and no record for the Middle-Late Miocene (Hopely *et al*., 2019; Stynder, 2011).

Although the fossil phytolith record from the African Miocene is poor, recent dates of about 80,000 years have a positive track record on phytolith significance to understanding past environments. Important Southern African examples are the Tsodilo Hills in Botswana, the Border Cave in South Africa, and the Sibudu Cave in KwaZulu-Natal. For example, at Tsodilo Hills, climate change has resulted in a shift from forests to grasslands throughout the previous 20,000 years, as reported by Geppert *et al*. (2021). Simultaneously, Geppert *et al*., (2021) demonstrated, based on phytolith evidence discovered at this location that a transition from wooded to open settings occurred during the late Pleistocene, coinciding with periods of fluctuating climate. Changes in forest-grassland throughout time in Sibudu Cave also reflect a complicated interaction between human adaption techniques and moisture levels (Wadley *et al*., 2004).

These results demonstrate how useful phytolith research is for understanding the climatic and ecological circumstances of human evolution and adaptation in southern Africa, as well as for recreating historical environments. Researchers can produce thorough reconstructions of past landscapes by combining phytolith data with other paleoenvironmental proxies, such as pollen, stable isotopes, and archaeological evidence. These simulations teach us important lessons about possible future environmental reactions to ongoing climate change in addition to previous ecosystems.

Table 1.1. Mark Stalmans' Vegetation Samples in Gorongosa National Park, 2008

Vegetation type	**Grass species**	**Tree species**	**other**
Low Dambo Grassland	*Setaria sphacelata- P*	*Combretum adegonium*	*Sesbania sp.*
	Loudetia- P	*Syzygium*	
	Trachypogon spicatus-P	*Julbernadia*	
	Schizachyrium- P	*Piliostigma thonningii*	
	Digitaria eriantha- P		
Short Open to Closed Pan Grassland	*Paspalidium obtusifolium- P*	*Hyphaene petersiana*	*Water lily*
	Echinochloa sp. - P		*Pistia stratiodes*
	Oryza longistaminata- O		
	Hemarthria altissima- P		
Tall *Echinochloa- Vetiveria* Floodplain Grassland	*Echinochloa- P*		
	Vetiveria- P		
Tall *Setaria* Floodplain Grassland	*Setaria incrassata- P*	*Combretum imberbe*	
	Panicum maximum- P	*Hyphaene*	
	Cynodon dactylon- C	*Acacia sieberana*	
	Vetiveria nigritana- P	*Acacia xanthophloea*	
	Echinochloa- P	*Faidherbia albida*	
		Philenoptera violacea	
		Piliostigma thonningii	
Cynodon dactylon- Digitaria swazilandensis Low Grassland	*Cynodon dactylon- C*	*Mimosa pigra*	*Sesbania sp.*

	Digitaria swazilandensis- P		
Open to Closed Tall *Hyphaene* and *Borassus* Palm veld	*Setaria incrassata- P*	*Hyphaene petersiana*	*Phoenix reclinata*
	Panicum maximum- P	*Borassus aethiopium*	
	Vetiveria nigritana- P	*Philenoptera violacea*	
	Hyparrhenia sp.- P	*Combretum adenogonium*	
		Acacia sieberana	
Colophosspermum mopane Tall Closed Woodland	*Panicum maximum- P*	*Colophosspermum mopane*	
	Digitaria eriantha- P	*cf. Boscia foetida*	
	Chloris sp. - C		
Piliostigma thonningii – Borassus aethiopium Closed Woodland/ Dry Forest	*Panicum maximum- P*	*Piliostigma thonningii*	Acanthaceous forbs
	Oplismenus sp. - P	*Borassus aethiopium*	
	Pennisetum purpureum - P	*Tabernamontana*	
		Hyphaene petersiana	
		Annona senegalensis	
Dichrostachys cinerea Tall/High Closed Shrubland	*Panicum maximum- P*	*Dichrostachys cinerea*	
	Brachiaria deflexa - P		
Dalbergia melanoxylon Low Closed Woodland	*Panicum maximum- P*	*Dalbergia melanoxylon*	
	Heteropogon contortus - P	*Ziziphus mucronata*	

	Aristada sp. - A	*Spiristachys africana*	
	Sporobolus sp. - P	*Acacia nigrescens*	
		Dichrostachys cinerea	
		Sclerocarya birrea	
		Combretum imberbe	
		Commpihera sp.	
Acacia xanthophloea Open to Closed Tall Woodland	*Panicum maximum- P*	*Acacia xanthophloea*	*Mimosa pigra*
	Setaria incrassata- P	*Hyphaene*	
	Cynodon dactylon- C	*Faidherbia*	
Faidherbia albida Open to Closed Tall Woodland	*Cynodon dactylon- C*	*Faidherbia albida*	
	Digitaria swazilandensis- P	*Acacia xanthophloea*	
	Echinochloa- P	*Hyphaene*	
Sparse/ Open *Acacia* Woodland with Saline Grassland	*Panicum maximum- P*	*Acacia robusta*	
	Panicum coloratum- P	*Acacia nigrescens*	
	Sporobolus iocladus - P	*Boscia salicifolia*	
	Urochloa mossambicensis - P	*Ziziphus mucronata*	
	Dactyloctenium- C	*Salvadora persica*	
		Maerua angolensis	
		Capparis sp.	
Acacia - Combretum Open to Closed Short to Tall Woodland	*Panicum maximum- P*	*Combretum adenogonium*	
	Digitaria eriantha- P	*Combretum imberbe*	

	Heteropogon contortus - P	*Acacia nigrescens*	
	Themeda triandra - P	*Acacia cf. robusta*	
	Urochloa mossambicensis - P	*Sclerocarya birrea*	
		Dalbergia melanoxylon	
		Philenoptera violacea	
		Ziziphus mucronata	
Short to Tall Dry Forest and Thicket	*Brachia deflexa - P*	*Cleistochlamys kirkii*	
	Digitaria sp. - P	*Diospyros senesis*	
	Oplismenus sp. - P	*Craibia zimmermannii*	
		Alchornea laxiflora	
		Milletia stuhlmannii	
		Markhamia acuminata	
		Capparis sp.	
		Thilachium africannum	
		Sclerocarya birrea	
Combretum Short Open Woodland in Miombo	*Digitaria eriantha- P*	*Combretum adenogonium*	
	Panicum maximum- P	*Diplorynchus condylocarpon*	
	Heteropogon contortus - P	*Acacia nigrescens*	
	Diheteropogon amplectens- P	*Crossopteryx febrifuga*	
	Loudetia simplex - P	*Lannea stuhlmannii*	

	Pogonarthria squarrosa - C	*Garcinia livingstonei*	
	Rottboellia exaltata- P		
	Hyparrhenia spp.- P		
Tall to High Limestone Gorge Forest		*Khaya anthotheca*	
		Antiaris toxicaria	
		Breobadia salicina	
		Craibia zimmermannii	
		Mimusops sp.	
		Croton sp.	
		Euphorbia sp.	
		Androstachys johnsonii	
Tall Miombo Riverine Forest	*Oplismenus sp. - P*	*Breobadia salicina*	
	Panicum maximum- P	*Khaya anthotheca*	
		Sterculia appendiculata	
		Bombax rhodognaphalon	
		Phoenix reclinata	
		Rinorea elleptica	
		Furtumia africana	
		Brachystegia boehmii	
Tall Closed Miombo- *Acacia nigrescens* woodland	*Panicum maximum- P*	*Brachystegia boehmii*	
	Digitaria eriantha- P	*Julbernadia globiflora*	
	Themeda triandra- P	*Acacia nigrescens*	
	Sporobolous sp.- P	*Diplorynchus condylocarpon*	

		Sterculia quinqueloba	
		Strychnos potatorum	
		Pterocarpus rotundifolius	
Tall Closed Humid Miombo Woodland	*Digitaria eriantha- P*	*Brachystegia spiciformis*	*Platycerium sp.*
	Themeda triandra- P	*Brachystegia tamarindoides*	Ferns
	Oplismenus sp. - P	*Milletia stuhlmannii*	
		Sideroxylon imerme	
Short Open to Closed *Acacia- Combretum-Milletia* Woodland	*Urochloa mossambicensis - P*	*Milletia stuhlmannii*	
	Heteropogon contortus - P	*Acacia nigrescens*	
	Panicum maximum- P	*Combretum adenogonium*	
	Digitaria eriantha- P	*Boscia salicifolia*	
	Themeda triandra- P	*Adansonia digitata*	
	Eragrostis rigidior- C		
	Andropogon gayanus- P		

Note- A= Aristidoideae, C= Chloridoideae, O= Oryzoideae, P= Panicoideae grass subfamilies

Fires are important to the maintenance of the African savanna landscapes (van Wilgen *et al*., 2000). Archibald *et al*, (2012) mentioned the use of fire across Africa to have been at its peak in 40 000 B.P especially in drier cold seasons, depleting most woody plants and thus leading to an expansion of grasslands (see also Lehmann *et al*, 2014). A publication by McWethy *et al*, (2016) reconstructed the Gorongosa palaeoenvironment from the Late Pleistocene to the Holocene, having records of vegetation dynamics from 27,000 years ago until the present. (McWerthy *et al*., 2016) extracted a peat core for palynological studies; the records showed climatic impacts such as warmer temperatures to have sustained subtropical forests with Podocarpus, and Ericaceae vegetation thriving, however, the increasing temperatures led to an expansion of grassland. Overall, moisture and biofuel content in an ecosystem can control how much fires affect tree density (van Wilgen et al., 200). Hence, this study uses phytoliths to determine the aridity index and moisture context and microcharcoal to know the fire regime of Gorongosa in the modern landscapes. Breman *et al*., (2019) and Bremond (2008) used phytolith indices 1) the Broadleaf index that compared dicots globular granulate with short cell Poaceae for overall shaded vs non-shaded vegetation, 2) the Aridity index to measure the drought tolerance vs resistance. They also used, 3) Climatic index to distinguish between C3 and C4 pathways, 4) Water stress index to deduce water availability and lastly, 5) I_c which tests grass cover dominancy.

1.3. Aims and Objectives

Based on research carried out by other researchers, as outlined in the section above, it can be assumed that the vegetation of an area is controlled by several factors: climate, soils, hydrology, topography and external factors such as grazing, fire, human influence and catastrophes (volcanic eruptions, major floods, sea-level fluctuations, etc). Based on data of

modern vegetation types and the local climate, we can relate the species diversity to the local climate tolerances (Utescher *et al*., 2007). If the composition of the fossil plants can be identified, and compared with the modern sets, it is possible to reconstruct the vegetation type and climate of the fossil deposit. For the Gorongosa fossil deposit, some fossil woods have been identified. The fauna gives a mixed signature of estuarine, coastal and inland fauna (check this). Another proxy for the vegetation and climate is the micro-fossil record, namely pollen and phytoliths.

There are two aims of this research project, the first aim is to reconstruct the vegetation and climate of the Early Miocene fossil deposit using the micro-fossil record of pollen, phytoliths and charcoal from GPL-12. The second aim is to improve the interpretation of the findings by testing the fidelity (taphonomic bias) of the modern pollen, phytolith, and micro-charcoal remains recorded in the soils of the known vegetation types in the park.

Objectives

In order to accomplish the aims the objectives of the project are to

a. Collect samples from the various strata exposed in the excavations at GPL-12 for fossil micro-remains analyses
b. Identify and quantify the micro-fossils and reconstruct the past vegetation with reference of modern micro-remains collected from modern soils
c. Infer the climate from the proxies
d. Collect soil samples of pollen, phytoliths and micro-charcoal from modern soils,
e. Map the local vegetation for each sample site
f. Compare the results of the macro- and micro- components, i.e, test the fidelity of the potential fossil record in the modern soils

g. Use the modern record to help interpret the fossil record

2. CHAPTER TWO- MATERIALS AND METHODS

2.1. Introduction

This section elaborates on the processes of extracting microremains from fossil sediments and modern soils. The softwares used to generate the data are also discussed.

2.2. Fossil Sampling

At the GPL-12 open excavation, 14 sediment samples were taken from the profile with a spatula after cleaning the surface. These samples (about 50-100g) were placed in clean, labelled ziplock bags. Sediment samples were collected from the fossil strata exposed in the 2022 excavation at GPL-12 by Prof Bamford. The layers were labelled B1-B14.

Miocene Sediment Descriptions

- **B1-** top of GPL-12 just below modern soil. Grey clay.
- **B2-** collected about 40cm below B1. Light brown clay with some grey.
- **B3-** brown sandy clay.
- **B4-** red band, clay.
- **B5-** grey clay.
- **B6-** brown clay.
- **B7-** grey clay.
- **B8-** brown clay.
- **B9-** some red with carbonate layer.
- **B10-** brown clay.

- **B11-** a mixture of grey and brown sandy clay.
- **B12-** grey brown sandy clay.
- **B13-** red-grey clay with fossils.
- **B14-** red sandy lenses with a large pelvis or rib.



Figure 2.1. Miocene deposit with stratigraphic layers which sediment samples were collected from. (Image credits: Prof Marion Bamford)

2.3. Modern Sampling

In August 2022, Prof Bamford collected 26 modern soil samples from a variety of vegetation types in the GNP. At each site, the surrounding vegetation was recorded. Surface soil and mulch were scraped away, and a clean spatula was used to excavate about 50-100g of soil at a depth of 5cm below the surface. Soils were placed in clean, labelled ziplock plastic bags. Pollen and phytoliths were extracted from these samples, and the processes are explained below.

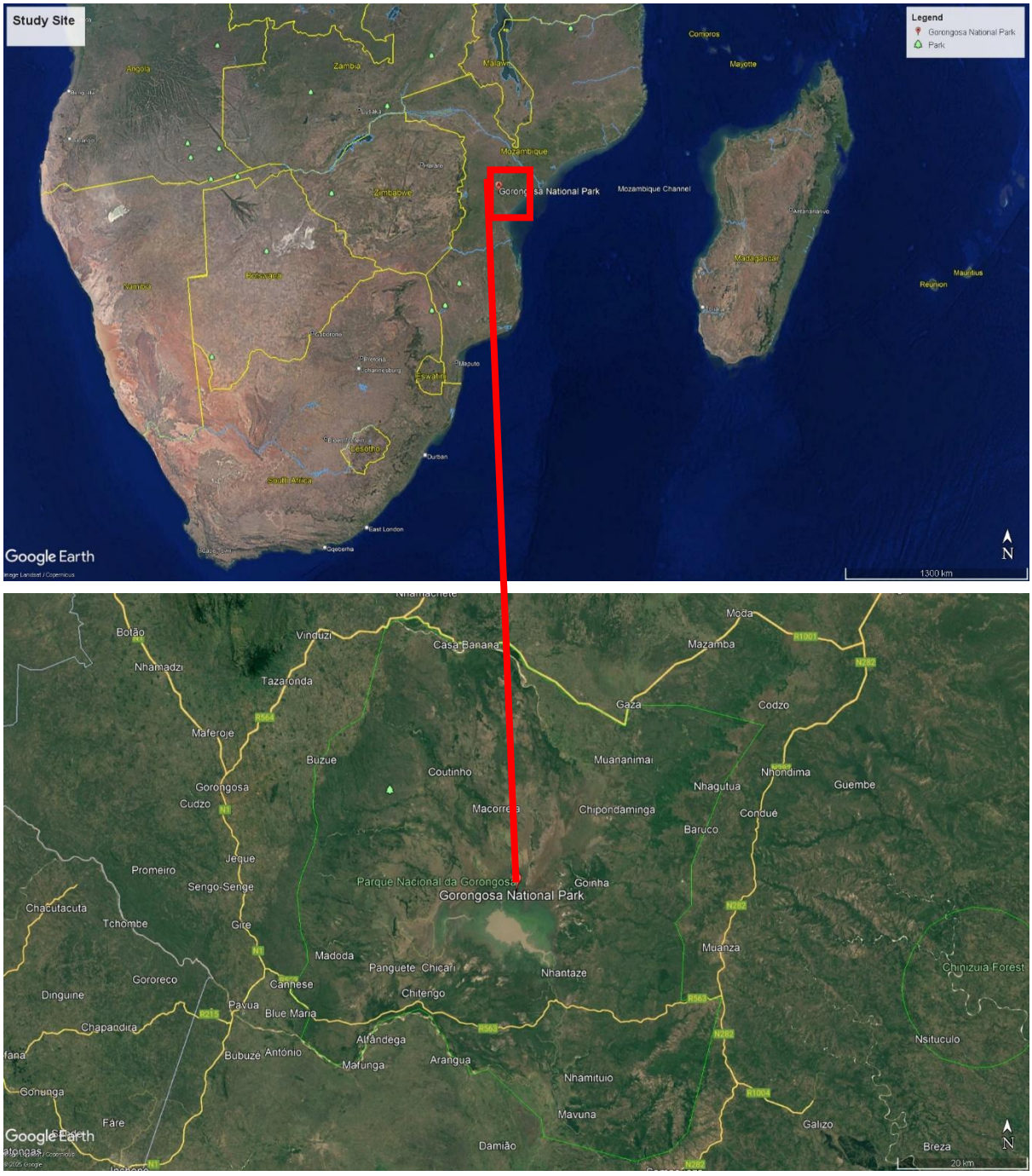


Figure 2.2. Study site, Gorongosa National Park in central Mozambique.

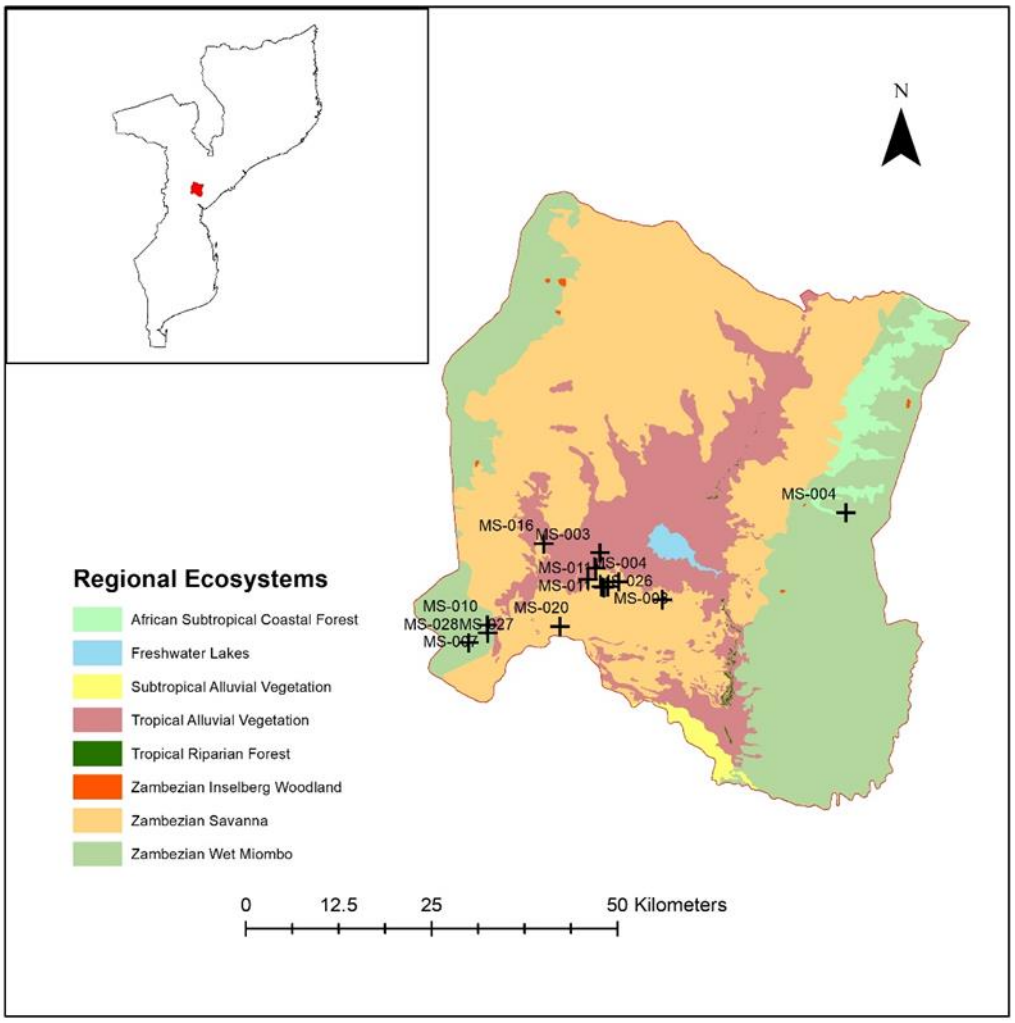


Figure 2.3. GNP regional ecosystems with sampling sites showing samples MS-003, 005, 011, and 027 at boundaries of vegetation types.

2.4. Laboratory method

2.4.1. Pollen Processing

The pollen samples for both fossil sediments and modern soils were processed in the palynology laboratory at the University of the Witwatersrand at the Evolutionary Studies Institute (ESI). Using the standard method following Faegri *et al*., (1989), which involves acid treatment with HF to destroy silicates, HCl to remove carbonates, acetolysis for the

removal of organics such as cellulose, and finally heavy mineral separation with a $ZNCl_2$ solution and centrifuging (Wood *et al*. 1996). Slides were mounted in a permanent mountant (glycerol).

An Olympus BX51 light microscope was used to identify and count a minimum of 300 pollen grains per sample pollen at X400 magnification. Pollen references were obtained from peer-reviewed from Southern Africa.

2.4.2. Phytolith Processing

Phytolith analysis for both fossil sediments and modern soils followed the standard procedures of Albert *et al*., (1999), Albert and Weiner (2001), and Kealhofer and Piperno (1998). Ms Prosper Bande and I weighed 1g of each soil sample and treated it with 3N HCl and 3 N HNO3 suspended in boiling water for 30 minutes. We did this to get rid of carbonates and phosphates. For sample acid wash, we transferred the sample to a 15 ml polypropylene centrifuge tube, filled it up with distilled water and centrifuged at 3000 rpm for 5 minutes. Each time before centrifugation, the samples passed through a shaker to stop soil particles from adhering to each other, thus washing the samples thoroughly. The centrifugation was repeated 3 times. The next step was to destroy organic components; to do this; we poured 10 ml of 30% hydrogen peroxide, and placed the sample in 70˚C water on a hot plate. The sample were dried and ready for the heavy liquid separation. Albert *et al*., (1999) calls the remainder the insoluble fraction of inorganic acid (AIF).

Again, in a 15 ml polypropylene centrifuge tube with the AIF, 5 ml of sodium polytungstate solution with a density of 2.4 g/ml was added to concentrate the phytoliths. To mix the contents well, each samples passed through the shaker and centrifuged again at 3000 rpm for 5 minutes. There was a floating fraction that was transferred into a second 15 ml tube

and the fraction that remained was transferred into a 1.5 ml Eppendorf vial. Into the 15 ml tube with the floating fraction, 1 ml of distilled water was added using a precision pipette. We centrifuged again. A second fraction of the floating substance was transferred into another 15 ml tube, with the remainder deposited into another 1.5 ml vial. The light fraction was centrifuged 3 times and each time we added distilled water up to the 14 ml mark to rinse off the heavy liquid. The samples were then dried in an oven at 50˚C. After drying they were combined with glycerol, and the suspension was covered with a cover slip. An Olympus BX51 light microscope was used to count and photograph a minimum of 450 phytolith morphotypes per sample at X400 magnification. Phytolith references were obtained from peer-reviewed from Southern Africa (Barboni and Bremond 2009; Lloyd Russow doctoral thesis, 2009; Murungi doctoral thesis, 2017).

The following equations were used for phytolith indices (Bremond et al., 2005; Cordova, 2023):

DP index= Sum of spheroid phytoliths/Sum of all GSSC

Panicoid index= All Panicoideae phytoliths/ Panicoideae + Chloridoideae GSSC

Water-stress index= bulliform flabellates/ Sum of all GSSC- elongates

2.5. Data analysis

The software program used was R-Studio and python to get PCA values and other graphs for the phytolith variables. ChatGPT was used to assist with generating codes and working on scripts when errors were encountered during coding.

3. CHAPTER THREE- Fossil Pollen Results

3.1. Introduction

This chapter discusses the pollen and non-pollen palynomorphs outcomes from the fossil sediment samples taken from the Miocene profile at GPL-12.

3.2. Results

3.2.1. Fossil Pollen

There are no phytolith or pollen results from the fossil sediment samples except for B8 and 13. B8 layer produced four Poaceae fossil pollen grains, cf. Convolvulaceae, and cf. Aquifoliaceae (see fig.4). The B13 layer produced an unidentifiable pollen grain; however, they are insufficient to quantify a pollen analysis for these layers. Overall, we got negative results from the fossil deposit. Microcharcoal (both <100 µm and >100 µm) occurred in B8 and B13.

Layers B3, B4, B8, and B13 produced some identifiable and reliable non-pollen palynomorphs.

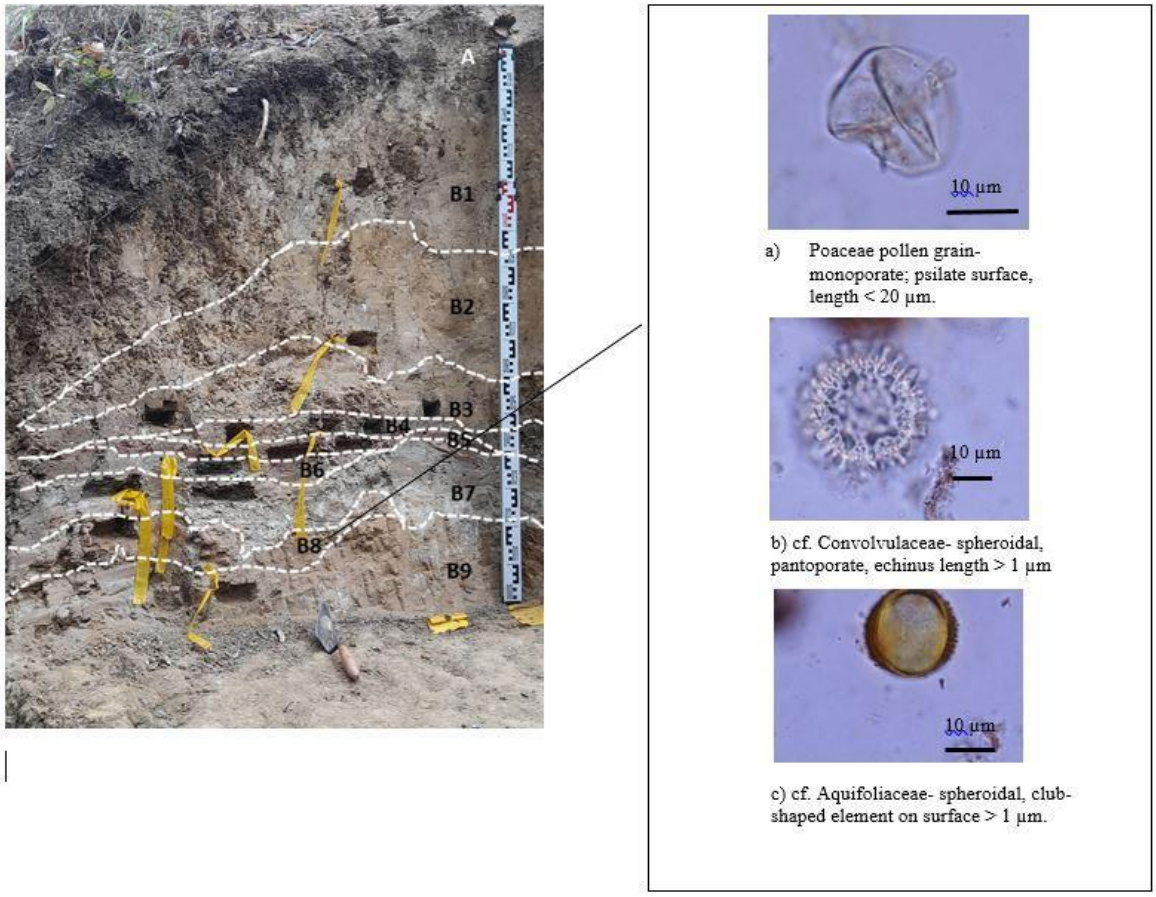


Figure 3.1. Fossil pollen from layers B8 A: a) Poaceae, b) cf. Convolvulaceae, and c) cf. Aquifoliaceae.

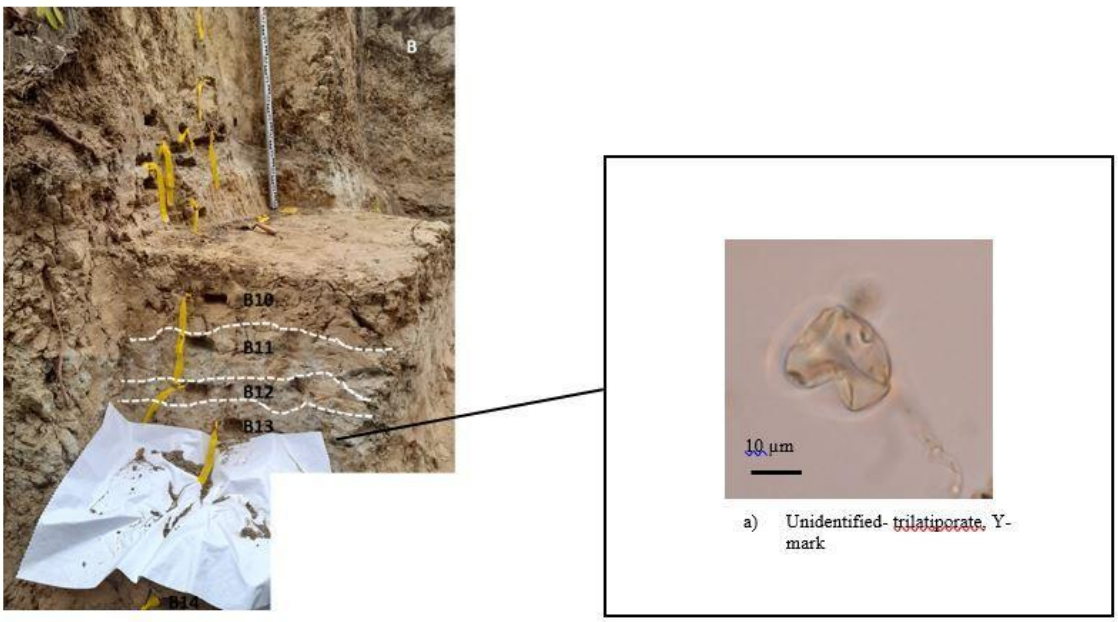


Figure 3.2. Fossil pollen from layer B13 with B: a) unidentified pollen grain respectively.

3.2.2. Fossil Non-Pollen Palynomorphs

Table 3.1 Fossil NPPs and their Affiliated Environments

Species	**Plate**	**Affiliated environment and/or behaviour**
Diporotheca sp.	I, a	Eutrophic/mesotrophic environments
Glomus type	I, b-c	Erosion and mycorrhizal relations
cf. *Iodamoeba* cyst	I, d-e	Megafauna intestines
cf. *Mangrovia hallii*	I, f	Mangrove swamps and algal mats
Sporormiella type	I, h	Coprophilous fungi
Aff. *Tomentella* type	III, c-e	Shallow stagnant water
Unknown fungal remains	I, i-k	Unknown
Unknown NPPs	I, g; II, a-i; III, f-l	Possible aquatic environments
Ustilina deusta	II, j	Rust fungi

Plate 1

***Diporotheca* sp.** (Plate 1, a) - brown fungi with anastomosing ribs (van Geel *et al*., 2011). Size is ~35 µm.

Habitat: Occurs in eutrophic to mesotrophic environments (van Geel *et al*., 2011).

***Glomus* type** (Plate 1, b-c) - ranges from 18-138 µm and can be with or without hyphal attachment in slides.

Habitat: First recorded with the melting of the Wisconsin ice (van Geel, 2001); thrives in erosive environments—and indicates mycorrhizal relationships in peat deposits and the presence of some of *Betula* species (Kołaczek *et al*., 2013; van Geel, 2001).

cf. *Iodamoeba* cyst (Plate 1, d-e) **–** a very small palaeoparasite (Camacho *et al*., 2020) ranging between 5 and 20 µm.

Habitat: Found in the intestines of mammals.

cf. *Mangrovia hallii* A. Kumar, sp. nov. (Plate 1, f) – flask-shaped greyish shell (Kumar, 2023). Length of shell >40 µm. The body is almost rectangular.

Habitat: Occurs in mangrove swamps and algal mat environments.

Unknown remains (Plate 1, g) – longer than 45 µm.

***Sporormiella* type- Type HdV-113** (Plate 1, h) – fungal spore almost 20 µm in diameter. Spherical with a slit at the equator.

Habitat: Inhabits dung of megafauna in fossil sediments (Davis and Shafer, 2006) and livestock dung in the Holocene (Van Geel *et al*., 2011).

Unknown fungal remains (Plate 1, i-k) – i- dark brown monoseptate, psilate body and crenate margin and terminal lobes.

j- A tomato-shaped fungal spore, size >40 µm.

k- Psilate surface, multiseptate.

Plate 2

Unknown NPPs (Plate 2, a-d) – a- bean-shaped micro remains ~10 µm.

b- Mushroom-shaped light brown micro remains.

c- Light brown-yellowish multiseptate corn-shaped NPP.

d- Complex morphology, possible fungi.

Unknown cyst (Plate 2, e) – very large yellowish and spherical. Diameter >100 µm.

Unknown fungal spores (Plate 2, f-h) – f- spheroidal with echinus, size >20 µm.

g- Brown, monoseptate and crenate margin. Psilate body with flat ends.

h- Multiseptate fungi with a slit at the equator.

Unknown cluster (Plate 2, i) – clustered remains with more than six individuals in each group.

***Ustulina deusta*, ascospores** (Plate 2, j) - very small monocolpate fungi and <10 µm in size. Brown to dark brown.

Habitat: mild parasite causing soft rot of wood in northwest Europe temperate species such as *Salix*, *Acer*, and Oak (van Geel, 2001). In Africa, these species require cooler and wetter conditions.

Plate 3

Possible dinocysts (Plate 3, a-b) **–** Spherical with centric openings, about 40 µm in diameter.

Aff. *Tomentella* type (Plate 3, c-e) – spherical psilate or ornamented. Body size between 8-15 µm. Very thin and long echinus.

Habitat: Stagnant and shallow open water (Halbwachs *et al*., 2021).

Unknown (Plate 3, f-l) – f- triangular-shaped pore and infolds creating a colpus.

g- saccate spheroid <20 µm.

h- pentagon-ish shape and monocolpate at the centre.

i-j- spheroidal with undulating margin.

k- possible shell for aquatic microorganisms.

l- elliptic shape, >20 µm.

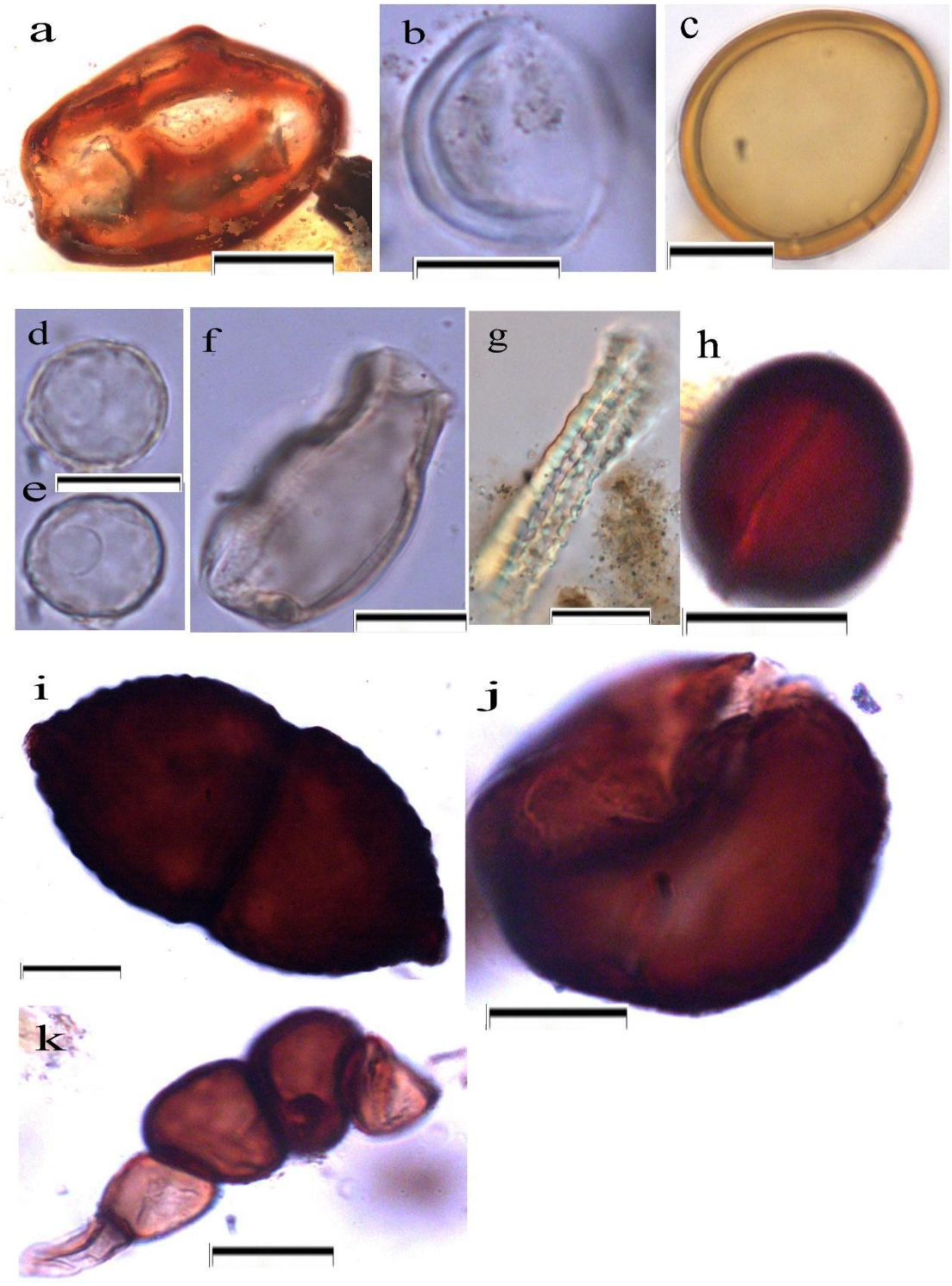


Plate 1. a: *Diporotheca* sp.; b-c: *Glomus* type; d-e: cf. *Iodamoeba* cyst; f: cf. *Mangrovia hallii;* g: possible invertebrate remains; h: *Sporomiella* type- Type HdV-113; i-k: unknown fungal spores. Scale bar = 10 µm

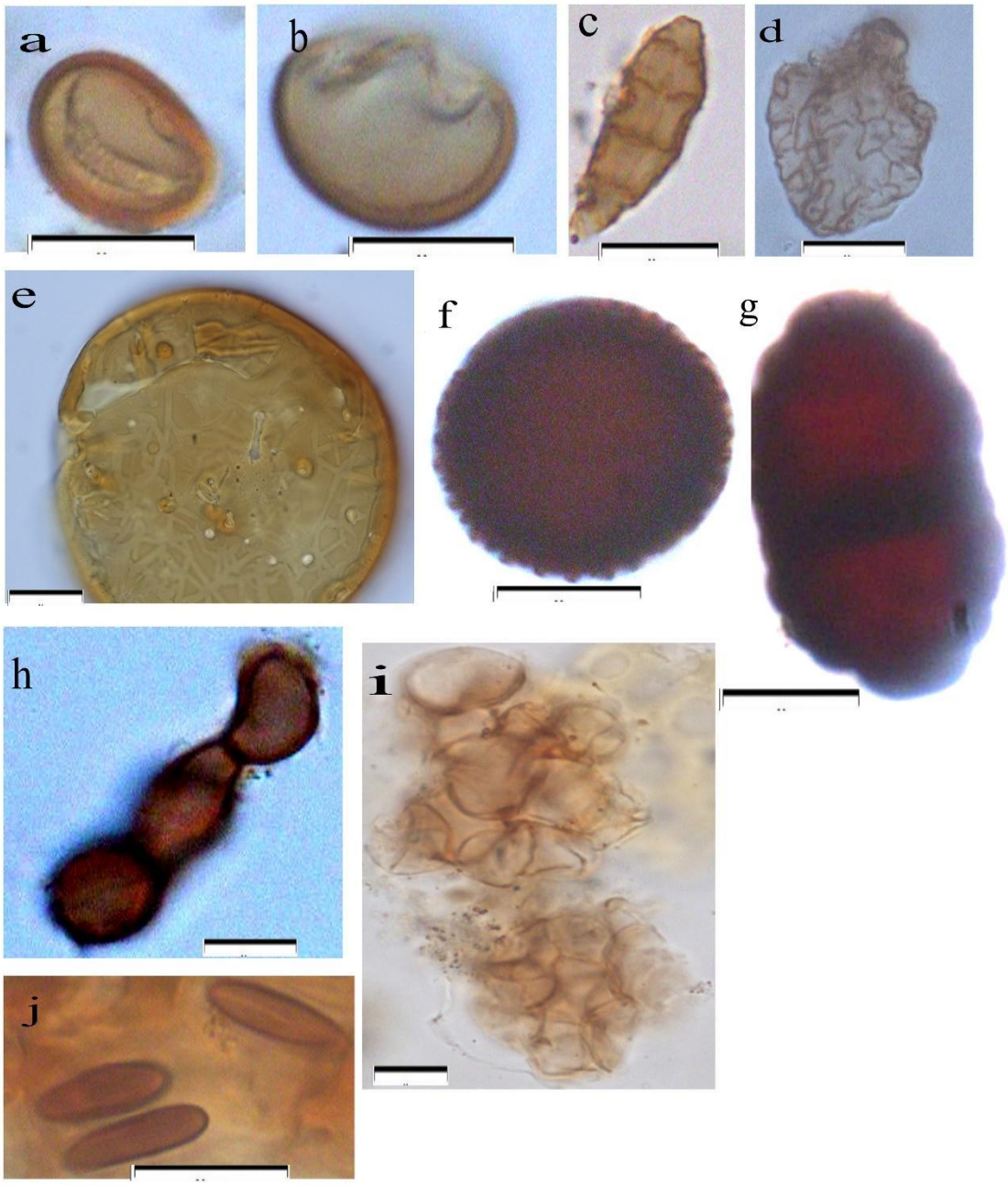


Plate 2. a-d: Unknown; e: Cyst type; f-h: Unknown fungi; i: Unknown cluster; j:*Ustulina duesta*. Scale bar= 10 µm.

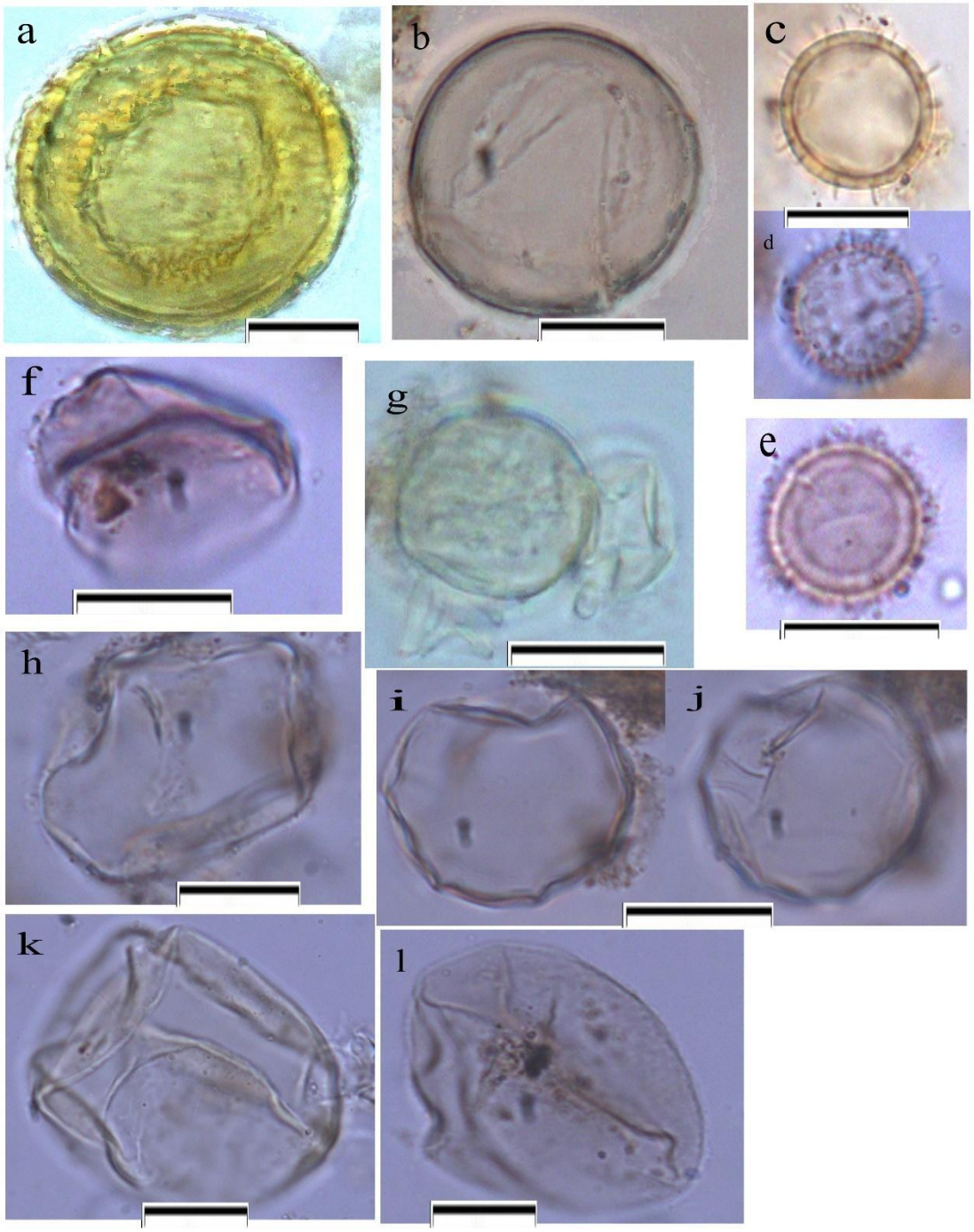


Plate 3. a-b: Possible dinocysts; c-e:Aff. *Tomentella* type; f: Unknown; g-l: Unknown possible aquatic NPPs. Scale bar= 10 µm.

Table 3.2. Fossil non-pollen palynomorphs groupings and possible affiliated environments following the scoring and grouping of Shumilovskikh and van Geel (2020).

NPP Type	B3	B4	B8	B13	Marine	Lacustrine	Peat	Soil
Arbuscular mycorrhizal fungi	0	0	3	0	0.5	1	2	3
Coprophilous fungi	0.5	0.5	0.5	0.5	0.5	1	2	1
Dinocysts	0	0	3	0	2	0.5	0	0
Prasinophyta	0.5	0	1	0	2	0	0	0
Rust fungi	1	0.5	0.5	0.5	0.5	1	2	0.5
Unidentified NPP	1	1	1	1	1	1	1	1

0- Absent, 0.5- present but uncertain identification, 1- present, 1.5- abundant but with uncertain identification, 2- abundant, 3- very abundant

Overall, fungal material dominated most of the slides. Arbuscular mycorrhizal fungi dominated layer B8 along with dinocysts (see fig 3.2). Possible coprophilous fungi did not have any dominance however were present in all four layers. Dinocysts were strongly in B8 and absent everywhere else. *Mangrovia hallii* was absent in layers B4 and B13 and showed a possible presence in B3. Rust fungi occurred in B3 and possibly in B4, B8, and B13. Layers B3, B4, and B13 showed a close correlation to each other while B8 was isolated towards marine environments. Out of the three layers mentioned, B4 and B13 were closely related.

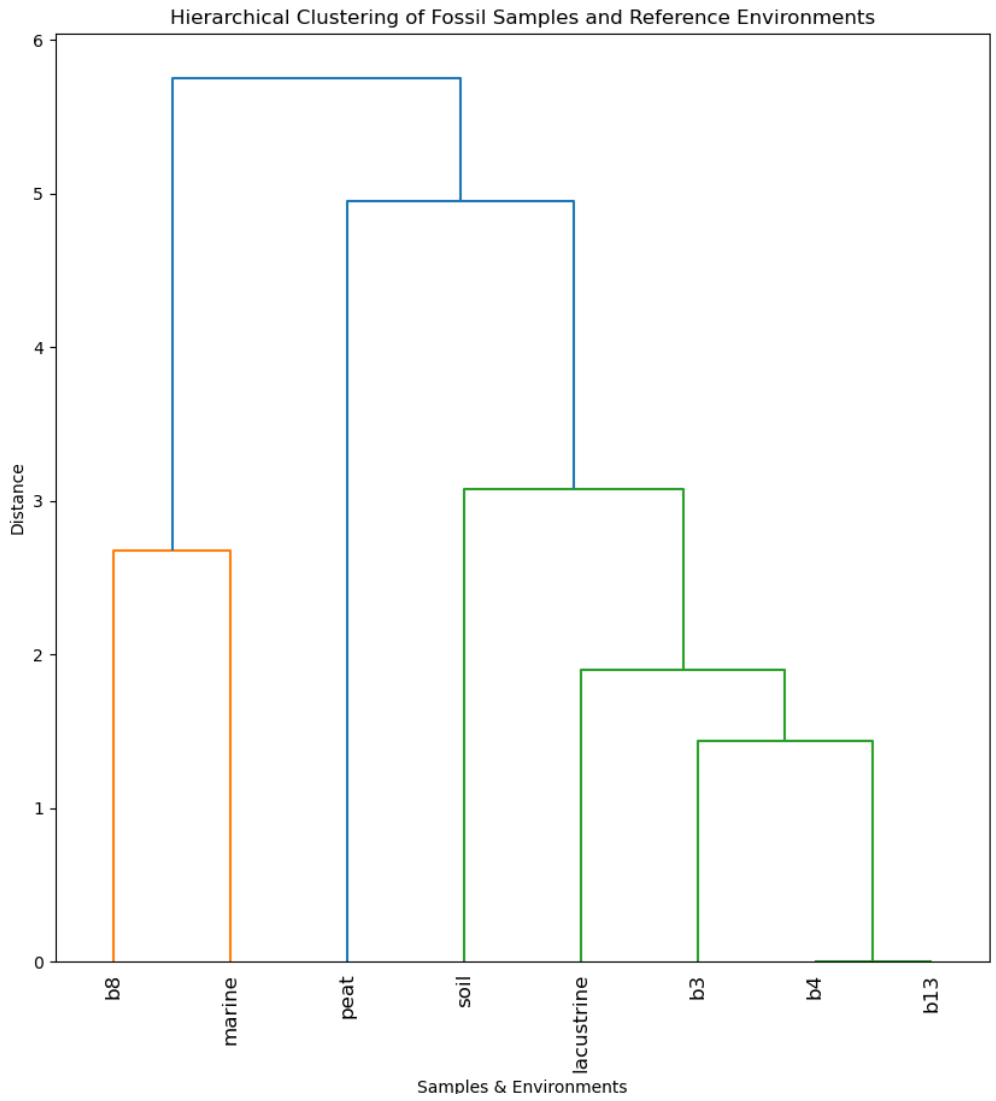


Figure 3.3. Fossil samples' clustering across reference environments (marine, lacustrine, peat, and soil).

4. CHAPTER FOUR- Modern Samples Results

4.1. Introduction

This chapter analyses the pollen and phytolith assemblages from selected modern habitats in Gorongosa. Modern non-pollen palynomorphs are also incorporated. Here, we pay deeper attention to the distribution of phytolith morphotypes in different vegetation types using R Studio, as well as pollen fidelity.

A non-parametric ANOVA was used to compare the morphotypes in different habitats. A minimum of 11 250 individual phytoliths were counted and analysed. Phytolith indices (Woody/Grass ratio, Panicoid index, and Water-stress index) were further analysed. In addition, the influences of fire on vegetation change were also analysed using the length and frequency of microcharcoal through the PCA.

4.1.1. Modern Pollen Results

Table 4.1 Pollen family and species as observed.

Family	Species	Plate
Acanthaceae	*Metarungia*	IV, a-b
Amaranthaceae	cf. *Chenopodium*	IV, c
Anacardiaceae	*Sclerocarya birrea* subsp. *caffra*	IV, d
Asteraceae	cf. *Cineraria deltoidea*	IV, e
	Tarchonanthus-Brachylaena type	IV, f-g
	cf. Tubuliflorae sp.	IV, h
Capparaceae	cf. *Boscia salicifolia*	V, a
Convulvulaceae		V, b-c
Cucurbatiaceae	cf. *Momordica boivinii*	V, d
Cyperaceae		VII, a,i
Euphorbiaceae	*Croton*	V, e-j
	cf. *Croton megalocarpus*	VI, a
Fabaceae	cf. *Crotalaria axillaris*	VI, b
Iridaceae		VII, b

Malvaceae		VI, c-d
Nymphaeaceae	*Nymphaea*	VII, h,j
Oxalidaceae	cf. *Oxalis*	VI, e-f
Poaceae		VII, c-e
Proteaceae		VII, f
Rubiaceae	spore	VI, g
	cf. *Anthospermum* type	VI, h-i
Santalaceae	cf. *Thesium dolichomeres*	VI, j
Unknown		VII, k -l

Plate 4

Acanthaceae

Metarungia sp. (Plate 4, a-b).

Shape – thick oblong peanut-shaped, ~25 µm in length.

Apertures: tricolporate, multiple rows of insulae.

Exine: reticulate.

Habitus: shrub, can grow up to 5 m high (Edwards *et al*., 2001).

Habitat: woody habitats- thickets and forests.

Distribution: afrotemperate forests.

Amaranthaceae

cf. *Chenopodium* sp. (Plate 4, c).

Shape - circular pollen grain, 10-15 µm across diameter.

Apertures: periporate.

Exine: tectate, columellate.

Habitus: annual herb.

Habitat: usually weed or in abandoned cultivated grounds, adapted to a wide variety of environments (Stadnicka-Futoma and Nobis, 2024), including dry and halophytic habitats (Scott, 1982).

Distribution: tropical and subtropical regions and temperate.

Anacardiaceae

Sclerocarya birrea (A.Rich.) Hochst. subsp. *caffra* (Sond.) Kokwaro (Plate 4, d).

Shape - elliptic pollen grain, ~33 µm.

Apertures: monocolpate, with colpus almost equal to the pollen length.

Exine: atectate.

Habitus: Medium to large tree (can grow 6-18 m high).

Habitat: Occurs in bushlands, riverine woodlands, and wooded grasslands. Thrives in well-drained sandy-loamy soils (Maroyi, 2014; Muok *et al*., 2007).

Distribution: Eastern tropical Africa, South tropical Africa, and Southern Africa.

Asteraceae

cf. *Cineraria deltoidea* Sond. (Plate 4, e).

Shape – spheroidal pollen grain, circular-triangular (Schüler and Hemp, 2016) and <10 µm in size.

Apertures: tricolporate.

Exine: a very thin tectate (Schüler and Hemp, 2016) and echinate short spines.

Habitus: herbaceous, can either trail or be erect for about 3 m (Schüler and Hemp, 2016).

Habitat: Afromontane, afroalpine, and grasslands (Cron, 2005)

Distribution: Tropical southern Africa.

Tarchonanthus-Brachylaena type L. (Plate 4, f-g).

Shape - pollen grain subspherical, size ranges between 19-25 µm.

Apertures: tricolporate.

Exine: tectate with clavae <1 µm.

Habitus: ranges from small to large trees

Habitat: Species distribution varies from forests to thickets, mountains, bushes, savannas, woodlands, and grasslands (Herman, 2002).

Distribution: Widely across southern Africa.

cf. Tubuliflorae (Plate 4, h).

Shape – spheroidal to triangular, pollen grain <20 µm.

Apertures: Tricolporate (Zavada and de Villers, 2000).

Exine: heart-shaped-like nexine, and thick broad echinate.

Habitus: Herbaceous.

Habitat: Grasslands, karoo, habitats vary.

Distribution: Widely distributed, from subpolar to tropics.

Plate 5

Capparaceae

cf. *Boscia salicifolia* Oliv. (Plate 5, a).

Shape –elliptic pollen grain, size < 25 µm.

Apertures: monocolpate

Exine: atectate.

Habitus: Small-medium tree, can grow up to 15 m (Maroyi, 2019).

Habitat: Semi-arid, Miombo woodlands, hot and dry open woodlands, and sometimes on termite mounds (Maroyi, 2019; https://www.mozambiqueflora.com/).

Distribution: Globally distributed in tropical and subtropical regions.

cf.Convulvulaceae (Plate 5, b-c).

Shape - Spheroidal pollen grain, ~30µm.

Apertures: inapertutate.

Exine: tectate, columellate with clavae ~ 1µm.

Habitus: Perennial or annual herb, climbers or trailers, and woody plants but rarely erect trees (Meeuse, 1957).

Habitat: Moist forests, Savanna, and disturbed vegetation.

Distribution: Widely spread.

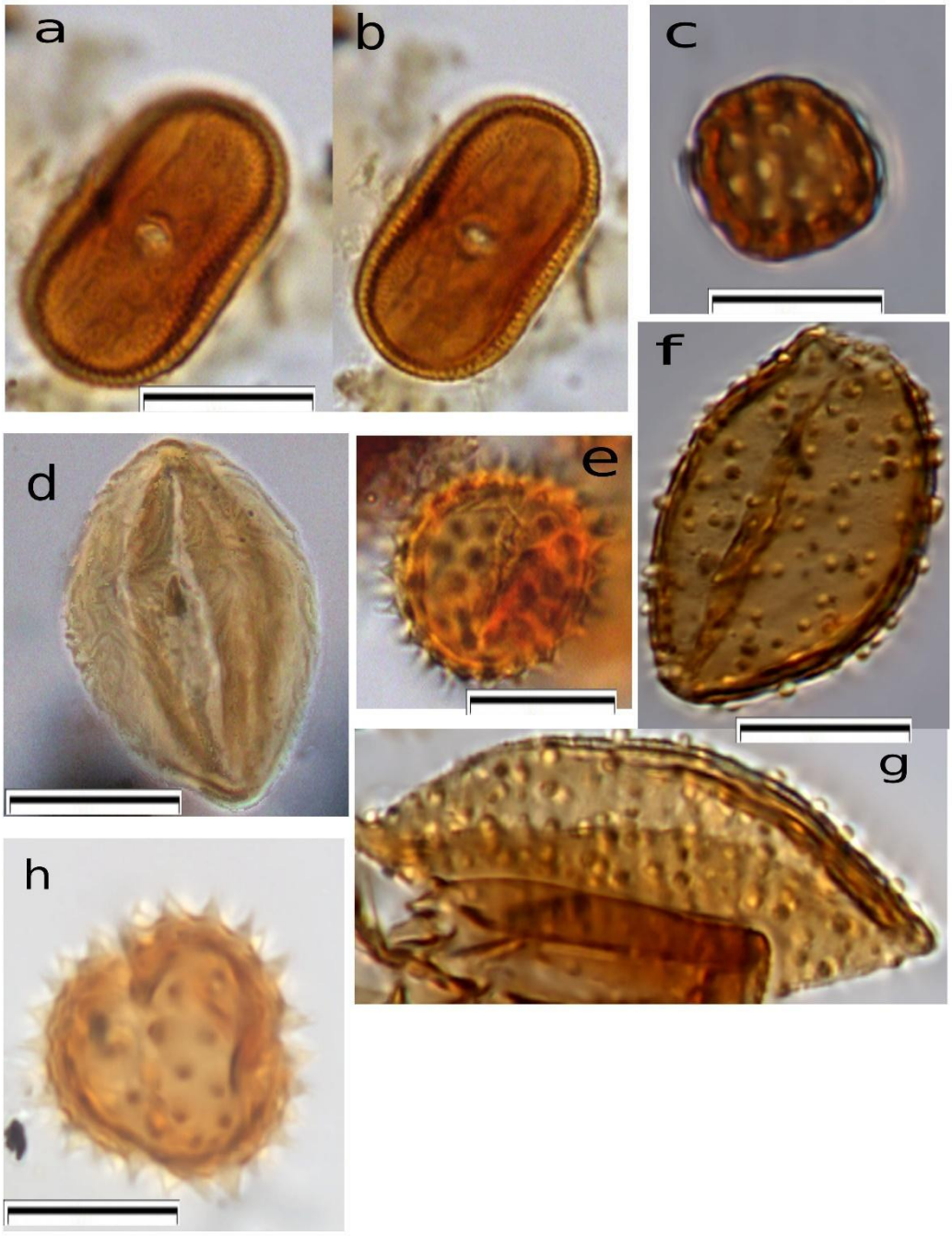


Plate 4. Acanthaceae: a-b- *Metarungia* sp., Amaranthaceae: c- cf. *Chenopodium* sp., Anacardiaceae: d- *Sclerocarya birrea*, Asteraceae: e- cf. Cineraria deltoidea, f-g- *Tarchonanthus-Brachylaena* type, h- cf. Tubuliflorae. Scale bar= 10µm

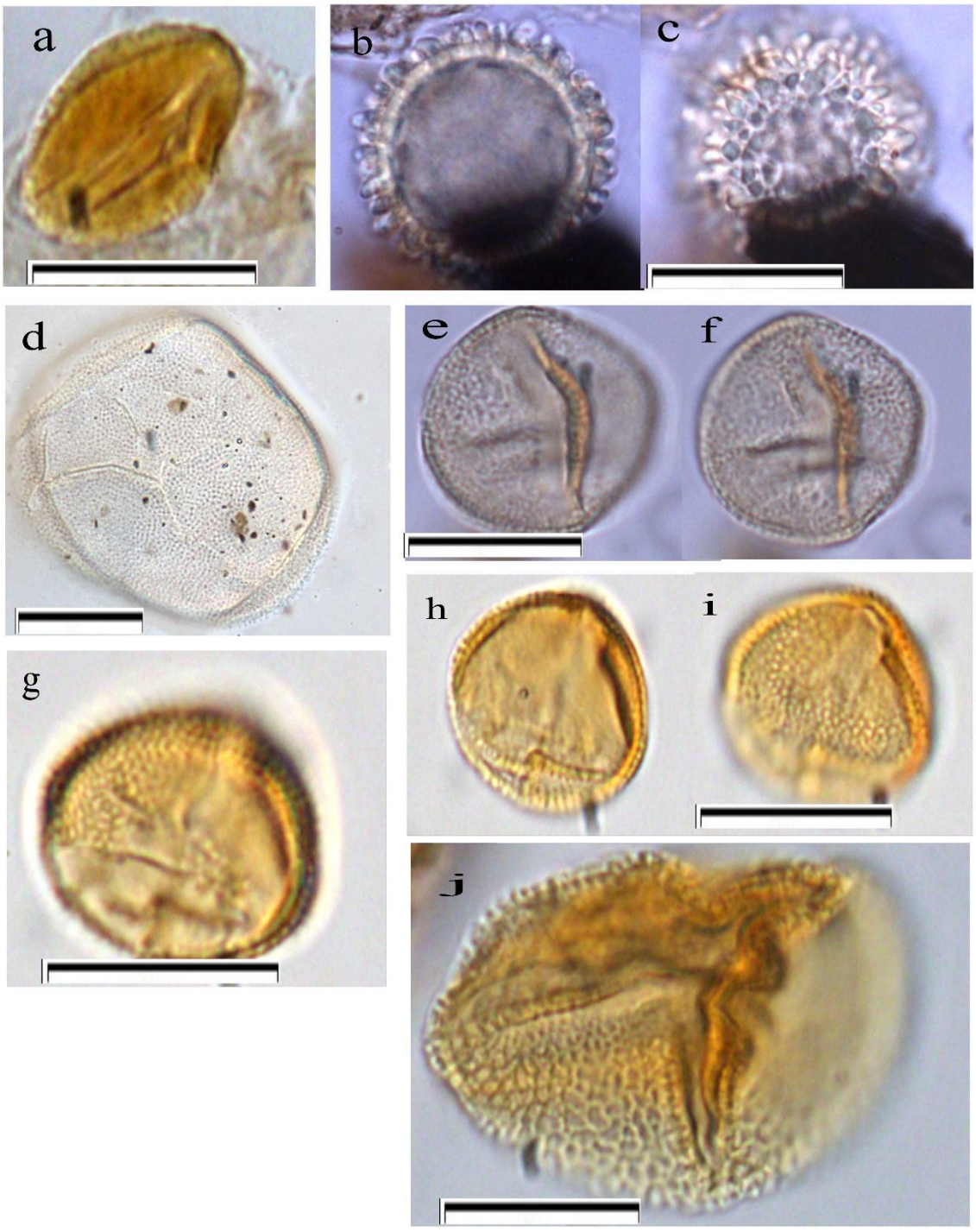


Plate 5. a: cf. *Boscia salicifolia*, b- c: cf. Convulvoluceae, d: cf. *Momordica boivinii*, e-j: *Croton* sp. Scale bar= 10µm.

cf. Cucurbitaceae

cf. *Momordica boivinii* Baill (Plate 5, d).

Shape – spherical, pollen grain size >60 µm.

Apertures: subprolate.

Exine: tectate, granulate.

Habitus: herbaceous climber or trailer.

Habitat: wooded grassland, woodland, thicket.

Distribution: Eastern Africa.

Euphorbiaceae

Croton sp. (Plate 5, e-j).

Shape- spherical, 10-30 µm.

Apertures: monocolpate.

Exine: tectate, reticulate.

Habitus: herbs, shrubs, and trees (Scott, 1982).

Habitat: succulent environment and widely distributed in tropical and subtropical regions, are highly adaptable to a variety of environments (Moremi *et al*., 2021; Scott, 1982).

Plate 6

Euphorbiaceae

cf. *Croton megalocarpus* Hutch (Plate 6, a).

Shape - spheroidal monad pollen grain. Size ~46 µm.

Apertures: inapeturate.

Exine: tectate, wall ornamented with clavicles.

Habitus: a flat-crowned deciduous tree that can exceed the height of 35 m (Thijssen, 1996).

Habitat: Occurs in wooded grasslands, riverine woodlands, evergreen forests, and sometimes rocky outcrops in tropical regions (Scheuler and Hemp, 2016; Scott, 1982).

Distribution: Tropical East Africa- Mozambique, Rwanda, Zambia, Malawi, Burundi.

Fabaceae

cf. *Crotalaria axillaris* Aiton (Plate 6, b).

Shape - pollen grain has a rectangle-like shape, and size <30 µm.

Apertures: tricolporate, slightly pinched at the equator.

Exine: tectate.

Habitus: Small shrub or woody herb growing between 1 and 4 m tall (Schüler and Hemp, 2016).

Habitat: Occurs in open vegetation, semi-deserts and mountains, forest margins, bushlands, grasslands, abandoned cultivations, and deciduous woodlands (Schüler and Hemp, 2016)

Distribution: Tropical and sub-tropical Africa.

Malvaceae (Plate 6, c-d).

Shape- spheroidal pollen grain large sized ~80 µm.

Apertures: inaperturate.

Exine: tectate, columellate. Echinate, spikes hooked at the terminal.

Habitus: herbs and subshrubs (Scott, 1982).

Habitat: grasslands, shrubs, Savanna

Distribution: Tropical and subtropics of southern Africa.

cf. Oxalidaceae

cf. *Oxalis* sp. (Plate 6, e-f).

Shape – circular, spheroidal ~ 30 µm.

Apertures: tricolpate. Aperture membrane ornamented (Halbritter, 1998).

Exine: atectate, wall reticulate.

Habitus: herbs to sub-shrubs.

Habitat: occupy vernal pools- temporary wetlands (Oberlander et al., 2014).

Distribution: widely distributed in tropical, subtropical, and temperate regions globally.

Rubiaceae

spore (Plate 6, g).

Shape- corpus spherical, size ~50 µm.

Apertures: bisaccate.

Exine: wringed corpus.

cf. *Anthospermum* type L. (Plate 6, h-i).

Shape – small to medium-sized sub-oblate (Robbrecht, 1982), ~20 µm.

Apertures: tricolporate pollen grain, narrow ectocolpus.

Exine: rugulate with grooves and regulated wall.

Habitus: can be either herbs, shrubs, or sub-shrubs.

Habitat: Affiliated with rocky outcrops on small hills, or rocky grasslands

Distribution: East Africa and southwestern Arabian Peninsula.

cf. Santalaceae

cf. *Thesium dolichomeres* Brenan (Plate 6, j).

Shape - pollen grain convex triangular pyramid, dyad ~26 µm.

Apertures: colpate.

Exine: tectate, wall echinate.

Habitus: erect woody herb.

Habitat: Rocky mountainous grasslands

Distribution: Zimbabwe and Chimanimani Mts in Mozambique

Plate 7

Cyperaceae (Plate 7, a,i).

Shape- pear-shaped, pollen and size ~30 µm.

Apertures: Y-mark colpi.

Exine: tectate, wall granulate.

Habitus: Perennial or annual herb and can exceed 1 m in height.

Habitat: Semi-aquatic, shallow waters, local swamps, or damp soils (Scott, 1999).

Distribution: Wet tropics

i-triangular, ~20 µm. Monoporate with a centric pore. Granulated surface and exine regulate.

cf. Iridaceae (Plate7, b).

Shape- elliptic, ~30µm.

Apertures: monosulcate.

Exine: tectate reticulate, wall granulate with micro papillae (Goldblatt *et al*., 2004).

Habitus: herbs and shrubs (Goldblatt, 1983).

Habitat: highly adaptive to rocky mountains, grasslands, forests, wetlands and marshes.

Distribution: widely distributed and thrives mostly in Southern Africa. Occurs in the tropics and temperate regions.

Poaceae (Plate 7, c-e).

Shape- circular, spheroidal, 25-40 µm.

Apertures: monoporate.

Exine: atectate, pollen wall granulate or psilate.

Habitus: Herbaceous and ranges from short to tall (can grow up to 2 m tall).

Habitat: Occurs in bushes, woodlands, savannah, and in both open and closed vegetation.

Distribution: Globally distributed on every continent.

Fern spores (Plate 7, f-g).

(Plate 7, f).

Shape- triangular, ~25 µm.

Apertures: triporate, circular pori.

Exine: very thin (Schüler and Hemp, 2016).

Habitus: fronds or creepers.

Habitat: occur in both arid and wet environments (Anthelme *et al*., 2011).

Distribution: globally distributed.

(Plate 7, g).

Shape- triangular, <20 µm.

Apertures: tricolpate.

Exine: tectate regulate.

Habitus: fronds or creepers.

Habitat: dry forest, riverbanks, roadbanks, rocky shaded areas (Schüler and Hemp, 2016).

Distribution: globally distributed.

Nymphaeaceae (Plate 7, h, j)

Nymphaea

h- triangular convex, ~30 µm. Tricolporate, exine tectate and regulate.

j- triangular-rectangular, ~25 µm. Tricolpate, exine thick.

Habitus: floating leaves.

Habitat: ponds and wetlands.

Distribution: West, East, and parts of South Africa (Nzei *et al*., 2021)

Unknown spores (Plate 7, k-l).

k- circular, spheroidal, <40 µm. Inapeturate. Bacculate projections.

l- circular, spheroidal, <15 µm. Inapeturate. Thick and short clavae projections.

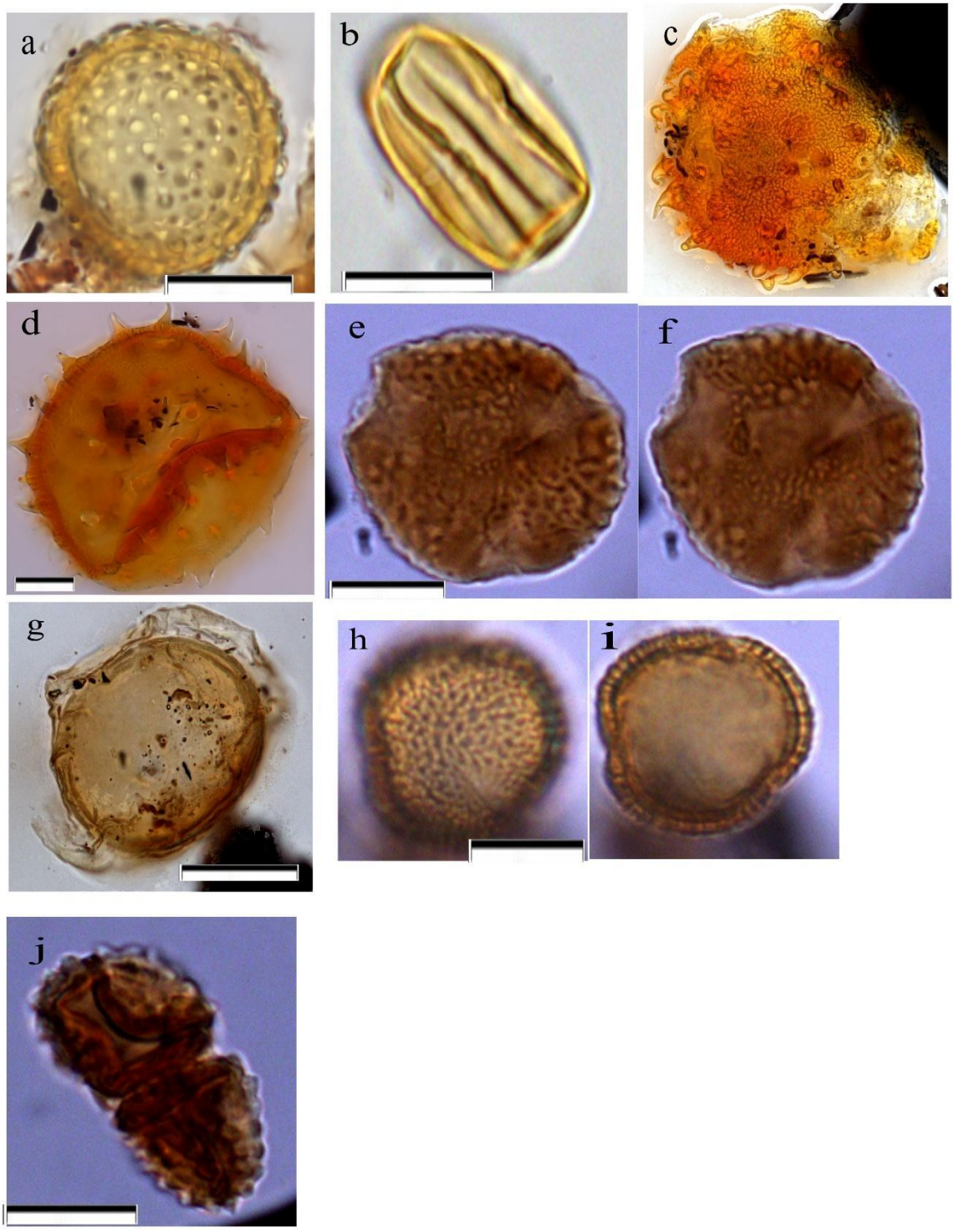


Plate 6. Euphorbiaceae: a- cf. *Croton megalocarpus;* Fabaceae: b- cf. *Crotalaria axillaris;* c-d: cf. Malvaceae; cf. Oxalidaceae: e-f- cf. *Oxalis* sp.; Rubiaceae: g-spore, h-i- *Anthospermum* type; cf. Santalaceae: j- cf. *Thesium dolichomeres*. Scale bar= 10 µm.

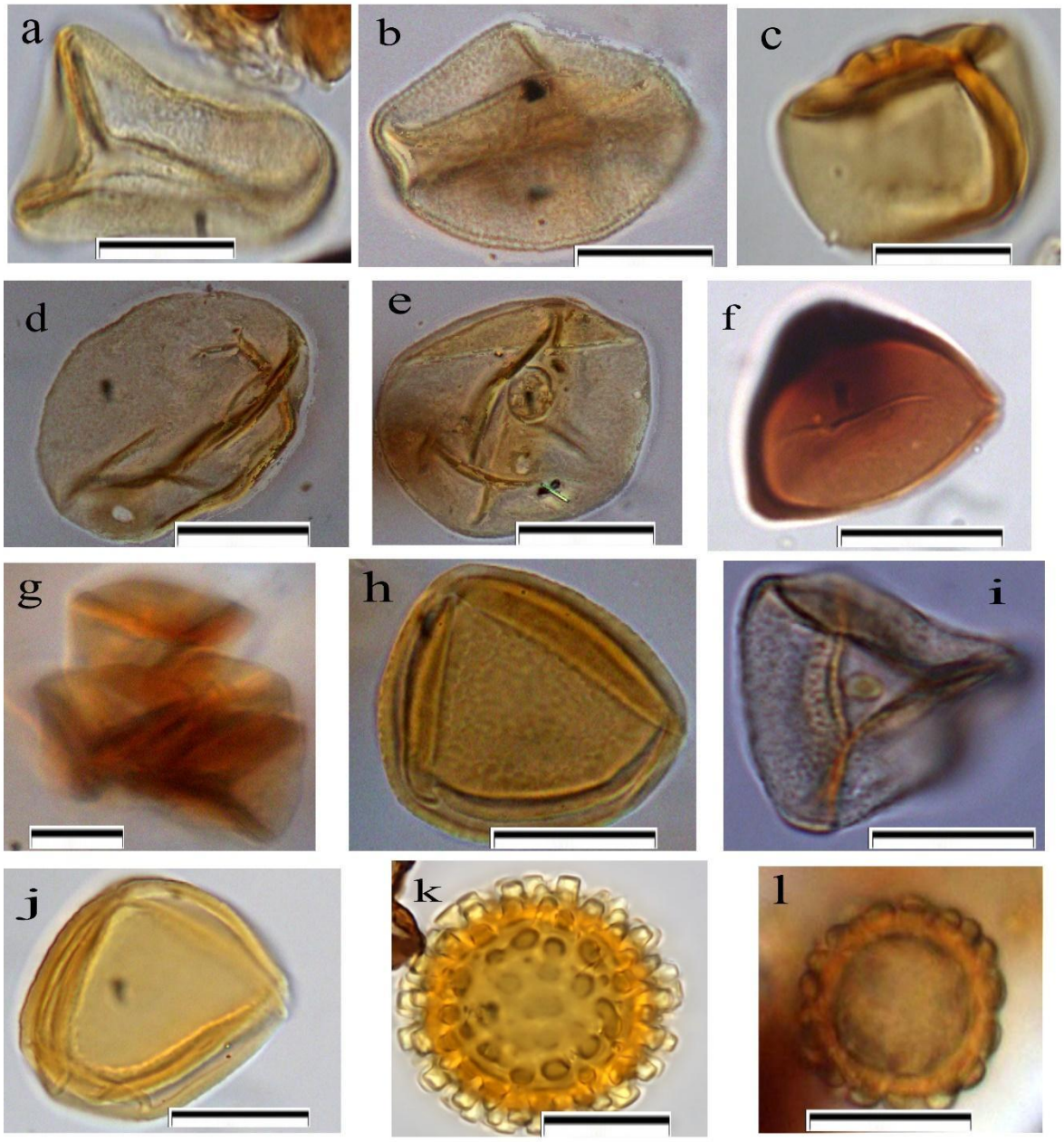


Plate 7. a,i: Cyperaceae; b: cf. Iridaceae; c-e: Poaceae; f-g: Fern spores; h,j: Nymphaea: k-l: Unknown spores. Scale bar= 10 µm.

4.2. Non-Pollen Palynomorphs from Modern Soils

Table 4.2 A list of modern non-pollen palynomorphs and their affiliated environment and/or predominant behaviour

Species	**Plate**	**Affiliated environment and/or behaviour**
cf. *Bactrodesmium* type	VIII, a	Occurs on decaying wood
cf. *Calcidiscus* sp.	VIII, d	Marine
cf. *Cirrenalia* sp.	IX, i	Woody vegetation
cf. *Coniochaeta* sp.	VIII, e	Predominantly coprophilous fungi
cf. Corolla capsule-tintinnomorph type	VIII, f	Marine
cf. *Gelasinosporia* sp.	VIII, g	Coprophilous fungi
Glomus sp.	VIII, h-I; IX, b	Erosive environments and mycorrhizal relations
cf. *Inocybe* UY-176	VIII, j	Saprophytic fungi in swamps
cf. *Katora arabica* A. Kumar, sp. nov.	X, a	Intertidal sediments
cf. *Lasiodiplodia theobromae*	X, b	Rust fungi
cf. *Meliola*	X, c	Woody vegetation
Neorhabdocoela oocyte	IX, d-f	Freshwater
cf. *Puccinia* sp.	IX, d-f	Rust fungi
Tetraploa aristata - Type HdV-89	IX, g	Rust fungi
Type UG-1320	VIII, c	Unknown
Unknown	VIII, k-l; IX, h-k; X, e-l	Unknown

Plate 8

cf. *Bactrodesmium* type- Type UG-1091 (Plate 8, a).

Shape- ellipsoid and asymmetrical, size <20 µm.

Habitat: occurs on decaying wood (Hernández-Restrepo *et al*., 2013).

cf. *Calcidiscus* sp. (Plate 8, b).

Shape- circular disk-like shape coccolith with a peripheral columnar pattern, size ~17 µm.

Habitat: they are autotrophic marine flagellates (Young, 2020).

cf. *Coniochaeta* sp. (Plate 8, c).

Shape- ellipsoid to circular, size = 14 µm. Potentially colporate.

Habitat: coprophilous and also found on wood (ref). In fossil samples, they imply wet and cooler environments (van Geel *et al*., 2011). Some species inhabit burned soil (Poswa *et al*., 2024; Wicklow, 1973).

cf. Corolla capsule- tintinnomorph type (Plate 8, d).

Shape- an elongated ellipsoid (Kumar, 2023), size = 84 µm.

Habitat: occurs in areas influenced by marine waters (Da Silva *et al*., 2017; Kumar, 2023).

cf. *Gelasinosporia* sp. (Plate 8, e).

Shape- ellipsoid, 35 µm. It is ornamented with pores and has a single infolding at the equator.

(Piasai and Sudsanguan, 2018; van Geel *et al*., 2011) associated the species with being of a coprophilous habit.

***Glomus* sp.** (Plate 8, f-g).

See (Plate 1, b-c).

cf. *Inocybe* UY-176 (Plate 8, h).

Shape- circular, spheroidal, ~12 µm.

Habitat: saprophytic fungi found in low amounts in swamps and pajonales (Leal *et al*., 2021).

Type UG-1320 (Plate 8, i).

Shape- a big ellipsoid, ~40 µm, whole body brown to dark brown and terminals subhyaline (van Geel *et al*., 2011).

Unknown (Plate 8, j-l).

j: oval-shaped, thick-walled, size ~ 18 µm.

k: hexagon outline, thick-walled, size ~ 18 µm.

l: circular-shaped with undulate lining, size = 91 µm.

Plate 9

cf. *Cirrenalia* sp. Type UG-1343 (Plate 9, a).

Shape- spiral-shaped, subglobose and multiseptate arranged in a spiral form.

Habitat: some species are marine and some are terrestrial occurring on wood in wet habitats (Gelorini *et al*., 2011). They have a positive correlation with closed vegetation and mostly occur in wooded sites (Dietre *et al*., 2012).

***Glomus* sp**. (Plate 9, b).

See (Plate 1, b-c).

cf. Neorhabdocoela (flatworm) sp. oocyte- T. UG-1224 (Plate 9, c).

Shape- ranges from ellipsoid to spherical. Surface microreticulate with ribs or psilate (Gelorini *et al*., 2011). Size >92 µm.

Habitat: occupy freshwater habitats worldwide (Haas, 1996; Young, 1977).

cf. *Puccinia* sp. (Plate 9, d-f).

Shape- septate fungus with a constricted septum, shaped like the number eight. It is thick-walled, and the surface can be psilate or ornamented. Size between 20-23 µm.

Habitat: rust fungi attacking wild and cultivated crops worldwide (Anikster *et al*., 1997; Böllmann and Scholler, 2006).

***Tetraploa aristata*- Type HdV-89** (Plate 9, g).

Shape- ellipsoid to rectangular, usually with 3 or 4 columns. Size > 73 µm. Surface with small hairs and looks granulated.

Habitat: hosted by plants in warm temperate climates (Karpinska-Kolaczek *et al*., 2010; Worobiec *et al*., 2009).

Unknown (Plate 9, h-k).

h: multiporate ~81 µm. Shape ellipsoid to circular.

i: multiseptate, ~21 µm.

j: circular with operculum, size is 30 µm.

k: translucent microremains with a basal flagellum-like stem. The yellowish-brown colour resembles the *Katora* sp. found in intertidal zones described by (Kumar, 2023).

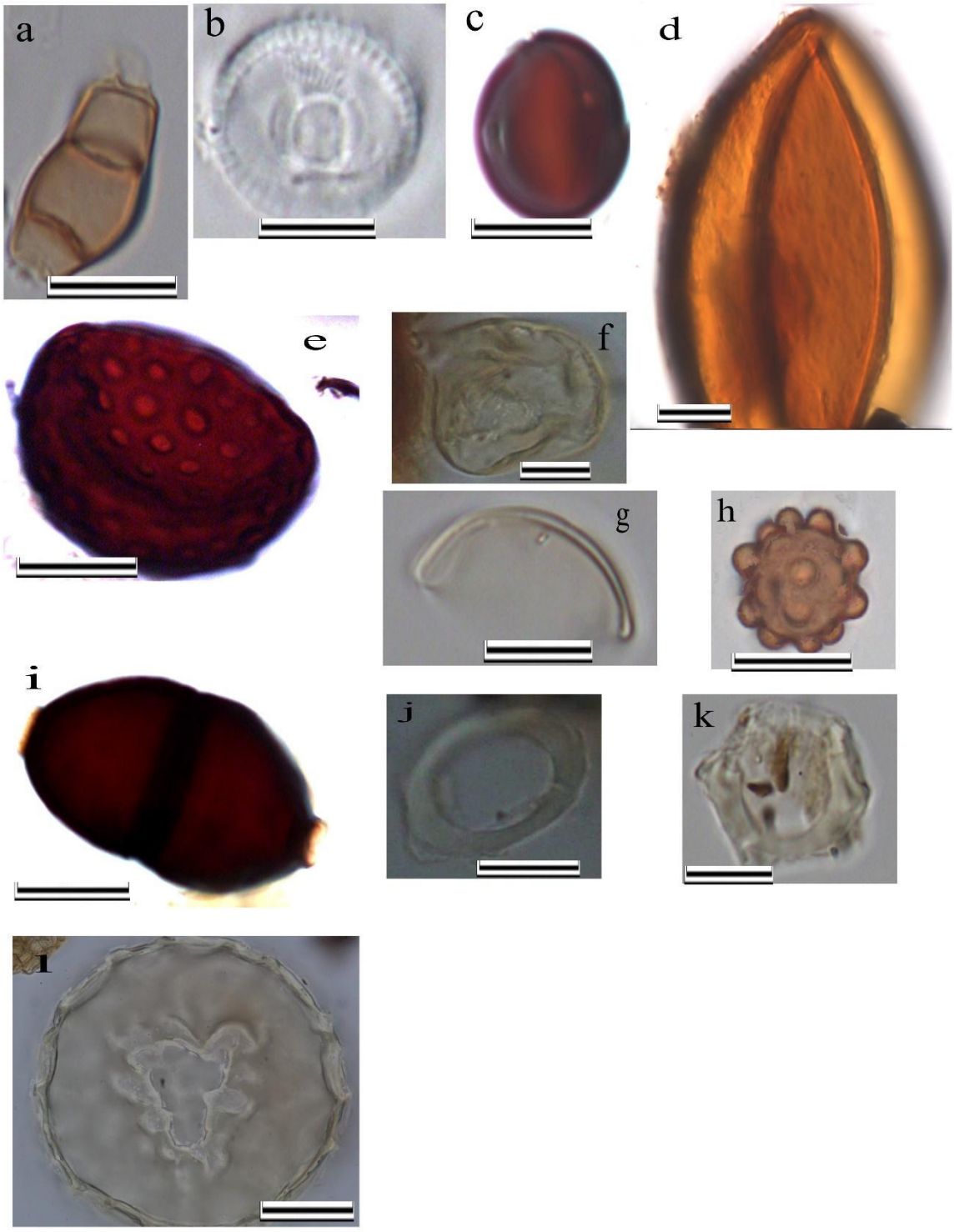


Plate 8. a: *Bactrodesmium* type; b: cf. *Calcidiscus* sp.; c: cf. *Coniochaeta* sp.; d: Corolla capsule- tintinnomorph type; e: *Gelasinospora* sp.; f-g: *Glomus* sp.; h: cf. Inocybe; i: Type UG-1320; j-l: Unknown NPPs. Scale bar= 10 µm.

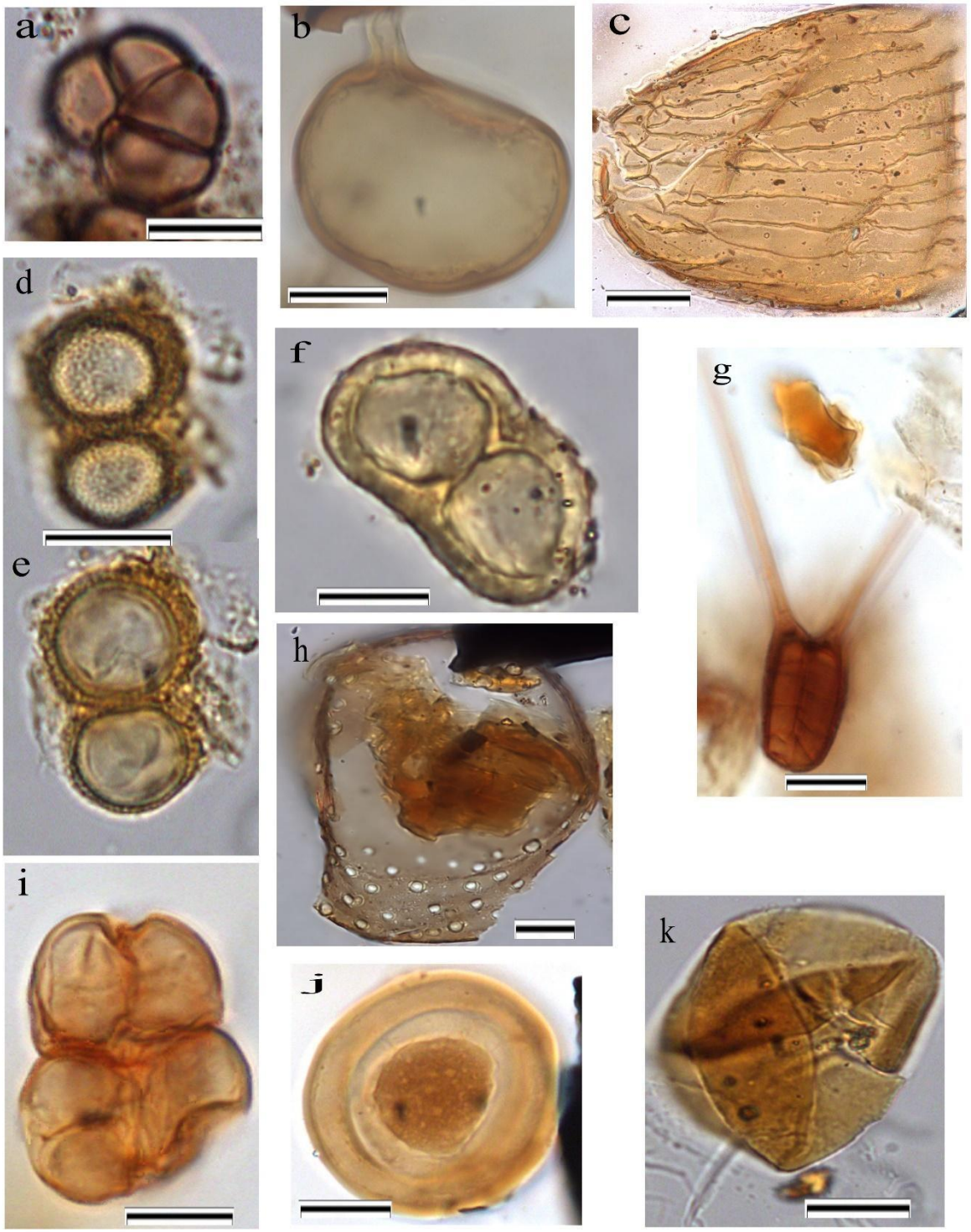


Plate 9. a: cf. *Cirrenalia* sp. Type UG-1343; b: *Glomus* sp.; c: *Neorhabdocoela* sp. (flatworm) oocyte; d-f: cf. *Puccinia* sp.; g: *Tetraploa aristata*- fungal spore- Type HdV-89; h-k: Unknown NPPs. Scale bar= 10 µm.

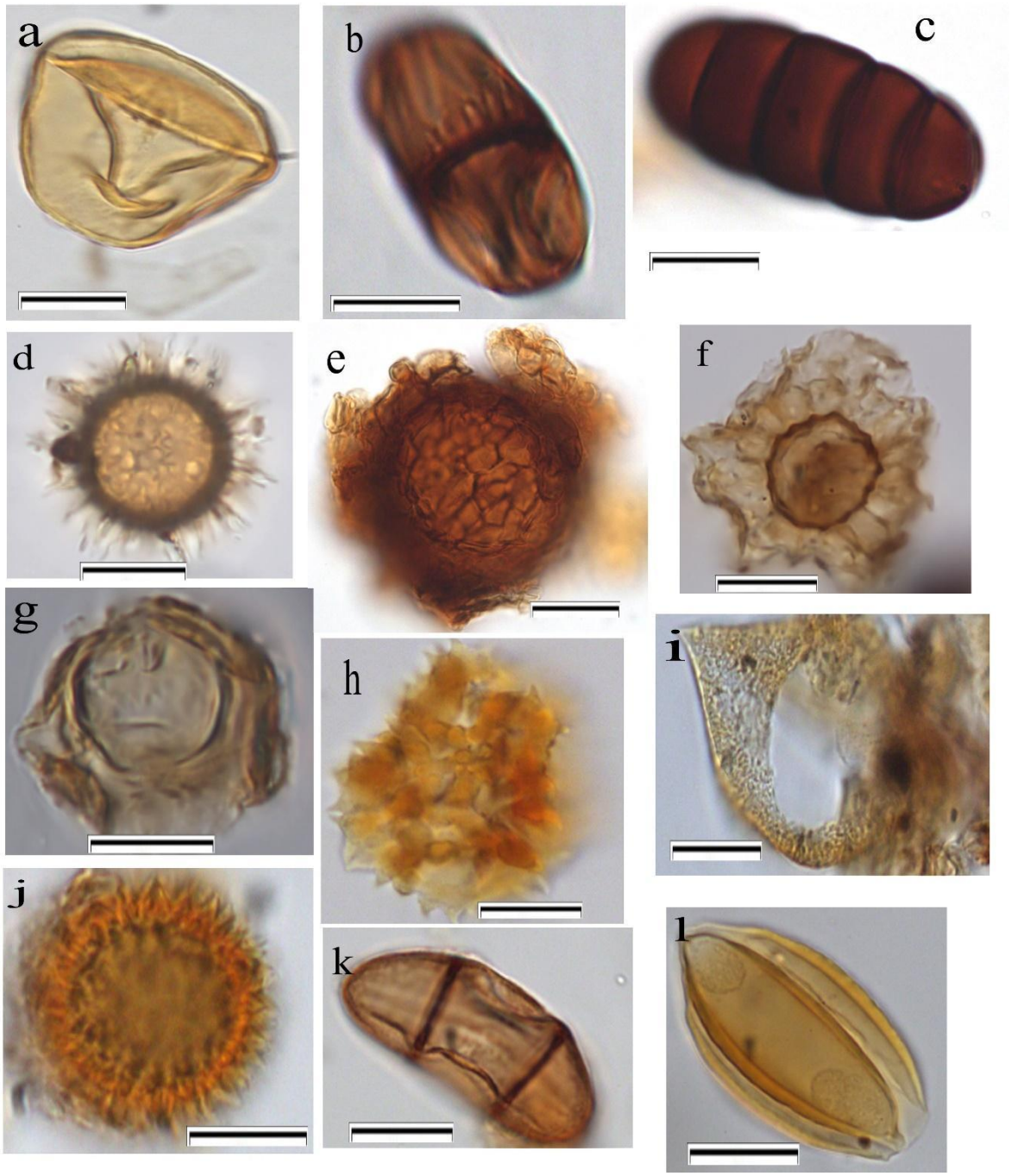


Plate 10. a: cf. *Katora arabica*; b: cf. *Lasiodiplodia theobromae*; c: cf. *Meliola;* d: Type HdV- 182; e-l: Unknown NPPs. Scale bar= 10µm.

Plate 10

cf. *Katora arabica* A. Kumar, sp. nov. (Plate 10, a).

Shape- yellow cup-shaped, with an anterior opening. Flagellum-like stem present. Size= 30 µm.

Habitat: (Kumar, 2023) found them in intertidal sediments in the southern Red Sea coast, Saudi Arabia.

cf. *Lasiodiplodia theobromae* – Type HdV-1043 (Plate 10, b).

Shape- ellipsoid uniseptate ascospore with longitudinal ridges (Gelorini *et al*., 2011), ~25 µm. Habitat: a pathogen of tropical trees (Mbenoun *et al*., 2008; Mohali *et al*, 2005), affecting plant growth even to the point of death and has a worldwide distribution in the tropics and subtropics.

cf. *Meliola* (Plate 10, c).

Shape- ellipsoidal 3-5 celled fungal spore (Leal *et al*., 2021), ~40 µm. Terminal cells are a semi-circle.

Habitat: a pathogen on woody vegetation (Doidge, 1921; Leal *et al*., 2021).

Unknown Type HdV-182 (Plate 10, d).

Shape- globose with a microreticulate surface. Looks like a micro sea urchin with long echinus. Size is 20 µm.

Habitat: Stagnant and shallow open water (Halbwachs *et al*., 2021; Revelles and van Geel, 2016).

Unknown (Plate 10, e-l).

e: circular, spheroidal fungal spore. Surface reticulate, ~40 µm across diameter.

f: lettuce-shaped-like micro remains. Monosaccate wall with blocky columellate ridges. Size = 32 µm.

g: cabbage-shaped, spherical interior and outer structure of an irregular shape with flagellum, ~22 µm.

h: shape irregular, spikes terminals hooked, ~30 µm.

i: leaf-like shape with a pointy terminal. Surface granulated. Size ~ 33 µm across the centre.

j: circular, spheroidal. Surface hetero-echinate. Size ~22 µm.

k: ellipsoidal fungal spore. Surface biseptate with longitudinal ridges, ~30 µm long.

l: small corolla capsule-like NPP, has longitudinal ribs, ~35 µm in size.

4.3. Modern Phytolith results

Table 4.3 Summary of phytolith morphotypes described by Lloyd Russow

Phytolith morphotypes	Description	Main taxonomic attribution	Illustration
Acicular	Needle-like, pointy sharp terminals	Non-specific	Fig 4.1, ah
Bulliform	Parallelepiped shaped	Poaceae	Fig 4.1, w
Elongate castellate	Margins columellate	Non-specific	Fig4.1, z
Elongate dentate	Margins echinate	Non-specific	Fig4.1, y
Flabellates	Fan-shaped	Poaceae	Fig 4.1, aa-ac
Lobates	Concave lobes and short thick shank	Panicoideae	Fig 4.1, a-b
	Convex lobes and short thick shank	Aristidoideae	Fig 4.1, c
	flat-end lobes and short shank	Chloridoideae	Fig4.1, d
	straight-end lobes and one slightly concave, short shank	Chloridoideae	Fig4.1, e
	Polylobate, extra lobe on shank, lobate narrow and long	Panicoideae	Fig4.1, f
	Polylobate, one lobate end slightly concave and one flat	Panicoideae	Fig4.1, g
	Extra lobe on thick short shank	Panicoideae	Fig4.1, h-i
	Crosses	Panicoideae	Fig4.1, j-l
	Narrow and concave lobes	Aristidoideae	Fig4.1, m

Oblong	long obovate ends	Poaceae	Fig4.1, x
Rondels	Small, narrow base	Arundinoideae	Fig4.1, s
	Hat-shaped with large funnels	Chloridoideae	Fig4.1, t-v
Saddle	Short saddle, concave plateau	Aristidoideae	Fig4.1, p
	Bed-like shape	Arundinoideae	Fig4.1, q
	Circular base	Chloridoideae	Fig4.1, r
Spheroid echinate	Circular spheroid with echinus ornamentation	Palms	Fig4.1, ad
Spheroid psilate	smooth spheroid	woody dicot	Fig4.1, ae
Tabular gibbate	Perforated ornamentation	Woody dicot	Fig4.1, af
Tabular psilate	No ornamentation, smooth-bodied	Woody dicot	Fig4.1, ag
Trapeziforms	Sides irregular and unequal in size	Chloridoideae	Fig4.1, n-o

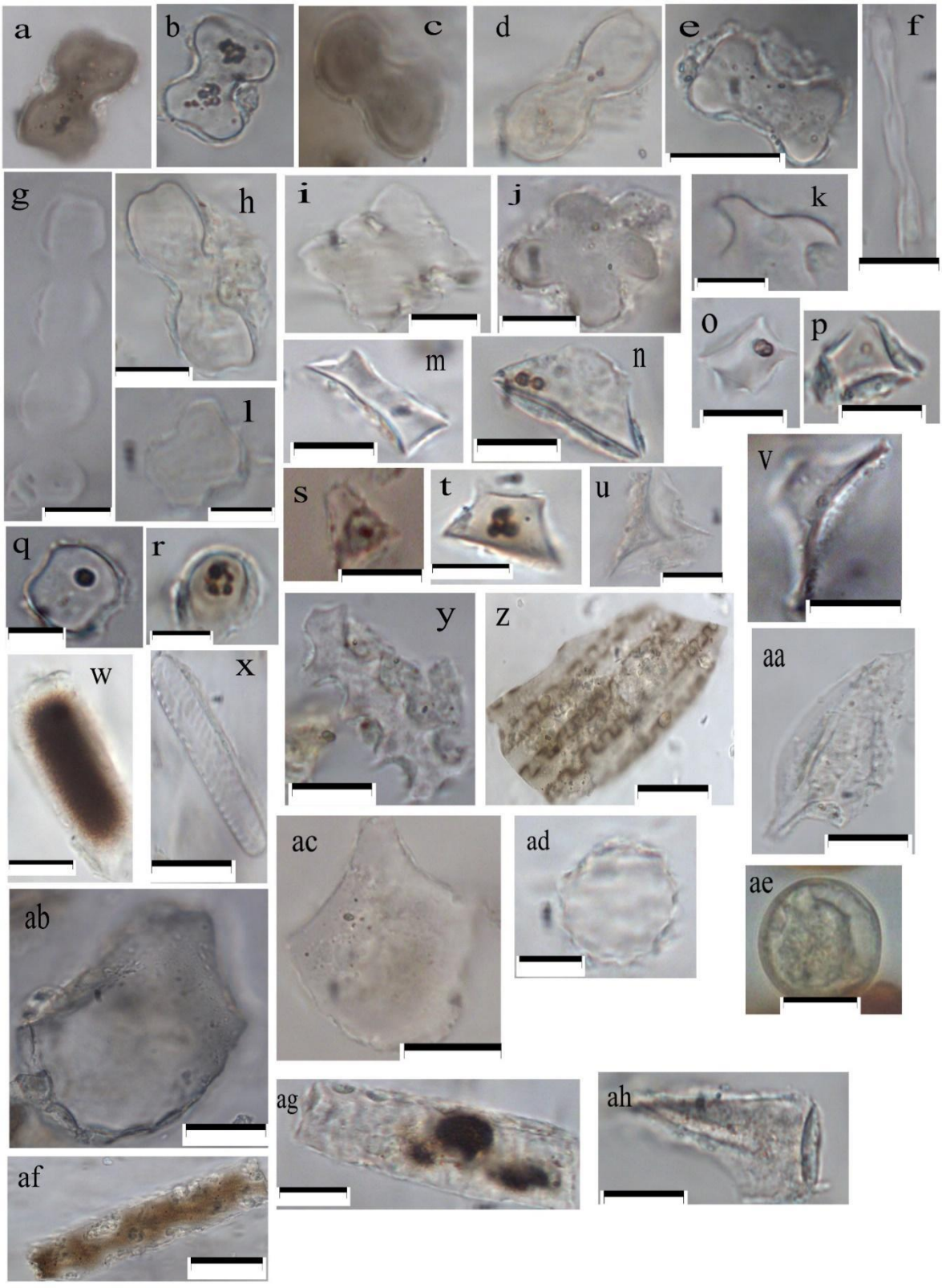


Figure 4.1. Phytolith morphotypes from modern soil samples. GSSC: Lobates (a-m): a-b-

Bilobate with concave lobes, short thick shank- **Panicoideae**; c- Bilobate with convex lobes, short thick shank- **Aristidoideae**; d- Bilobate with flat ends round lobes and short shank- **Chloridoideae**; e- Bilobate with straight-end lobes and one slightly concave, medium thick shank- **Chloridoideae**. f- Polylobate, extra lobe on shank, lobate narrow, long and thin- **Panicoideae**; g- Polylobate, one lobate end slightly concave and one flat- **Panicoideae**; h-i- Extra lobe on thick short shank- **Panicoideae**. Crosses (j-l): **Panicoideae**; m- Bilobate narrow and concave lobes- **Aristidoideae**. Trapeziforms (n-o): **Chloridoideae**. Saddle (p-r): p- Short saddle, concave plateau and base- **Aristidoideae**; q- **Arundinoideae**; r- **Chloridoideae**. Rondels (s-v): s- **Arundinoideae**; t-v- **Chloridoideae**. w- Bulliform; x- Oblong; y- elongate dentate; z- elongate castellate. Fan-shaped flabellates (aa-ac). Spheroidal (ad-ae): ad- Spheroid echinate- Palms; ae- Spheroid psilate- woody dicot. af- Tabular gibbate; ag- Tabular psilate; ah- Acicular. Scale bar= 10µm.

Table 4.4 Sample data from GNP showing lithology, vegetation types and GPS localities where

Field No	Date Collected	Lithology	Vegetation above	Area	Vegetation type	Vegetation key	Code	Laboratory code	Latitude	Longitude
MS-001	2022-07-31 00:00:00	sandy clay	*Hyphaene petersiana; Senegalia nigrescens; Vachellia robusta; Urochloa mossambicensis*	Picada 4, bones under Acacia	grassland-woodland palm	Grassland1	MS-001	S1	-18,92223	34,38128
MS-002	2022-07-31 00:00:00	sandy clay	*Salvadora persica; Grewia sp.; Ziziphus mucronata; Hypoestes sp.; Chromalaena odorata; Achyranthes aspera; Setaria incrassata; Urochloa mossambicensis*	Carcass 89	pan mixed woodland and grassland	Woodland1	MS-002	S2	-18,90862	34,39093
MS-003	2022-07-31 00:00:00	sandy clay	*Faidherbia albida; Hyphaene petersiana; Chromalaena odorata; Acalypha.*	Carcass 84	woodland-herbaceous understory	Woodland2	PPG2022-B-84	S3	-18,89034	34,39594
MS-004	2022-07-31 00:00:00	sandy loam	*Vachellia robusta; Setaria sp.;*	Carcass 97	open woodland-medium grassland	Woodland3	PPG2022-B-140	S4	-18,92539	34,41876
MS-004	2022-07-31 00:00:00	sandy loam	*Vachellia robusta; Setaria sp.;*	Carcass 97	as above	as above	PPG2022-B-97	S4	-18,84185	34,69361
MS-005	2022-07-31 00:00:00	sandy clay	*Solanum incanum; Achyranthes aspera; Chromalaena odorata;*	Picada 6	disturbed-long flooding open veld	Floodplain1	MS-005	S5	N/A	N/A
MS-006	2022-07-31 00:00:00	clay	Pan- *Cyperus articulatus; Fuirena sp.; Marsilea; sp. Kyllinga sp.*	Carcass 82, pan nearby	permanent pan margin	Ecotone1	PPG2022-B-82	S6	-18,931265	34,40551
MS-007	2022-07-31 00:00:00	sand	*Hyphaene petersiana; Ziziphus mucronata; Vachellia robusta; Urochloa mossambicensis.*	about 20m from MS006	mixed palm woodland	Woodland4	MS-007	S7	-18,98695	34,26027

MS-008	2022-07-31 00:00:00	sodic sand	*Salvadora persica; Ximenia caffra; Commiphora, Cissus sp.; Eragrostis iocladus; Kalanchoe sp.*	Carcass 103 - 2021	sodic area-shrub and tree patches	Woodland5	PPG2021-B-103	S8	-18,93234	34,40043
MS-008B	2022-07-31 00:00:00	crust on sand	*as above*	N/A	as above	as above	PPG2021-B-103	S8	-18,93234	34,40043
MS-009	2022-08-01 00:00:00	clay	*Combretum adegonium; Millettia stuhlmannii*	Picada 2	tall woodland	Woodland6	MS-009	S9	N/A	N/A
MS-010	2022-08-02 00:00:00	sandy clay	*Ehretia rigida; Ziziphus mucronata; Philenoptera violacea*	Sanctuario; Carcass 104	medium tall woodland	Woodland7	PPG2022-B-104	S10	-18,97759	34,25991
MS-011	2022-08-02 00:00:00	sandy clay	*short grassland; very few herbs*	Carcass 107	floodplain grassland	Floodplain2	PPG2022-B-107	S11	-18,93119	34,39774
MS-011	2022-08-02 00:00:00	sandy clay	*short grassland; very few herbs*	Carcass 107	as above	Floodplain2	PPG2022-B-107	S11	-18,93119	34,39774
MS-013	2022-08-03 00:00:00	clay	*Vachellia robusta; Senegalia nigrescens; Combretum adegonium; Setaria sp.; Urochloa mossambicensis*	Sanctuario; chasing vultures to thick bush	open woodland w medium grasses	Woodland8	MS-013	S13	N/A	N/A
MS-014	2022-08-03 00:00:00	loam	*Vachellia robusta; Boscia salicina; Combretum imberbe; Urochloa mossambicensis*	Picada 1	open woodland w short grasses	woodland9	MS-014	S14	N/A	N/A
MS-016	2022-08-03 00:00:00	loam	*labiatae; Heteropogon contortus*	Carcass 109	medium grassland	Grassland2	PPG2022-B-109	S16	-18,87959	34,32764
MS-018	2022-08-03 00:00:00	clay	*Piliostigma thonningii; Hyphaene petersiana; Combretum adegonium; Combretum imberbe; Setaria sp.; Hyparrhenia hirta*	small road parallel to main road, Sanctuario	medium woodland with tall grasses	Woodland10	MS-018	S18	N/A	N/A
MS-019	2022-08-05 00:00:00	sand	*Combretum appiculatum; Combretum adegonium; Senegalia*	Mhenguere Hill	N/A	N/A	MS-019	S19	N/A	N/A

			nigrescens; Diplorhynchus condylocarpon; Hyparrhenia hirta.							
MS-020	2022-08-08 00:00:00	sandy clay	*Ziziphus mucronata; Gymnosporia heterophylla; Vachellia robusta; Combretum adegonium; Setaria sp.; Panicum maximus*	Carcass 119	open woodland1	Woodland11	PPG2022-B-119	S20	-18,97928	34,34769
MS-021	2022-08-08 00:00:00	clay	*Faidherbia albida; Cynodon dactylon; Chromalaena odorata; Acalypha sp.*	Picada 4	floodplain grassland-woodland margin	Ecotone2	MS-021	S21	N/A	N/A
MS-022	2022-08-09 00:00:00	clay	*Vachellia robusta; Senegalia nigrescens; Setaria sp.; Urochloa mossambicensis*	Sanctuario	grassland-woodland margin	Ecotone3	MS-022	S22	N/A	N/A
MS-023	2022-08-09 00:00:00	sandy clay	*Setaria sp.; Hypoestes; underground Combretum?*	Sanctuario, just beyond 3-lion intersection	distal floodplain	Floodplain3	MS-023	S23	N/A	N/A
MS-024	2022-08-09 00:00:00	sand	*Combretum adegonium;* Termite mound - *Albizia sp.; Grewia sp.; Gymnosporia heterophylla; Hypoestes sp. Achyranthes aspera*	Termite mound	Termite mound	Ecotone4	MS-024	S24	N/A	N/A
MS-025	2022-08-09 00:00:00	loam	*Philenoptera violacea; Combretum adegonium; Heteropogon contortus; Setaria sp. dominating grassland*	grassland nearby to termite mound	grassland nearby to termite mound	Grassland3	MS-025	S25	N/A	N/A
MS-026	2022-08-10 00:00:00	sandy clay	*Vachellia robusta; Sporobolus sp.*	Picada 6	open woodland2	Woodland12	MS-026	S26	-18,94695	34,47123
MS-027	2022-08-11 00:00:00	sandy clay	burned grass	Sanctuario, fresh burned area near camp	Sanctuario1-Miombo	Woodland13	MS-027	S27	-18,99908	34,2368
MS-028	2022-08-11 00:00:00	sandy clay	burned shrubs and grass	Sanctuario, fresh	Sanctuario2-Miombo	Woodland14	MS-028	S28	-18,99908	34,2368

				burned area near camp						

The non-parametric ANOVA gave a P-value of 0,4615973 at a 95% confidence interval. In total, 14 phytolith morphotypes were found across the modern soil samples, i.e., acicular, bulliform, circular, claviform, elongate, flabellate, lobate, oblong, rondel, saddle, scutiform, spheroid, tabular, and trapeziform (see fig. 4.1). Overall, the ecotone vegetation types have an average of about 60% tabular morphotypes, ~8% spheroidal, almost 20% bulliform, and the saddle, trapeziform, along with rondel morphotypes had a means of less than 3% (see fig. 4.2). The floodplain vegetation is comprised of 30% tabular morphotypes, ~20% spheroidal, ~15% for both bulliform and elongate and about 8% of saddle morphotypes. Grassland vegetation composition had tabular morphotypes amounting to almost 38%, lobates close to 20%, and both bulliforms and elongates were less than 12,5%, with a peak of ~8% in rondel morphotypes. On average, woodlands had about 36% tabular morphotypes, ~18% bulliforms, ~20% spheroidal, and close to 8% for both bulliforms and elongates. The bulliform, lobates, spheroidal, and tabular morphotypes were the major contributors to the composition of the different vegetation types (see fig. 4.3). The elongate and lobate morphotypes were consistent in most vegetation types but not all.

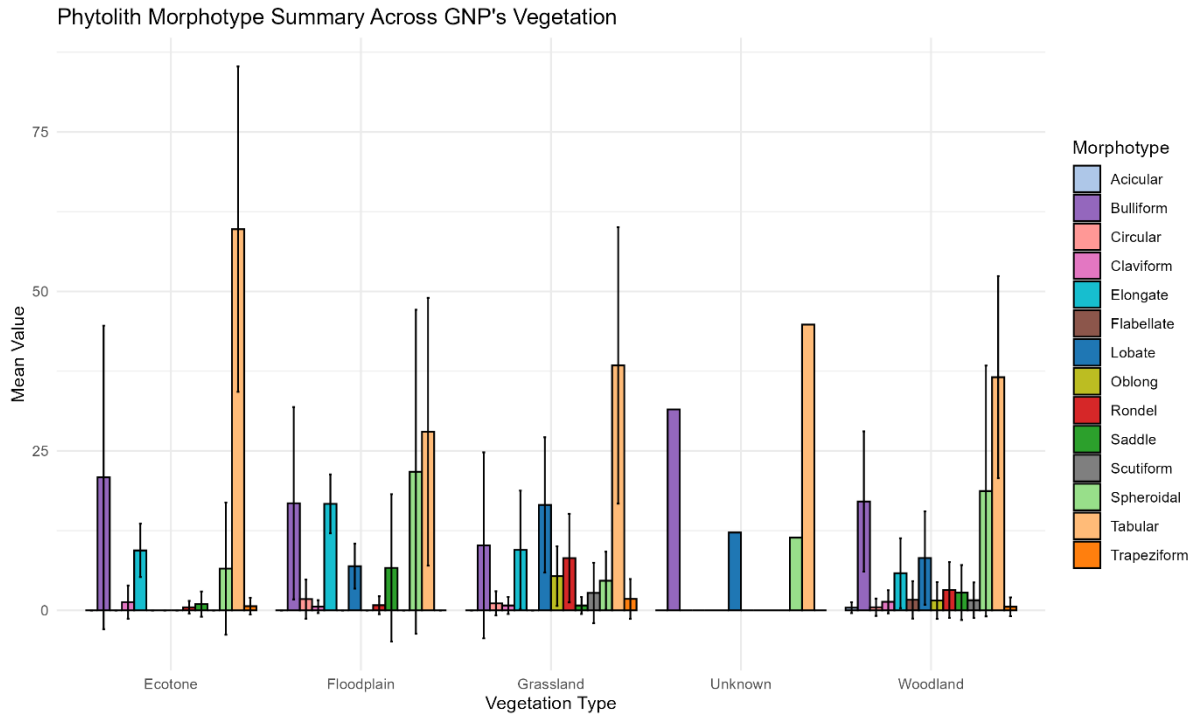


Figure 4.2. The summary of phytolith morphotypes in different biomes at GNP.

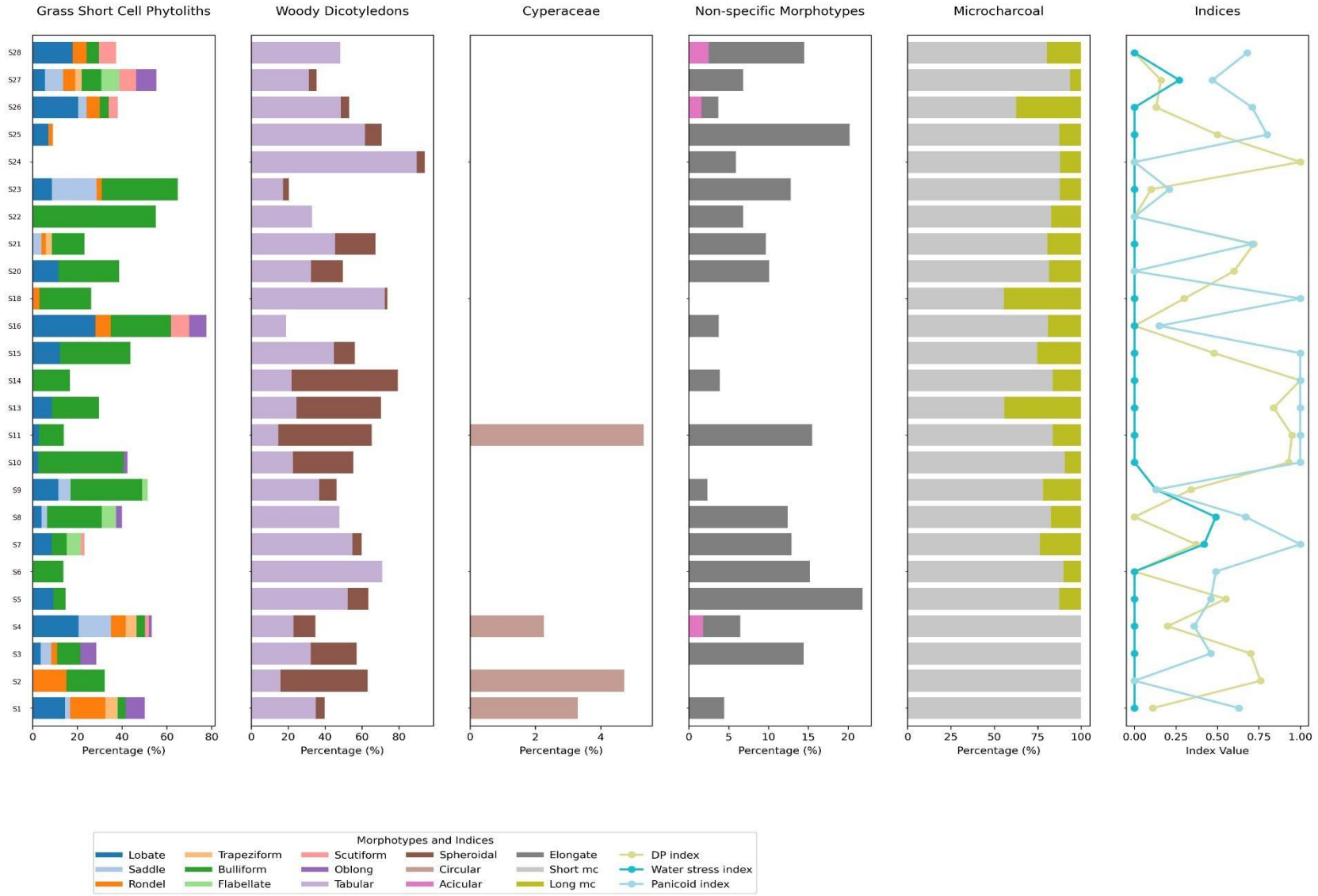


Figure 4.3. Phytolith morphotypes distribution and abundace across Gorongosa National Park.

Out of the 14 phytolith morphotypes, nine belong to grasses (i.e., bulliform, claviform, flabellate, lobate, oblong, saddle, scutiform, and trapeziform), acicular appear in more than one plant group, and elongate in both grasses and trees, spheroidal and tabular morphotypes are associated with woody dicots and Cyperaceae (sedges) with circular morphotypes. The Grass Silica Short-Cells (GSSC) occupied at least 50% of the slides in samples from ecotone 3(S22), floodplain 3(S23), grassland 1(S1) and 2(S16), and woodland 3(S4), 6(S9), and 13(S27) (see fig. 4.3). Majority of samples with 50% or more woody vegetated phytoliths were from woodlands i.e. (S2, S3, S7, S10, S13, S14, S18, and S26), followed by ecotones (S6, S21, S24), floodplains (S5, S11), and grassland (S25). Circular phytolith morphotypes occupied less than 5% of the slides in samples S1 (grassland), woodlands- S2, S4, and S11 (floodplain).

Short microcharcoal dominated all the slides with ≥ 50% coverage in the samples and up to 100% in some. Long microcharcoal had lower percentages.

The water-stress index added up to zero in the ecotones, floodplains, grasslands, and some of the woodlands; a few peaks ranged between 0.3-0.5 in some of the woodlands. The DP and Panicoid indices ranged between 0.0-1.0. The DP index values in the ecotones, floodplains, and woodlands were relatively high, with only a few drops ranging below 0.5-0.0. The Panicoid index overlapped with the DP index occasionally.

Taxa associated with the phytolith morphotypes found in Gorongosa were Arecaceae (palms), grass subfamilies- Aristidoideae, Arundinoideae, Chloridoideae, and Panicoideae, as well as Cyperaceae (see fig. 4.4). On average, the top 3 taxa appearing in different vegetation types arranged from most dominant to least, in the ecotones were Arecaceae (~42%), Panicoideae (close to 18%) and Cyperaceae (< 10%). Arecaceae had a high

percentage and covered about 25% of the floodplains, followed by 23% of Chloridoideae, and 21% of Panicoideae. Grasslands were covered by 25% Panicoideae, 23% Arecaceae, and 17% Aristidoideae. The woodlands were dominated by 38% Arecaceae, 36% Panicoideae, and 22% Chloridoideae. Overall, Arecaceae was the most common taxa in most vegetation types.

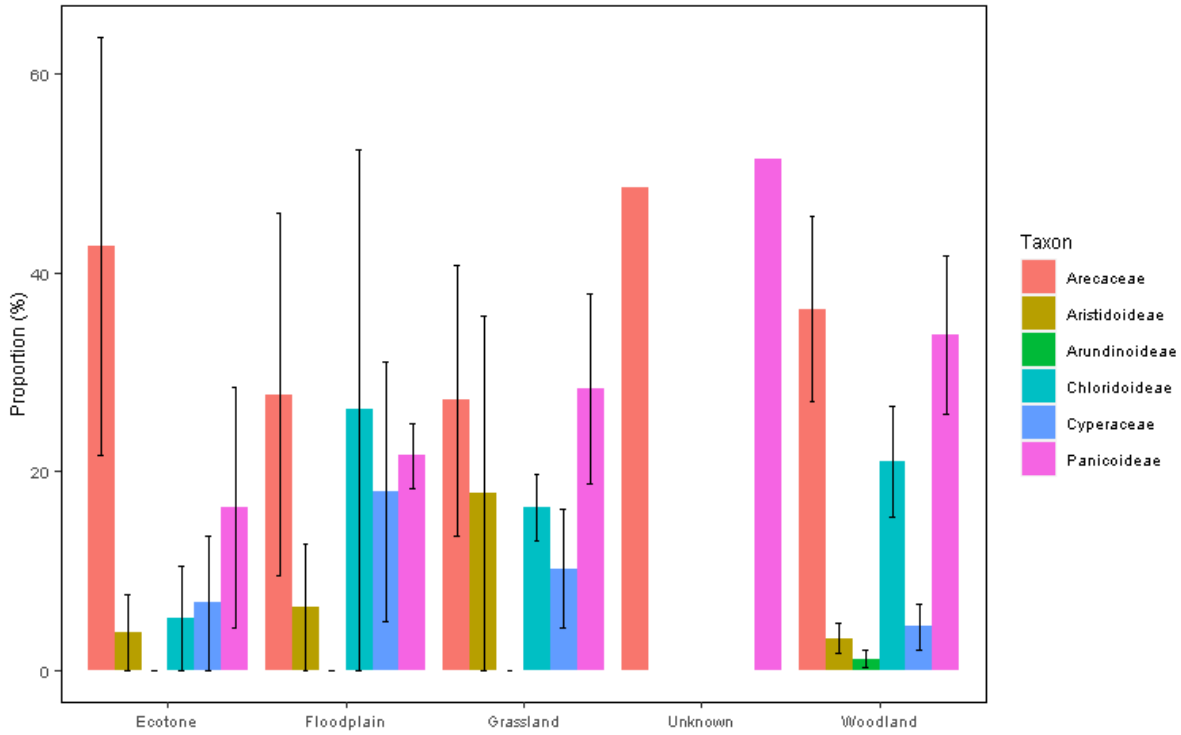


Figure 4.4. Summary of taxa and their proportions in the different vegetation types across Gorongosa National Park.

The PCA plot shows dimension 1 to contribute 24,6 % of the variance and 20,7% for dimension 2 (see fig.4.5). There is also a positive correlation between the DP index and Arecaceae, Panicoid index is clustered together with long microcharcoal (Long mc), Arundinoideae with short microcharcoal (Short mc) and finally, Aristidoideae with

Chloridoideae and Cyperaceae. The water stress index and Arundinoideae point in different directions; the arrows of the variables are orthogonal. The Panicoid index shows a negative correlation to Arundinoideae, Cyperaceae, Aristidoideae, Chloridoideae, and short microcharcoal. Samples 1, 3, 5 and 6 are more similar. Samples 10, 11, and 14 also show similarities. Arecaceae, DP index, microcharcoal (both short and long), Panicoid index and Panicoideae, have longer arrows compared to all the variables. Arundinoideae, Cyperaceae, and the water stress index have shorter arrows compared to the other variables.

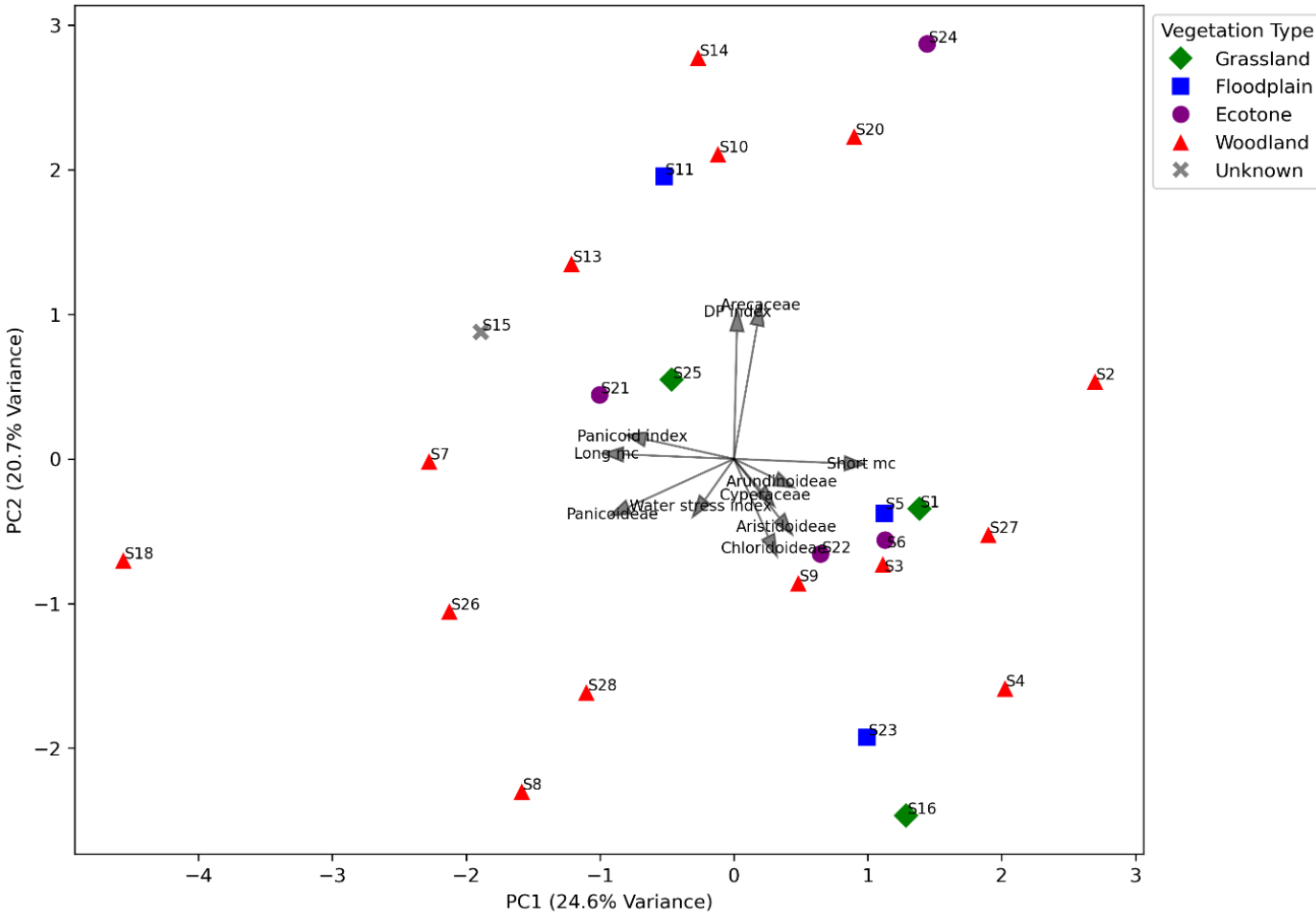


Figure 4.5. The distribution and correlation of multivariable factors influencing the vegetation of GNP.

5. CHAPTER FIVE- DISCUSSION

5.1. Introduction to Discussion

This chapter elaborates on fossil and modern non-pollen palynomorphs, modern pollen and phytoliths as environmental indicators and their viability to reconstruct palaeoenvironments. We dive in on how these micro remains serve palaeoecological significance, aiding us in comparing past and modern ecosystem dynamics.

5.2. Fossil Palynomorphs Preservation

The overall non-pollen palynomorphs (NPPs), pollen, and phytolith preservation were very poor at the GPL-12 Miocene sediment deposit. No phytoliths were observed or recorded from the slides. The pollen count was extremely low due to corrosion, oxidation (Albert *et al*., 2016), possible microbial attack (Havinga, 1967; Zhang *et al*., 2017), and chemical effects in the laboratory. The annual flooding in Gorongosa leaves the area waterlogged for at least 120 days. Waterlogged environments are not be an issue for pollen of some plant species (Turner, 1985), however, after desiccation, the fossil deposits are exposed to direct sunlight that fuels up oxidation (Albert *et al*., 2016; Havinga, 1967; Turner, 1985) and the destruction of pollen, hence the poor preservation. There were also signs of modern roots penetrating the fossil deposits (see fig 3.1); this possibly created modern root contamination that led to microbial activity, hence the low count of palynomorphs and non-pollen palynomorphs in addition to the zero phytolith count.

The Miocene stratigraphic profile also had a lot of layers overlapping each other depicting erosion (Frye, 1949). The depth and rate of the loss of soil implies the source of erosion is water (Balasubramanian, 2017), which supports the notion that Gorongosa was much closer to the sea in the past compared to now (Habermann *et al*., 2019) and GPL-12 had an estuarine environment (Bobe *et al*., 2023).

Although the number of palynomorphs recovered from the Miocene deposits were not enough to reconstruct the palaeoenvironment and palaeoclimate, the Poaceae pollen found tells us that grasses were present in the area, as well as tropical and temperate woody vegetation from cf. Aquifoliaceae and cf. Convolvulaceae (see fig 3.1). Unfortunately, we cannot deduce the abundance and dominance of grasses over woody vegetation; however,

the non-pollen palynomorphs insinuate the terrestrial environment to have been more involved with the aquatic ecosystem.

Fossil NPP records (see Plate 1-3) had arbuscular mycorrhizal fungi- *Glomus* (which is a good indicator for erosion and mycorrhizal relations (Kołaczek *et al*., 2013; van Geel, 2001), as well as coprophilous fungi associated with megafauna (for example, a deinotherium) in fossil deposits (Davis and Shafer, 2006). The *Tomentella* type signifying shallow and stagnant open water (Halbwachs *et al*., 2021), and possibly, an *Iodamoeba* cyst known to occupy the intestines of mammals (Camacho *et al*., 2020) were present. These NPPs support the dendrogram depiction that layers B3, B4, and B13 resemble lacustrine environments (see fig 3.2). It is possible that browsers described by Habermann *et al*., (2019) and other herbivores visited the localities regularly to forage and drink water; hence the coprophilous fungi and intestinal cysts were present in the soil samples. The B8 layer clustered around a marine environment after it produced high numbers of dinocysts and other aquatic eggshells, *Diporotheca* fungi representing eutrophic and/or mesotrophic environments (van Geel, 2011), and *Mangrovia hallii* species (see fig 3.2). This is again supported by Habermann *et al*., (2019), the authors recovered fossil barnacles, and muricid gastropods which are mostly marine species; in addition to the mixture of crocodile, sharks, turtles, suids, and proboscideans evidence suggesting a brackish estuarine environment. The presence of microcharcoal, grass pollen, and *Ustulina deusta* shows the presence of fires, as well as woody vegetation to host the fungal parasite (van Geel, 2001).

Even though the fossil palynomorphs data were not sufficient to quantify to properly produce a viable pollen diagram, their presence still gives a supported insight into the Miocene palaeoenvironment.

5.3. Modern Climate and Vegetation

5.3.1. Pollen Interpretation

Similar to fossil preservation, modern samples yielded very low pollen counts, some with weathered walls due to poor preservation. We suspect that the annual floods alter the soil pH by leaching out some soil minerals and thus increasing oxidation (Havinga, 1967). In addition, microbial activity could be contributing to the low counts (Dimbleby, 1957; 1961) as Gorongosa has a diverse fauna and increasing in population size, therefore, the soil trampling and dung deposits could be adding to bacterial, fungal, and/or microfauna responsible for microbial activities in the soil (Cycoń and Piotrowska-Seget, 2016), hence the microbial attacks on pollen.

Even though the pollen counts were very low, most of the identified pollen grains belonged to shrubby and tall woody dicots and less of the herbaceous (see Plate 4-7). Mark Stalmans and Beilfuss' vegetation mapping in 2008 also reported six different types of grasslands and sixteen different types of woodlands.

Although the pollen count was not quantifiable and viable enough to distinguish similar vegetation types, woody vegetation seems to still be dominant in Gorongosa landscapes, as mentioned by Herrero *et al*., (2017). The pollen species also show diverse habitats in Gorongosa, from tropical to subtropical, temperate, afromontane forests, and rocky outcrops. With more palynological and reconstruction of past environments, we can be able to trace ecological changes and compare these past environments with the current.

5.3.2. Non-pollen palynomorphs

Compared to fossil non-pollen palynomorphs, the modern NPPs were mostly fungal and less marine (see Plate 8-10). The fungal spores were mostly of terrestrial relations rather than of aquatic habitats, possibly due to increased animal interaction with the environment. However, there were a few that showed marine influence such as coccoliths, corolla capsules of a tintinnomorph type, and cf. *Katora arabica*, signifying inland haline intertidal zone (Da Silva *et al*., 2017; Kumar, 2023, Young, 2020). The flooding season could be responsible for haline microbes deposits in the soil. There were also a few freshwater NPPs, i.e. cf. *Inocybe* UY-176, flatworm oocytes, and Unknown Type HdV-182. Coprophilous fungi were the most dominant in most of the slides, along with lignitic fungi, and fungi hosted by woody dicots. Rust fungi cf. *Puccinia* sp. and *Tetraploa aristata*- Type HdV-89 which are pathogens were also present with *Tetraploa* recurring multiple times. Again, these fungi pointed to the dominance of woody vegetation in Gorongosa. The limitations faced again were having at least 50% of the NPPs unidentified because they were unknown.

5.4. Phytolith, Microcharcoal, and Indices

5.4.1. Phytolith Assemblages

Out of all the microscopic remains, phytoliths from modern vegetation were the most well preserved to make viable interpretations (see fig 4.1). Overall, tabular and spheroidal morphotypes dominated most of Gorongosa, meaning that Gorongosa has a high number of woody vegetation as studied by Herrero *et al*., (2017). The spheroids were dominated by spheroidal echinate; palms were responsible for most of the woody cover. Unfortunately, tabular morphotypes are commonly found in all woody dicots and cannot be classified into species or family levels (Rossouw and Scott, 2011). Panicoideae contributed to most lobates

similar to those of Barboni *et al*., (1999), Barboni and Bremond (2009), followed by Chloridoideae. Most saddle morphotypes belonged to Chloridoideae. Aristidoideae and Arundinoideae had the least counts throughout. The phytolith morphotype composition was almost similar in the samples but the means distinguished ecotone vegetation types from grasslands, floodplains, and woodlands (see fig 4.2). Grasslands, woodlands, and floodplains look more similar in terms of phytolith assemblages. Floodplains and woodlands had almost similar percentages of bulliforms, lobates, and spheroidal morphotypes on average, meaning that the woody vegetation cover could be the same in these vegetation types. Moisture content, fire frequencies, and other abiotic and biotic factors are most likely to be the drivers that keep the vegetation dissimilar. Grasslands and woodlands had similar percentages of tabular morphotypes on average, as well as a high diversity of grass phytoliths compared to ecotones and floodplains. Although the different vegetation types had almost similar composition of phytolith morphotypes on average, it does not mean that they have similar plant species occurring in their populations, hence, we looked into grass subfamilies associated with the phytolith morphotype records.

Only C4 grasses were recorded from phytolith results. Only one grass species (*Oryza longistaminata)* using the C3 photosynthetic pathway was recorded by Stalmans and Beilfuss (2008) in a short open to closed pan grassland, but our samples had no C3 grasses, eluding high atmospheric CO2, semi-arid, tropical to subtropical environments (Ehleringer, 2005; Gowik and Westhoff, 2011; Ward *et al*., 1999). Arecaceae (Palms), Panicoideae, and Chloridoideae were the top three plant family and grass subfamilies respectively, to dominate the different vegetation types on average. Panicoideae increased with high occurrences of Arecaceae except in the floodplains where Chloridoideae preceded it. Since Panicoideae are moisture-loving and thrive mostly in humid low environments (Barboni *et*

al., 1999; Bremond *et al*., 2005; Cordova, 2023; Novello *et al*., 2012), in arid areas they are most likely to use woody vegetation as covering to remain in shady areas to preserve moisture in mesophytic environments (Bremond *et al*., 2005). Hence, when the D/P index peaked, the Panicoid index also peaked and lowered when the D/P index decreased. Where the Panicoid index remained low with a D/P index peak, it was an ecotone habitat on a termite mound with sandy soil indicating high aridity, with a water-stress index of 0. The Panicoid index decreased again with a peak of the D/P index where fire frequencies were high and much closer to the site with microcharcoal <100 μm. The water-stress index was mainly 0.0 and could be due to low preservation and count of fan-shaped flabellate phytoliths, or the dry miombo woodlands; also keeping in mind that some of the samples were collected near roads (picada).

Finally, the PCA (see fig. 4.5), showed the dominance of woodlands as mentioned earlier. The majority of the woodlands are positively correlated to long microcharcoal (indicating fires to be further away from the locality for most woody species). The woodlands thrive where the Panicoid index and water-stress index are high, indicating the moisture content in the soil required by trees. Two ecotone samples shifted towards woodlands. Ecotone environments are unstable and can become either grasslands or woodlands depending on moisture, fire frequency and nutrients in the soil. In this case, low fire frequencies and humidity influenced S21 to have more of a woody cover than grasses whereas, S24 was on a sandy picada, however, on a termite mound with high soil nutrition, hence the high percentages of Areceae and D/P index. Four woodland samples (i.e. S3, S4, S9, and S27) were more open with high Chloridoideae, and Aristidoideae content. These two grass subfamilies represent arid environments as well as vegetation openness. Aristidoideae can also indicate highly disturbed areas (Dingaan and Preez, 2017; Rasingam and Parthasarathy,

2009), that can affect the resistance and development of woodlands. Woodlands (S3, S4, and S9) show trends of arid and open habitats, as well as being grouped with grasslands and floodplains. The grazing, frequent fires, low soil moisture content and warm environments are most likely to affect woody dicots and could alter the woody cover and transform them into grasslands after some years.

There was high variability within the floodplains. One was influenced by moisture content (S5) and had high counts of Arundinoideae and Cyperaceae, while one was more arid, dry, and had similarities with grassland (S16). The last floodplain sample behaved more like a woodland with a high D/P index and high Arecaceae counts.

Overall, there has been a significant shift in the climate and environment from the past to the present. Environmental indicators (i.e. pollen, fungi, algae, cysts) show aquatic environments being more inland than today. The different types of grasses and woody vegetation occurring in each area show complicated ecosystem dynamics in vegetation types that may look similar.

Conclusion

There is still a lot to do when it comes to identifying non-pollen palynomorphs. Many of the NPPs found remain unknown thus making the results biased as they skew in one direction depending on how many NPPs we were able to identify and affiliate them to the correct environmental setting. More than 50% of the NPPs were unknown with unknown affiliations and ecology. No other pollen studies have been done in the area; therefore identifying pollen from soil deposits was difficult, especially when the walls are weathered.

Phytoliths favour grasses compared to trees, while pollen favour trees. We can get to grasses subfamilies with phytoliths and identify palms only from phytolith assemblages; tabular morphotypes representing woody dicots are not species-specific, therefore we cannot know the type of woody species present in an ecosystem using phytoliths. However, with pollen, we can get to genera level when identifying shrubs or trees and other herbs except for grasses. Poaceae pollen morphology is similar in most subfamilies and species, they are all monoporate, and pollen walls can be either psilate or granulate and can be affected by the acid treatments in the lab. The ornamentation can be lost as grass pollen does not have a thick wall or exine and thus limits classification to the species level even more. For future research, coring lakes and wetlands should increase the pollen and phytolith counts and reduce the high number of NPPs with improved pollen preservation. Modern sample numbers should be increased with habitats that are more diverse where possible since Gorongosa is a big region. Multiple Miocene locations should be sampled from Gorongosa for comparisons and additions to the Miocene palaeoenvironmental reconstruction studies.

Appendix 1

ICPN 2.0 (Neumann *et al*, 2019)	**Code for CA**
Lobate descriptions from (Barboni and Bremond, 2009)	
Bilobate concave lobes	Bil_con
Bilobate round lobes	Bil_ro
Bilobate truncated lobes	Bil_trun
Bilobate shank narrow + long	Bil_nl
Bilobate shank narrow + short	Bil_ns
Bilobate shank wide + short	Bil_ws
Bilobate with extra-lobe on shank	Bil_xtra
Cross	Cr
Short Saddle	Sad_s
Long Saddle	Sad_l
Rondel	Ron
Trapeziform	Trap
Bulliform	Bul
Tabular gibbate	Tab_gib
Tabular crenate	Tab_cre
Tabular dentate	Tab_den
Tabular faceted	Tab_fac
Tabular aerolate	Tab_aer
Tabular columnar	Tab_col
Tabular granulate	Tab_gran
Tabular pilate	Tab_pi
Tabular psilate	Tab_psi
Spheroidal cavate	S_cav
Spheroidal echinate	S_ech
Spheroidal psilate	S_psi
Flabellate	Fla
Claviform	Clavi
Elongate	Elon
Circular	Cir
Scutiform	Scut
Oblong	Obl
Acicular	Aci

Table 4.3 Raw phytolith counts

Sample	Bil_con	Bil_ro	Bil_trun	Bil_nl	Bil_ns	Bil_ws	Bil_xtra	Cr	Sad_s	Sad_l	Ron	Trap	Bul	Tab_gib	Tab_cre	Tab_den	Tab_fac	Tab_aer	Tab_col	Tab_gran	Tab_pi	Tab_psi	S_cav	S_ech	S_psi	Fla	Clavi	Elon	Cir	Scut	Obl	Aci	Total
S1	32	7	0	0	6	12	13	5	0	12	81	28	19	0	0	19	33	0	0	26	65	37	12	0	13	0	12	23	17	0	44	0	516
S2	0	0	0	0	0	0	0	0	0	0	74	0	83	28	0	0	16	0	0	33	0	0	64	71	95	0	0	0	23	0	0	0	487
S3	0	0	0	0	0	19	0	0	9	16	13	0	55	67	0	0	28	0	0	0	73	0	39	0	91	0	0	75	0	0	37	0	522
S4	17	0	19	70	0	19	0	11	65	32	43	33	25	39	47	0	12	0	0	0	0	54	63	16	0	0	22	31	15	11	9	12	665
S5	0	0	0	15	12	23	0	0	0	0	0	0	29	101	21	64	0	0	0	18	13	63	0	21	39	0	0	117	0	0	0	0	536
S6	0	0	0	0	0	0	0	0	0	0	0	0	61	123	76	26	42	0	0	56	0	0	0	0	0	0	0	67	0	0	0	0	451
S7	11	0	0	0	0	28	0	0	0	0	0	0	31	0	0	17	66	0	0	13	91	64	0	23	0	29	19	59	0	7	0	0	458
S8	9	0	0	0	0	11	0	0	12	0	0	0	121	53	0	12	0	0	0	21	56	93	0	0	0	31	0	61	0	0	13	0	493
S9	19	0	0	9	11	9	17	0	19	11	0	0	179	12	0	53	9	0	12	96	0	23	9	31	13	14	0	13	0	0	0	0	559
S10	0	0	0	0	0	0	0	13	0	0	0	0	193	16	0	23	0	11	0	35	0	29	45	28	93	0	11	0	0	0	9	0	506
S11	0	0	0	0	0	13	0	0	0	0	0	0	50	0	0	0	0	0	0	23	0	43	0	139	90	0	0	70	24	0	0	0	452
S13	0	0	0	22	0	0	0	18	0	0	0	0	98	0	0	0	0	14	0	29	0	71	7	142	63	0	0	0	0	0	0	0	464
S14	0	0	0	0	0	0	0	0	0	0	0	0	77	17	0	32	0	0	0	31	0	21	9	257	0	0	0	18	0	0	0	0	462
S15	0	0	0	0	15	23	0	21	0	0	0	0	152	51	0	46	0	0	0	61	0	58	21	34	0	0	0	0	0	0	0	0	482
S16	0	0	0	55	21	33	0	17	0	0	31	0	121	0	0	23	29	0	0	0	0	32	0	0	0	0	0	17	0	37	34	0	450
S18	0	0	0	0	0	0	0	0	0	0	14	0	104	64	0	69	0	0	42	63	0	88	6	0	0	0	0	0	0	0	0	0	450
S20	12	0	0	0	0	0	14	28	0	0	0	0	126	33	0	31	0	0	0	86	0	0	24	23	34	0	7	47	0	0	0	0	465
S21	0	0	0	0	0	0	0	0	18	0	9	12	66	56	0	23	67	0	0	39	21	0	19	21	59	0	0	44	0	0	0	0	454
S22	0	0	0	0	0	0	0	0	0	0	0	0	275	48	0	68	0	0	0	48	0	0	0	0	0	0	26	34	0	0	0	0	499
S23	0	0	0	0	0	39	0	0	91	0	11	0	154	19	0	18	0	0	0	41	0	0	0	0	15	0	8	58	0	0	0	0	454
S24	0	0	0	0	0	0	0	0	0	0	0	0	0	21	0	16	356	0	0	77	0	0	11	12	0	0	0	31	0	0	0	0	524
S25	0	0	0	0	0	17	0	15	0	0	9	0	0	23	0	0	103	0	0	88	0	64	12	29	0	0	0	91	0	0	0	0	451
S26	0	0	0	13	19	64	0	19	22	0	33	0	23	39	11	41	91	0	0	26	0	67	11	15	0	0	29	12	0	23	0	9	567
S27	0	0	5	7	13	0	20	0	65	0	44	23	71	0	21	42	31	0	0	0	67	91	0	33	0	65	21	55	0	61	72	0	807
S28	0	0	0	45	16	33	0	0	0	0	33	0	29	0	91	40	54	0	0	0	0	69	0	0	0	0	0	63	0	40	0	13	526

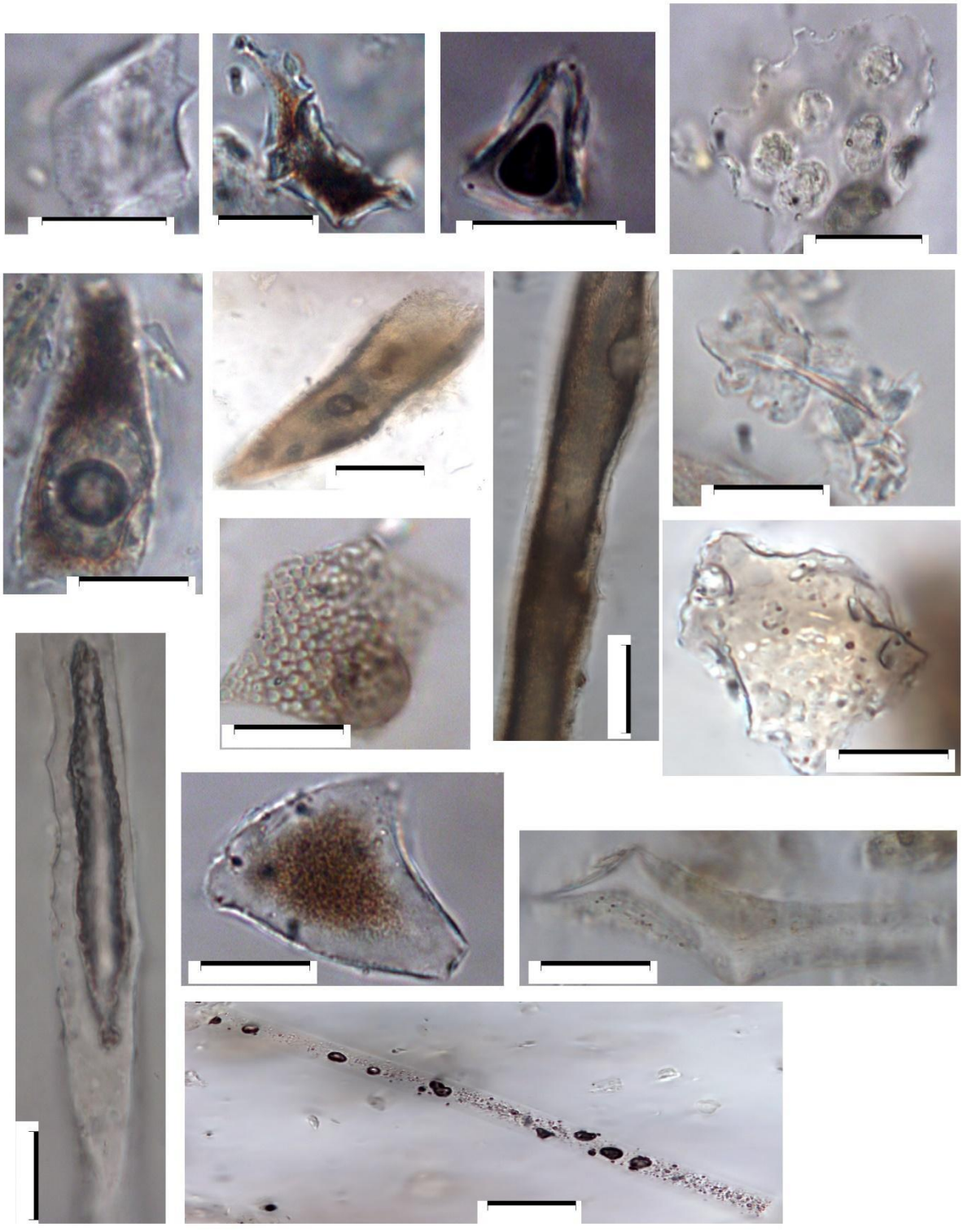


Figure 4.6 Other phytolith morphotypes occurring in the modern samples. Scale bar = 10 µm.

Table 4.5 Non-parametric ANOVA test on morphotypes

	Morphotype	p_value
1	Acicular	0.4615973
2	Bulliform	0.4615973
3	Circular	0.4615973
4	Claviform	0.4615973
5	Elongate	0.4615973
6	Flabellate	0.4615973
7	Lobate	0.4615973
8	Oblong	0.4615973
9	Rondel	0.4615973
10	Saddle	0.4615973
11	Scutiform	0.4615973
12	Spheroidal	0.4615973
13	Tabular	0.4615973
14	Trapeziform	0.4615973

REFERENCES

Albano, G., 2002. Tropical secondary forest management in Africa. Mozambique country report.

Albert, R.M., Lavi, O., Estroff, L., Weiner, S., Tsatskin, A., Ronen, A. and Lev-Yadun, S., 1999. Mode of occupation of Tabun Cave, Mt Carmel, Israel during the Mousterian period: a study of the sediments and phytoliths. Journal of Archaeological Science, 26(10), pp.1249-1260.

Albert, R.M. and Weiner, S., 2001. Study of phytoliths in prehistoric ash layers from Kebara and Tabun caves using a quantitative approach. Phytoliths: applications in earth sciences and human history, pp.251-266.

Albert, R.M., Bamford, M.K. and Cabanes, D., 2006. Taphonomy of phytoliths and macroplants in different soils from Olduvai Gorge (Tanzania) and the application to Plio-Pleistocene palaeoanthropological samples. Quaternary International, 148(1), pp.78-94.

Albert, R.M., Bamford, M.K. and Cabanes, D., 2009. Palaeoecological significance of palms at Olduvai Gorge, Tanzania, based on phytolith remains. Quaternary International, 193(1-2), pp.41-48.

Albert, B., Innes, J., Blackford, J., Taylor, B., Conneller, C. and Milner, N., 2016. Degradation of the wetland sediment archive at Star Carr: An assessment of current palynological preservation. Journal of Archaeological Science: Reports, 6, pp.488-495.

Alexandré, A., Meunier, J.D., Lézine, A.M., Vincens, A. and Schwartz, D., 1997. Phytoliths: indicators of grassland dynamics during the late Holocene in intertropical Africa. Palaeogeography, Palaeoclimatology, Palaeoecology, 136(1-4), pp.213-229.

Anikster, Y., Bushnell, W.R., Roelfs, A.P., Eilam, T. and Manisterski, J., 1997. Puccinia recondita causing leaf rust on cultivated wheats, wild wheats, and rye. Canadian journal of botany, 75(12), pp.2082-2096.

Anthelme, F., Abdoulkader, A. and Viane, R., 2011. Are ferns in arid environments underestimated? Contribution from the Saharan Mountains. Journal of Arid Environments, 75(6), pp.516-523.

Archibald, S., Staver, A.C. and Levin, S.A., 2012. Evolution of human-driven fire regimes in Africa. Proceedings of the National Academy of Sciences, 109(3), pp.847-852.

Balasubramanian, A., 2017. Soil erosion–causes and effects. Centre for Advanced Studies in Earth Science, University of Mysore, Mysore, 12, p.12.

Bamford, M. and Pickford, M., 2021. Stratigraphy, chronology and palaeontology of the Tertiary rocks of the Cheringoma Plateau, Mozambique. Fossil Imprint, 77(1), pp.187-213.

Barboni, D., Bonnefille, R., Alexandre, A. and Meunier, J.D., 1999. Phytoliths as paleoenvironmental indicators, west side Middle Awash Valley, Ethiopia. Palaeogeography, Palaeoclimatology, Palaeoecology, 152(1-2), pp.87-100.

Barboni, D., Bremond, L. and Bonnefille, R., 2007. Comparative study of modern phytolith assemblages from inter-tropical Africa. Palaeogeography, Palaeoclimatology, Palaeoecology, 246(2-4), pp.454-470.

Barboni, D. and Bremond, L., 2009. Phytoliths of East African grasses: an assessment of their environmental and taxonomic significance based on floristic data. Review of Palaeobotany and Palynology, 158(1-2), pp.29-41

Bengtsson, J., Bullock, J.M., Egoh, B., Everson, C., Everson, T., O'connor, T., O'farrell, P., Smith, H.G. and Lindborg, R., 2019. Grasslands—more important for ecosystem services than you might think. Ecosphere, 10(2), p.e02582.

Berihuete-Azorin, M., Kerfant, C., Allué, E., Burguet-Coca, A., Burjachs, F., Expósito Barea, I., Fernández Iriarte, T., Garay Palacios, B., Revelles, J., Robledo, A. and Rodríguez Antón, D., 2023. Archaeobotany in an era of change and challenge: potential and fragility of macro- and micro-remains. *World Archaeology*, *55*(3), pp.299-314.

Björck, S., Persson, T. and Kristersson, I., 1978. Comparison of two concentration methods for pollen in minerogenic sediments. Geologiska Föreningen i Stockholm Förhandlingar, 100(1), pp.107-111.

Blair, J., Nippert, J. and Briggs, J., 2014. Grassland ecology 14. Ecology and the Environment, 389, pp.389-423.

Bobe, R. and Behrensmeyer, A.K., 2004. The expansion of grassland ecosystems in Africa in relation to mammalian evolution and the origin of the genus Homo. Palaeogeography, Palaeoclimatology, Palaeoecology, 207(3-4), pp.399-420.

Bobe, R., 2006. The evolution of arid ecosystems in eastern Africa. Journal of Arid Environments, 66(3), pp.564-584.

Bobe, R., Martinez, F. and Carvalho, S., 2020. Primate adaptations and evolution in the Southern African Rift Valley. Evolutionary Anthropology, 29(3), pp. 94-101.

Bobe, R., Aldeias, V., Alemseged, Z., Archer, W., Aumaître, G., Bamford, M.K., Biro, D., Bourlès, D.L., Braun, D.R., Capelli, C. and Coelho, J.D.O., 2021. The first Miocene fossils from coastal woodlands in the southern East African Rift. bioRxiv.

Bobe, R., Aldeias, V., Alemseged, Z., Anemone, R.L., Archer, W., Aumaître, G., Bamford, M.K., Biro, D., Bourlès, D.L., Boyd, M.D. and Braun, D.R., 2023. The first Miocene fossils from coastal woodlands in the southern East African Rift. Iscience, 26(9), p.107644

Böhme, B., 2005. Geoecology of the Lake Urema/Central Mozambique. Freiberg Online Geology, 14, pp.1-114.

Böllmann, J. and Scholler, M., 2006. Life cycle and life strategy features of Puccinia glechomatis (Uredinales) favorable for extending the natural range of distribution. Mycoscience, 47(3), pp.152-158.

Bond, W.J., Midgley, G.F. and Woodward, F.I., 2003. The importance of low atmospheric CO2 and fire in promoting the spread of grasslands and savannas. Global Change Biology, 9(7), pp.973-982.

Bonnefille, R., 2010. Cenozoic vegetation, climate changes and hominid evolution in tropical Africa. Global and Planetary Change, 72(4), pp.390-411.

Bouley, P., Paulo, A., Angela, M., Du Plessis, C. and Marneweck, D.G., 2021. The successful reintroduction of African wild dogs (Lycaon pictus) to Gorongosa National Park, Mozambique. PLoS One, 16(4), p.e0249860.

Breman, E., Ekblom, A., Gillson, L. and Norström, E., 2019. Phytolith-based environmental reconstruction from an altitudinal gradient in Mpumalanga, South Africa, 10,600 BP–present. Review of Palaeobotany and Palynology, 263, pp.104-116.

Bremond, L., Alexandre, A., Peyron, O. and Guiot, J., 2005. Grass water stress estimated from phytoliths in West Africa. Journal of Biogeography, 32(2), pp.311-327.

Camacho, M., Perri, A. and Reinhard, K., 2020. Parasite microremains: preservation, recovery, processing, and identification. Handbook for the analysis of micro-particles in archaeological samples, pp.173-199.

Carlier, L., Rotar, I., Vlahova, M. and Vidican, R., 2009. Importance and functions of grasslands. Notulae Botanicae Horti Agrobotanici Cluj-Napoca, 37(1), pp.25-30.

Clayton, W.D., 1981. Evolution and distribution of grasses. Annals of the Missouri Botanical Garden, pp.5-14.

Coelho, J.D.O., Anemone, R.L. and Carvalho, S., 2021. Unsupervised learning of satellite images enhances discovery of late Miocene fossil sites in the Urema Rift, Gorongosa, Mozambique. PeerJ, 9, p.e11573.

Cordova, C.E., 2023. Soil surface grass phytolith morphotypes across bioclimatic gradients and biomes at about latitude 29° S in South Africa. Review of Palaeobotany and Palynology, 313, p.104887.

Cron, G.V., 2005. Cineraria L.(Senecioneae, Asteraceae)-its taxonomy, phylogeny, phytogeography and conservation (Doctoral dissertation).

Cycoń, M. and Piotrowska-Seget, Z., 2016. Pyrethroid-degrading microorganisms and their potential for the bioremediation of contaminated soils: a review. Frontiers in microbiology, 7, p.1463.

Daskin, J.H., Stalmans, M. and Pringle, R.M., 2016. Ecological legacies of civil war: 35-year increase in savanna tree cover following wholesale large-mammal declines. Journal of Ecology, 104(1), pp.79-89.

Davis, O.K. and Shafer, D.S., 2006. Sporormiella fungal spores, a palynological means of detecting herbivore density. Palaeogeography, Palaeoclimatology, Palaeoecology, 237(1), pp.40-50.

Dietre, B., Gauthier, É. and Gillet, F., 2012. Modern pollen rain and fungal spore assemblages from pasture woodlands around Lake Saint-Point (France). Review of Palaeobotany and Palynology, 186, pp.69-89.

Dimbleby, G.W., 1957. Pollen analysis of terrestrial soils. The New Phytologist, 56(1), pp.12-28.

DIMBLEBY, G., 1961. Soil pollen analysis. Journal of Soil Science, 12(1), pp.1-10.

Doidge, E.M., 1921. SOUTH AFRICAN PERISPORIACEAE: VI. The Haustoria of the Genera Meliola and Irene. Transactions of the Royal Society of South Africa, 9(2), pp.117-127.

Edwards, T.J., Beaumont, A.J. and Styles, D., 2001. New records and distributional disjunctions from South Africa, Zimbabwe and Mozambique. Bothalia, 31(2), pp.200-202.

Edwards, E.J. and Smith, S.A., 2010. Phylogenetic analyses reveal the shady history of C4 grasses. Proceedings of the National Academy of Sciences, 107(6), pp.2532-2537.

Edwards, E.J., Osborne, C.P., Strömberg, C.A., Smith, S.A., C4 Grasses Consortium, Bond, W.J., Christin, P.A., Cousins, A.B., Duvall, M.R., Fox, D.L. and Freckleton, R.P., 2010. The origins of C4 grasslands: integrating evolutionary and ecosystem science. science, 328(5978), pp.587-591.

Ehleringer, J.R. and Monson, R.K., 1993. Evolutionary and ecological aspects of photosynthetic pathway variation. Annual Review of Ecology and Systematics, pp.411-439.

Ehleringer, J.R., Cerling, T.E. and Helliker, B.R., 1997. C 4 photosynthesis, atmospheric CO 2, and climate. Oecologia, 112, pp.285-299.

Ehleringer, J.R., 2005. The influence of atmospheric CO2, temperature, and water on the abundance of C3/C4 taxa. In A history of atmospheric CO2 and its effects on plants, animals, and ecosystems (pp. 214-231). New York, NY: Springer New York.

Faegri, K., Kaland, P.E. and Krzywinski, K., 1989. Textbook of pollen analysis (No. Ed. 4). John Wiley & Sons Ltd.

Fitchett, J.M. and Bamford, M.K., 2017. The validity of the Asteraceae: Poaceae fossil pollen ratio in discrimination of the southern African summer-and winter-rainfall zones. Quaternary Science Reviews, 160, pp.85-95.

French, T.J., 2009. " Like Leaves Fallen by Wind": Resilience, Remembrance and the Restoration of Landscapes in Central Mozambique (Doctoral dissertation, Boston University).

Frye, J.C., 1949. Use of fossil soils in Kansas Pleistocene stratigraphy. Transactions of the Kansas Academy of Science (1903-), 52(4), pp.478-482.

Gallaher, T.J., Peterson, P.M., Soreng, R.J., Zuloaga, F.O., Li, D.Z., Clark, L.G., Tyrrell, C.D., Welker, C.A., Kellogg, E.A. and Teisher, J.K., 2022. Grasses through space and time: An overview of the biogeographical and macroevolutionary history of Poaceae. Journal of Systematics and Evolution, 60(3), pp.522-569.

Gelorini, V., Verbeken, A., van Geel, B., Cocquyt, C. and Verschuren, D., 2011. Modern non-pollen palynomorphs from East African lake sediments. Review of Palaeobotany and Palynology, 164(3-4), pp.143-173.

Geppert, M., Riedel, F., Gummersbach, V.S., Gutjahr, S., Hoelzmann, P., Garzón, M.D.R., Shemang, E.M. and Hartmann, K., 2021. Late Pleistocene hydrological settings at world heritage Tsodilo Hills (NW Kalahari, Botswana), a site of ancient human occupation. *Quaternary Science Advances*, *3*, p.100022.

Goldblatt, P., 1983. Geography of Iridaceae in Africa. Bothalia, 14(3/4), pp.559-564.

Goldblatt, P., Le Thomas, A. and Suarez-Cervera, M., 2004. Phylogeny of the Afro-Madagascan Aristea (Iridaceae) revisited in the light of new data on pollen morphology. Botanical Journal of the Linnean Society, 144(1), pp.41-68.

Gowik, U. and Westhoff, P., 2011. The path from C3 to C4 photosynthesis. Plant physiology, 155(1), pp.56-63.

Grass Phylogeny Working Group, Barker, N.P., Clark, L.G., Davis, J.I., Duvall, M.R., Guala, G.F., Hsiao, C., Kellogg, E.A., Linder, H.P., Mason-Gamer, R.J. and Mathews, S.Y., 2001. Phylogeny and subfamilial classification of the grasses (Poaceae). Annals of the Missouri Botanical Garden, pp.373-457.

Guyton, J.A., Pansu, J., Hutchinson, M.C., Kartzinel, T.R., Potter, A.B., Coverdale, T.C., Daskin, J.H., da Conceição, A.G., Peel, M.J., Stalmans, M.E. and Pringle, R.M., 2020. Trophic rewilding revives biotic resistance to shrub invasion. Nature Ecology & Evolution, 4(5), pp.712-724.

Haas, J.N., 1996. Neorhabdocoela oocytes—palaeoecological indicators found in pollen preparations from Holocene freshwater lake sediments. Review of Palaeobotany and Palynology, 91(1-4), pp.371-382.

Habermann, J.M., Alberti, M., Aldeias, V., Alemseged, Z., Archer, W., Bamford, M., Biro, D., Braun, D.R., Capelli, C., Cunha, E. and da Silva, M.F., 2019. Gorongosa by the sea: First Miocene fossil sites from the Urema Rift, central Mozambique, and their coastal paleoenvironmental and paleoecological contexts. Palaeogeography, Palaeoclimatology, Palaeoecology, 514, pp.723-738.

Halbritter, H., 1998. Preparing living pollen material for scanning electron microscopy using 2, 2-dimethoxypropane (DMP) and critical-point drying. Biotechnic & Histochemistry, 73(3), pp.137-143.

Halbritter, H., Ulrich, S., Grímsson, F., Weber, M., Zetter, R., Hesse, M., Buchner, R., Svojtka, M. and Frosch-Radivo, A., 2018. Illustrated pollen terminology. Springer.

Halbwachs, H., Bässler, C. and Worobiec, E., 2021. Palynomorphs in Baltic, Bitterfeld and Ukrainian ambers: a comparison. Palynology, 45(3), pp.441-457.

Havinga, A.J., 1967. Palynology and pollen preservation. Review of Palaeobotany and Palynology, 2(1-4), pp.81-98.

Herman, P.P.J., 2002. Revision of the Tarchonanthus camphoratus complex (Asteraceae-Tarchonantheae) in southern Africa. Bothalia, 32(1), pp.21-28.

Hernández-Restrepo, M., Mena-Portales, J., Gené, J., Cano, J. and Guaarro, J., 2013. New Bactrodesmiastrum and Bactrodesmium from decaying wood in Spain. Mycologia, 105(1), pp.172-180.

Herrero, H.V., Southworth, J., Bunting, E. and Child, B., 2017. Using Repeat Photography to Observe Vegetation Change Over Time in Gorongosa National Park. African Studies Quarterly, 17(2).

Herrero, H., Waylen, P., Southworth, J., Khatami, R., Yang, D. and Child, B., 2020. A Healthy Park Needs Healthy Vegetation: The Story of Gorongosa National Park in the 21st Century. Remote Sensing, 12(3), p.476.

Hopley, P.J., Reade, H., Parrish, R., De Kock, M. and Adams, J.W., 2019. Speleothem evidence for C3 dominated vegetation during the Late Miocene (Messinian) of South Africa. *Review of Palaeobotany and Palynology*, *264*, pp.75-89.

Huntley, B.J., 2023. Gorongosa National Park: Wilderness, War and Wildlife Recovery. In Strategic Opportunism: What Works in Africa: Twelve Fundamentals for Conservation Success (pp. 39-51). Cham: Springer Nature Switzerland.

Jacobs, B.F., 2004. Palaeobotanical studies from tropical Africa: relevance to the evolution of forest, woodland and savannah biomes. Philosophical Transactions of the Royal Society of London. Series B: Biological Sciences, 359(1450), pp.1573-1583.

Karpinska-Kolaczek, M., Kolaczek, P., Heise, W. and Worobiec, G., 2010. Tetraploa aristata Berkeley and Broome (Fungi, Pleosporales), a new taxon to Poland. Acta Societatis Botanicorum Poloniae, 79(3).

Kealhofer, L. and Piperno, D.R., 1998. Opal phytoliths in Southeast Asian flora. Smithsonian contributions to botany, 88, pp.1-43.

Kellogg, E.A., 2001. Evolutionary history of the grasses. Plant physiology, 125(3), pp.1198-1205.

Kołaczek, P., Zubek, S., Błaszkowski, J., Mleczko, P. and Margielewski, W., 2013. Erosion or plant succession—How to interpret the presence of arbuscular mycorrhizal fungi

(Glomeromycota) spores in pollen profiles collected from mires. Review of Palaeobotany and Palynology, 189, pp.29-37.

Kumar, A., 2023. New form taxa of non-pollen palynomorphs (NPP) from southern Red Sea coastal sediments of Saudi Arabia. Geophytology, 53(1), pp.1-24.

Lamb, W.H., 1912. The phylogeny of grasses. The Plant World, 15(11), pp.264-269.

Leal, A., Martínez-Blanco, X., Beri, Á. and del Puerto, L., 2021. A combined catalog of non-pollen palynomorphs (NPPs) of fungal origin from soil and airborne samples of Uruguay. Review of Palaeobotany and Palynology, 293, p.104488.

Lehmann, C.E., Anderson, T.M., Sankaran, M., Higgins, S.I., Archibald, S., Hoffmann, W.A., Hanan, N.P., Williams, R.J., Fensham, R.J., Felfili, J. and Hutley, L.B., 2014. Savanna vegetation-fire-climate relationships differ among continents. Science, 343(6170), pp.548-552.

Linder, H.P., 1987. The evolutionary history of the Poales/Restionales: a hypothesis. Kew Bulletin, pp.297-318.

Macphail, M.K. and Hill, R.S., 2002. Palaeobotany of the Poaceae. Flora of Australia, 43, pp.37-70.

Maroyi, A., 2014. Traditional and medicinal uses of essential oil producing tree Sclerocarya birrea in south-central Zimbabwe. Journal of Essential Oil Bearing Plants, 17(5), pp.776-786.

Maroyi, A., 2019. Boscia salicifolia: review of its botany, medicinal uses, phytochemistry and biological activities. Journal of Pharmaceutical Sciences and Research, 11(8), pp.3055-3060.

Masubelele, M.L., Hoffman, M.T., Bond, W.J. and Gambiza, J., 2014. A 50 year study shows grass cover has increased in shrublands of semi-arid South Africa. Journal of Arid Environments, 104, pp.43-51.

Mbenoun, M., Momo Zeutsa, E.H., Samuels, G., Nsouga Amougou, F. and Nyasse, S., 2008. Dieback due to Lasiodiplodia theobromae, a new constraint to cocoa production in Cameroon. Plant Pathology, 57(2).

McWethy, D.B., Neumann, F.H., Steinbruch, F., Ryan, C.M. and Valsecchi, V., 2016. Late Quaternary vegetation development and disturbance dynamics from a peatland on Mount Gorongosa, central Mozambique. Quaternary Science Reviews, 137, pp.221-233.

Meeuse, A.D.J., 1957. The South African Convolvulaceae. Bothalia, 6(4), pp.643-792.

Moran, V.C., Hoffmann, J.H., Donnelly, D., Zimmermann, H.G., Van Wilgen, B.W. and Spencer, N.R., 2000, July. Biological control of alien, invasive pine trees (Pinus species) in South Africa. In Proceedings of the X international symposium on biological control of weeds (Vol. 941, pp. 941-953). Bozeman, MT, USA: Montana State University.

Moremi, M.P., Makolo, F., Viljoen, A.M. and Kamatou, G.P., 2021. A review of biological activities and phytochemistry of six ethnomedicinally important South African Croton species. Journal of Ethnopharmacology, 280, p.114416.

Muala, D.J., 2016. Gorongosa: A history of an African landscape, 1921-2014. Utah State University.

Muok, B.O., Matsumura, A., Ishii, T. and Odee, D.W., 2007. Genetic diversity within Sclerocarya birrea populations in Kenya. Journal of arid environments, 71(1), pp.1-11.

Murungi, M.L., 2017. Phytoliths at Sibudu (South Africa): implications for vegetation, climate and human occupation during the MSA (Doctoral Dissertation, University of the Witwatersrand).

Murungi, M.L. and Bamford, M.K., 2020. Revised taxonomic interpretations of Cyperaceae phytoliths for (paleo) botanical studies with some notes on terminology. Review of Palaeobotany and Palynology, 275, p.104189.

Neumann, F.H., Stager, J.C., Scott, L., Venter, H.J. and Weyhenmeyer, C., 2008. Holocene vegetation and climate records from lake Sibaya, KwaZulu-Natal (South Africa). Review of Palaeobotany and Palynology, 152(3-4), pp.113-128.

Neumann, F.H. and Bamford, M.K., 2015. Shaping of modern southern African biomes: Neogene vegetation and climate changes. Transactions of the Royal Society of South Africa, 70(3), pp.195-212.

Novello, A., Barboni, D., Berti-Equille, L., Mazur, J.C., Poilecot, P. and Vignaud, P., 2012. Phytolith signal of aquatic plants and soils in Chad, Central Africa. Review of Palaeobotany and Palynology, 178, pp.43-58.

Nzei, J.M., Ngarega, B.K., Mwanzia, V.M., Musili, P.M., Wang, Q.F. and Chen, J.M., 2021. The past, current, and future distribution modeling of four water lilies (Nymphaea) in Africa indicates varying suitable habitats and distribution in climate change. Aquatic Botany, 173, p.103416.

Oberlander, K.C., Roets, F. and Dreyer, L.L., 2014. Pre-Pleistocene origin of an endangered habitat: links between vernal pools and aquatic Oxalis in the Greater Cape Floristic Region of South Africa. Journal of Biogeography, 41(8), pp.1572-1582.

Owen, R., 2004. The Millennium Ecosystem Assessment (MA): GM SAFMA Hydrogeology condition and trend report. Mineral Resources Centre, University of Zimbabwe.

Palmer, A.R. and Ainslie, A.M., 2005. Grasslands of South Africa. Grasslands of the World, 34, p.77.

Piasai, O. and Sudsanguan, M., 2018. Morphological study of Gelasinospora from dung and antagonistic effect against plant pathogenic fungi in vitro. Agriculture and Natural Resources, 52(5), pp.407-411.

Pickford, M., 2013. Gorongosa palaeontology survey. Retrieved from Gorongosa National Park.

Polissar, P.J., Rose, C., Uno, K.T., Phelps, S.R. and Demenocal, P., 2019. Synchronous rise of African C4 ecosystems 10 million years ago in the absence of aridification. Nature Geoscience, 12(8), pp.657-660.

Poswa, S.B., Manyevere, A. and Mashamaite, C.V., 2024. Responses of fungal diversity and community composition after 42 years of prescribed fire frequencies in semi-arid savanna rangelands. Frontiers in Environmental Science, 12, p.1355278.

Prasad, V., Stromberg, C.A., Alimohammadian, H. and Sahni, A., 2005. Dinosaur coprolites and the early evolution of grasses and grazers. Science, 310(5751), pp.1177-1180.

Pringle, R.M. and Gonçalves, D., 2022. Gorongosa National Park, Mozambique. Routledge Handbook of Rewilding.

Retallack, G.J., 1992. Middle Miocene fossil plants from Fort Ternan (Kenya) and evolution of African grasslands. Paleobiology, 18(4), pp.383-400.

Revelles, J. and Van Geel, B., 2016. Human impact and ecological changes in lakeshore environments. The contribution of non-pollen palynomorphs in Lake Banyoles (NE Iberia). Review of Palaeobotany and Palynology, 232, pp.81-97.

Robbrecht, E., 1982. Pollen morphology of the tribes Anthospermeae and Paederieae (Rubiaceae) in relation to taxonomy. Bulletin du Jardin botanique national de Belgique/Bulletin van de Nationale Plantentuin van Belgie, pp.349-366.

Roberts, D.L., Matthews, T., Herries, A.I., Boulter, C., Scott, L., Dondo, C., Mtembi, P., Browning, C., Smith, R.M., Haarhoff, P. and Bateman, M.D., 2011. The regional and global context of the Late Cenozoic Langebaanweg (LBW) palaeontological site: West Coast of South Africa. Earth-Science Reviews, 106(3-4), pp.191-214.

Roberts, D.L., Sciscio, L., Herries, A.I., Scott, L., Bamford, M.K., Musekiwa, C. and Tsikos, H., 2013. Miocene fluvial systems and palynofloras at the southwestern tip of Africa: Implications for regional and global fluctuations in climate and ecosystems. Earth-science reviews, 124, pp.184-201.

Rossouw, L. and Scott, L., 2011. Phytoliths and pollen, the microscopic plant remains in Pliocene volcanic sediments around Laetoli, Tanzania. Paleontology and Geology of Laetoli: Human Evolution in Context: Volume 1: Geology, Geochronology, Paleoecology and Paleoenvironment, pp.201-215.

Rossouw, L., 2009. The application of fossil grass-phytolith analysis in the reconstruction of Cainozoic environments in the South African interior (Doctoral dissertation, University of the Free State).

Sage, R.F., 2004. The evolution of C4 photosynthesis. New phytologist, 161(2), pp.341-370.

Sage, R.F., Sage, T.L. and Kocacinar, F., 2012. Photorespiration and the evolution of C4 photosynthesis. Annual review of plant biology, 63(1), pp.19-47.

Schueler, L. and Hemp, A., 2016. Atlas of pollen and spores and their parent taxa of Mt Kilimanjaro and tropical East Africa. Quaternary International, 425, pp.301-386.

Sciscio, L., Neumann, F.H., Roberts, D., Tsikos, H., Scott, L. and Bamford, M., 2013. Fluctuations in Miocene climate and sea levels along the southwestern South African coast: inferences from biogeochemistry, palynology and sedimentology. Palaeontologia Africana, 48(1), pp. 2-18.

Scott, L., 1982. Late Quaternary fossil pollen grains from the Transvaal, South Africa. Review of Palaeobotany and Palynology, 36(3-4), pp.241-278.

Scott, L. and Neumann, F.H., 2018. Pollen-interpreted palaeoenvironments associated with the Middle and Late Pleistocene peopling of Southern Africa. Quaternary International, 495, pp.169-184.

Scott, L., 1999. Vegetation history and climate in the Savanna biome South Africa since 190,000 ka: a comparison of pollen data from the Tswaing Crater (the Pretoria Saltpan) and Wonderkrater. Quaternary International, 57, pp.215-223.

Scott, L., 2002. Grassland development under glacial and interglacial conditions in southern Africa: review of pollen, phytolith and isotope evidence. Palaeogeography, Palaeoclimatology, Palaeoecology, 177(1-2), pp.47-57.

Ségalen, L., Lee-Thorp, J.A. and Cerling, T., 2007. Timing of C4 grass expansion across sub-Saharan Africa. Journal of Human Evolution, 53(5), pp.549-559.

Shumilovskikh, L.S. and van Geel, B., 2020. Non-pollen palynomorphs. Handbook for the analysis of micro-particles in archaeological samples, pp.65-94.

Squires, V.R. and Feng, H., 2018. Brief history of grassland utilization and its significance to humans. In Grasslands of the world (pp. 17-26). CRC Press.

Stadnicka-Futoma, A. and Nobis, M., 2024. Geographical–Historical Analysis of the Herbarium Specimens Representing the Economically Important Family Amaranthaceae (Chenopodiaceae-Amaranthaceae Clade) Collected in 1821–2022 and Preserved in the Herbarium of the Jagiellonian University in Krakow. Biology, 13(6), p.435.

Stalmans, M. and Beilfuss, R., 2008. Landscapes of the gorongosa national park. Report prepared for Gorongosa Research Center, Gorongosa National Park, Mozambique.

Stalmans, M.E., Massad, T.J., Peel, M.J., Tarnita, C.E. and Pringle, R.M., 2019. War-induced collapse and asymmetric recovery of large-mammal populations in Gorongosa National Park, Mozambique. PloS one, 14(3), p.e0212864.

Stockey, R.A., 2006. The fossil record of basal monocots. *Aliso: A Journal of Systematic and Floristic Botany*, *22*(1), pp.91-106.

Stockmarr, J., 1971. Tables with spores used in absolute pollen analysis. Pollen et spores, 13, pp.615- 621.

Strömberg, C.A., 2011. Evolution of grasses and grassland ecosystems. Annual review of Earth and planetary sciences, 39, pp.517-544.

Stynder, D.D., 2011. Fossil bovid diets indicate a scarcity of grass in the Langebaanweg E Quarry (South Africa) late Miocene/early Pliocene environment. *Paleobiology*, *37*(1), pp.126-139.

Thijssen, R., 1996. Croton megalocarpus, the poultry-feed tree: how local knowledge could help to feed the world. commercialization of non-timber, p.226.

Tinley, K.L., 1977. Framework of the Gorongosa ecosystem (Doctoral dissertation, University of Pretoria).

Turner, C., 1985. Problems and pitfalls in the application of palynology to Pleistocene archaeological sites in western Europe. Palynologie archéologique, pp.347-373.

Twiss, P.C., Suess, E. and Smith, R.M., 1969. Morphological classification of grass phytoliths. Soil Science Society of America Journal, 33(1), pp.109-115.

Utescher, T., Erdei, B., François, L. and Mosbrugger, V., 2007. Tree diversity in the Miocene forests of Western Eurasia. *Palaeogeography, Palaeoclimatology, Palaeoecology*, *253*(1-2), pp.226-250.

van Geel, B., 2001. Non-pollen palynomorphs. Tracking environmental change using lake sediments: terrestrial, algal, and siliceous indicators, pp.99-119.

Van Wilgen, BW*, Biggs, HC**, O'Regan, SP***, Mare, N., 2000. A fire history of the savanna ecosystems in the Kruger National Park, South Africa, between 1941 and 1996. South African Journal of Science, 96(4), pp.167-178.

Wadley, L., Hodgskiss, T. and Grant, M., 2009. Implications for complex cognition from the hafting of tools with compound adhesives in the Middle Stone Age, South Africa. Proceedings of the National Academy of Sciences, 106(24), pp.9590-9594.

Wang, M., Yang, Q., Yang, W., Shi, L., Zhang, Y., Zhou, Z., Zhang, W. and Zheng, H., 2022. Surface phytolith and pollen assemblages of a low-latitude subtropical region in Southwest China and their implications for vegetation and climate. Frontiers in Plant Science, 13, p.1007612.

Ward, J.K., Tissue, D.T., Thomas, R.B., And and Strain, B.R., 1999. Comparative responses of model C3 and C4 plants to drought in low and elevated CO2. Global Change Biology, 5(8), pp.857-867.

Wicklow, D.T., 1973. Microfungal populations in surface soils of manipulated prairie stands. Ecology, 54(6), pp.1302-1310.

Williams, G.L., Fensome, R., Miller, M. and Bujak, J., 2018. Microfossils, Palynology. Encyclopedia of Petroleum Geoscience, pp.1-15. Springer Encyclopedia of Earth Sciences Series.

Wing, S.L. and Sues, H.D., 1992. Mesozoic and early Cenozoic terrestrial ecosystems. In: Behrensemeyer, A.K., Damuth, J.D., DiMichele, W.A., Potss, R., Sues, H.-D., Wing, S.L. (Eds.), Terrestrial ecosystems through time: evolutionary paleoecology of terrestrial plants and animals. University of Chicago Press, Chicago, pp.327-416.

Wood, G.D., 1996. Palynological techniques - processing and microscopy. In. Jasonius, J. and McGregor, DC eds., Palynology: Principles and Application. American Association of Stratigraphic Palynologists Foundation, 1, pp.29-50.

Worobiec, E., Worobiec, G. and Gedl, P., 2009. Occurrence of fossil bamboo pollen and a fungal conidium of Tetraploa cf. aristata in Upper Miocene deposits of Józefina (Poland). Review of Palaeobotany and Palynology, 157(3-4), pp.211-217.

Young, J.O., 1977. Six new species and records of two established species of Dalyelliidae (Turbellaria: Neorhabdocoela) from freshwater habitats in Kenya, East Africa. Journal of Natural History, 11(1), pp.1-15.

Young, J.R., 2020. Coccoliths and other marine microfossils in microparticle analysis. Handbook for the Analysis of Micro-Particles in Archaeological Samples, pp.7-21.

Zavada, M. and de Villiers, S., 2000. Pollen of the Asteraceae from the Paleocene-Eocene of South Africa. Grana, 39(1), pp.39-45.

Zhang, W., Lu, H., Li, C., Dodson, J. and Meng, X., 2017. Pollen preservation and its potential influence on paleoenvironmental reconstruction in Chinese loess deposits. Review of Palaeobotany and Palynology, 240, pp.1-10.